NUMERICAL SOLUTIONS OF THE INERTIAL MODES OF THE EARTH'S FLUID CORE: FROM THE OUTSTANDING PROBLEM OF THE INCOMPRESSIBLE FLUID SHELL TO MORE REALISTIC UP TO DATE CORE MODELS

HOSSEIN NASERI

Bachelor of Science, University of Mohaghegh Ardabili, 2007
Master of Science, Institute for Advanced Studies in Basic Sciences (IASBS), 2010

A Thesis
Submitted to the School of Graduate Studies
of the University of Lethbridge
in Partial Fulfillment of the
Requirements for the Degree

MASTER OF SCIENCE

Department of Physics and Astronomy
University of Lethbridge
LETHBRIDGE, ALBERTA, CANADA

NUMERICAL SOLUTIONS OF THE INERTIAL MODES OF THE EARTH'S FLUID CORE: FROM THE OUTSTANDING PROBLEM OF THE INCOMPRESSIBLE FLUID SHELL TO MORE REALISTIC UP TO DATE CORE MODELS

HOSSEIN NASERI

Date of Defense: April 17, 2015

Dr. Behnam Seyed-Mahmoud		
Supervisor	Associate Professor	Ph.D.
Dr. Adriana Predoi-Cross		
Committee Member	Professor	Ph.D.
Dr. Hadi Kharaghani		
Committee Member	Professor	Ph.D.
Dr. Dr. Locke Spencer		
Chair, Thesis Examination Committee	Assistant Professor	Ph.D.

Dedication

To my Honey!

Abstract

In this work we study the inertial modes of a rotating spheroidal fluid shell proportional to the Earth's fluid core. We start with the long standing problem of the modes of an incompressible and inviscid spherical fluid shell. Traditionally, a second order equation describing the pressure field of the flow, subject to the impermeability boundary condition, is solved for the eigenfrequencies and eigenfunctions of the flow. These equations are scalar hyperbolic boundary value second-order Partial Differential Equations (PDEs) which are ill-posed problems in the sense that the existence of the analytical solutions depends on the geometry of the container. The problem admits analytical solutions in a sphere but not in a spherical shell.

We use the Galekin method to solve the momentum and the continuity equation together and compute the frequencies, pressure and displacement eigenfunctions for some of the low order, wavenumbers $m = 0$ and $m = 1$, inertial modes of this model. To show that our approach is correct we compute the inertial modes of a homogeneous, incompressible and inviscid fluid sphere for which analytical solutions for the inertial modes exist.

We also compute the inertial modes of a more realistic uniformly rotating, compressible, self gravitation and inviscid fluid core model. Finally, we extend the governing equations to include first order terms in the ellipticity. In order to minimize effects of the derivatives of the material properties which are poorly determined in the existing Earth models, a Clairaut coordinate system is used to map the elliptical equipotential surfaces into the spherical ones. Also, the divergence theorem is used to implement the boundary equations.

Acknowledgments

First and foremost I offer my sincerest gratitude to my supervisor, Dr. Behnam Seyed-Mahmoud, who has supported me throughout my thesis with his remarks, patience and knowledge. I attribute the level of my Masters degree to his encouragement and effort and without him this thesis would not have been completed or written. One simply could not wish for a better or friendlier supervisor.

Furthermore, I would like to thank my committee members, Professor Adriana Predoi-Cross and Professor Hadi Kharaghani for serving as my committee members. I also want to thank you for letting my defense be an enjoyable moment, and for your brilliant comments and suggestions, thank you.

I express my warm thanks to my officemates Ali and Zaman for their valuable comments and guidance, and all of my friends, specially Mazid, Amin, Mohi, Zaza, Shishil, Nahil, Xadij, Lapa, Haj Mehdi, Seyed, Hepi, Ali Boli, Ebi, Suzan, Ahadaa, Peday, Topal, Ouruf, Qatil, Salim, Notrino, Topugh, Tagh Dayi, Mesut, Aliriza, Ustad, Dr. Behbud and Dohtur Manzuri who supported me in this way.

The most special thanks goes to my best partner and friend, my wife. Robab, you gave me your unconditional support and love through all this long process. Gadasi :*

Contents

List of Tables

List of Figures

Chapter 1

Introduction

Undoubtedly, it is almost impossible to have direct access to the Earth's deep interior. Hence, our knowledge of the structural features and the composition of the internal structure of the Earth has to be obtained from indirect evidences. At present, two sets of evidences are mostly being considered: (i) observations of geophysical phenomena such as planetary motion of the Earth, traveling speed of Earthquake waves through the Earth, heat flux in the Earth's interior, gravitational attraction, and the magnetic field; and (ii) comparison of the Earth with other astronomical objects such as solar system planets, the sun, stars, and through meteorites which may be fragments of an old planet.

1.1   Structure of the Earth

Ideally, the interior of the Earth may be described as a sequence of concentric layers. As illustrated in Figure 1.1, there are three main structural components of the Earth, which are distinguished by sharp discontinuities at the boundary interfaces: (i) a very thin surface layer of crust; (ii) the mantle, extending over half distance towards the Earth's center; and (iii) the core, which makes up the rest of the Earth's interior.

Using Earthquake records, called *seismograms*, Oldham (1914) discovered that the core itself is divided into two layers: the inner core with a radius of 1221.5 km, and the outer core with a thickness of about 2258.5 km [according to PREM; the Preliminary Reference Earth Model (Dziewonski, 1981)](see Figure Figure 1.1). The outer core is liquid; it does not transmit the shear waves, and the speed of the pressure waves is reduced sharply in this
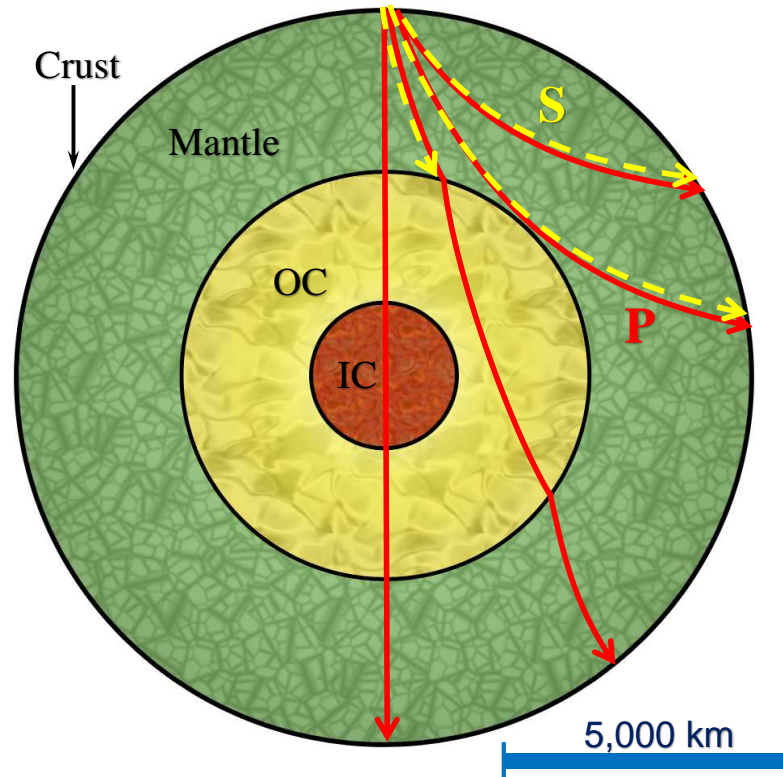
Figure 1.1: Cross section of the Earth with Inner-core (IC), outer-core (OC), mantle and crust. The paths curve because the speeds of these waves change as they travel through layers of different densities. Solid lines marked P are compressional waves; dashed lines marked S are shear waves.

region. Shear (*S*) and pressure (*P*) waves are the two main seismic wave generated by either Earthquakes or artificial large blasts near the Earth's surface. In 1936, Lehmann discovered, from seismic data available, that the inner core was solid.

The schematic ray paths of Earthquake waves are illustrated in Figure 1.1. The Earthquake waves are curved when they pass through the Earth's interior. This curvature is a refraction which indicates the change in velocity of these traveling body waves with respect to the distance from the surface of the Earth. Change in the speed of the waves is a result of change in the density (and other material properties), with Earth depth (Robertson, 1966).

1.2 Earth's Free Osculations: Observation and Theory

In order to obtain information about the detailed structure of the Earth, analyzing the variations of *P* and *S* wave velocities with depth is not sufficient. For instance, density profile within the Earth and the stability parameter (Pekeris, 1972), which is directly related to the density gradient in the core, cannot so far be accurately inferred from the seismological data. Therefore, to get a better insight into the Earth's deep interiors, traditional seismology is complemented with the *normal mode theory*. These modes are the Earth's natural vibrations, the free oscillations, which are excited as a result of a large Earthquake or other natural phenomena such as the gravitational pull of the Moon on the Earth's core. These vibrations are similar to the vibrations of a drum. When one hits the drum, it vibrates.

The observation of the free oscillations of the Earth was greatly enhanced in the 1960s with the invention of more sensitive and novel instruments, and by developing more precise recording and processing techniques (see Benioff, 1959; Alsop, 1961; Bolt, 1962). These studies resulted in new data on the internal structure of the Earth.

The conservation laws of physics applied to the Earth's interiors constitute the theoretical treatment of the free oscillations. This gives solutions consisting of the eignfrequencies of these natural vibrations, known as *normal modes* (Alterman, 1974).

For the Spherically symmetric, non-rotating, perfectly elastic and isotropic (SNREI) Earth model, theoretical angular frequencies can be precisely calculated. For this model, the components of the displacement vector can be described by the spherical harmonics $Y_n^m(\theta, \phi)$ and a function of the coordinate *r*. Then, the corresponding wave functions can be solved for spheroidal and toroidal oscillations (Alterman, 1959).

Calculating theoretical eignfrequencies is of great interest to many geophysicists. These researchers investigate the so-called *inverse normal mode* problem to compute the collection of all possible Earth models whose frequencies are overlapping with the observed frequencies of the free oscillations of the Earth. These findings are essential in in geophysical and astronomical studies and provides information about (i) the Earth's origin and evolu-

tion; (ii) the position of the Earth's inner core-outer core boundary; (iii) the core-mantle boundary; and (iv) the material properties of the Earth's interior such as density ρ, bulk modulus κ, the shear modulus μ, viscosity ν, and stratification parameter β (see Dorman, 1965; Derr, 1969; Dziewonski, 1971; Gilbert, 1975).

The rotation of the Earth and its gravitational interactions with the Moon and the Sun generate the standard model to investigate the instabilities in the Earth fluid core. One of the most significant results of this consideration is that it may generate turbulent flow in the electrically conducting fluid enclosed in the liquid core, which may play a role in the geodynamo. Especially, some of these instabilities are induced by the elliptic shape of the boundaries due to the tides (see Lumb et al., 1993; Kerswell, 1994). It is believed that the dynamo generated in the planetary fluid cores is the source of magnetic field of the Earth and other planets (Ronald, 1998). If an elliptical instability is excited in the core of planetary fluid cores, the energy it releases is sufficient to sustain the dynamo over the Earth's life time. Elliptical instability is excited as a result of interactions between the inertial modes of the rotating body (Seyed-Mahmoud, 2000).

1.3   Classification of the Normal Modes

The Earth is a rotating, self gravitating body in nearly hydrostatic equilibrium. The rotation of this body results in periodic perturbations in the shape, direction, and its rate of the rotation.These perturbations are known as tides, precession/nutation, and change in length of day. The spectrum of the Earth's free oscillations may be categorized as follow.

a) For short period oscillations called *seismic normal modes* with frequencies in the range of 5 min to 1 hour, and have elasticity as the main restoring force (Martinec, 1987). For these oscillations, deviation from sphericity of the real Earth are small enough that can be treated as first-order perturbations in the theoretical calculations of the normal mode eignfrequencies of SNREI Earth model. This assumption has been well established (see Alterman, 1974; Backus, 1962; Dahlen, 1968).

b) Translational modes of oscillation of the inner core, usually named the *Slichter modes*, are subject to gravitational and may be buoyancy restoring forces due to a density jump across the inner core boundary (ICB) (Slichter, 1961; Smith, 1976). For these modes, the period of oscillations is long enough (around 5.5 hours) that the effects of the Earth's rotation cannot be confidently regarded as a simple small perturbation. (Rochester, 1993).

c) *Gravity waves* (or the core undertones) are driven by buoyancy force that is the result of non-neutral density distribution in the ICB. The period of these oscillations is found to be up to 13 hours for most realistic Earth models (Dehant, 1990). This period is comparable to the Earth's rotational speed and hence the SNREI Earth model may not be valid for the computation of some of these modes (Crossley, 1975, 1980; Mamboukou, 2013).

d) For the long period oscillations, such as wobble and nutation and those confined mainly to the liquid outer core, the so-called *inertial modes* of the liquid outer core, the eignperiods are longer than 12 hours. Since, the Coriolis Effect is the driving force, the full effects of rotation and, in some cases, of ellipticity, must be taken into account ((Shen, 1983; Seyed-Mahmoud and Moradi, 2014; Guo, 2004).

There are five main rotational modes: (1) the Tilt-Over Mode (TOM) or Free Diurnal Nutation (FDN) of the whole Earth; (2) Chandler Wobble (CW), which is dominantly due to the rigid rotation of the Earth's elliptical mantle (Observed period of CW is about 430 days); (3) Inner Core Wobble (ICW) with a computed period of a few years (ICW has not been observed yet); (4) Free Inner Core Nutation (FICN); and (5) Free Core Nutation (FCN) (Mathews, 1991). Other than for the TOM, the eignperiods of all the rotational modes strongly depend on the ellipticity of the rotating Earth model (Rogister, 2004).

1.4 Normal Modes of a Uniformly Rotating Earth Model

Exploring the dynamic of the rotating Earth influenced by an ellipsoidal liquid-filled interior with rigid boundary has a long history. Long term motion of a fluid inside a rotating

container is a rigid rotation. Any disturbance to this motion causes relative motions of the fluid with respect to the walls of the container. This can result in either periodic changes of the orientation of the axis of rotation (wobble, nutation), or the intensity modulation of the angular velocity (length of a day) because of the relative motions of the fluid layers due to viscosity. Relative motions can also occur because of the deformation of the container induced by external forces (such as gravitational tides on a planet).

Assuming that the relative motion of the fluid versus the rigid rotation is small, equations of fluid motions for a homogeneous and incompressible fluid can be linearize as so-called *Poincaré* equations. The solutions for the Poincaré equation in the rigid boundary container are time periodic waves, called *inertial modes*, which must satisfy impermeability condition imposed by the boundaries.

For a cylindrical geometry, global solutions were investigated in the original work of Kelvin (1880). Calculation of these commonly called Kelvin modes were published by several authors (see e.g., Kerswell, 1993) on a basis of Bessel functions. Herreman (2009) extended this analysis to calculate the analytical eigenfrequencies of Kelvin modes in a cylindrical shell. The equations governing the inviscid inertial modes of an incompressible and homogeneous fluid sphere were established by Bryan (1889) and Poincaré (1910) using spherical harmonics and elliptic coordinates to analytically solve the equations of motion by separation of the variables (see also Zhang, 2004).

Experimentally, Aldridge (1969) found some of the axi-symmetric inertial modes by using pressure measurements in a librating sphere[1] at the excitation frequencies of these modes. Melchior and Ducarme (1986) and Aldridge (1987), claimed they had detected these modes in Earth's core, excited through a small perturbation in Earth's rotation after large, deep Earthquakes. Zrn et al. (1987) made a critical analysis of these observations but confirmed that inertial modes exist in planetary and stellar systems. The mechanical energy that drives deformation results in the excitation of inertial waves and also different types of

---

[1] longitudinal libration are small periodic oscillations of the spinning rate of a globally rotating sphere.

instabilities (e.g., elliptic instability, shear instability and centrifugal instability) (Le Bars, 2015).

Concerning a spheroidal geometry, Hopkins (1839) was among the first to find the free nutation of the Earth and numerically determined its amplitude by solving the equation of the motion for position of the Earth's pole. Chandler (1894) discovered the *Chandler Wobble* with a period of 427 days by studying the observed astronomical data. The theoretical period for a solid homogeneous, ellipsoidal Earth is 304 days. But if a homogeneous and incompressible liquid core is added then the period actually becomes 270 days. Once elasticity, presence of the oceans, the Earth's atmosphere, and electromagnetic and gravitational coupling at the CMB is considered, the period for a realistic Earth model becomes close to the observed value (Mathews and Shapiro, 1992).

Hough (1895) showed that for such a system a second free wobble of a nearly diurnal period exists in addition to the Euler (Chandler) wobble. The existence of this second free wobble was confirmed by Poincaré (1910), by using the natural coordinates for a rotating fluid (oblate spheroidal systems). It was from subsequent analyses of latitude and time data that Popov (1963), for the first time, observed this *nearly diurnal wobble*. Greenspan (1964), Kudlick (1966) calculated inertial oscillations of a rotating, incompressible, homogeneous, Newtonian fluid bounded by a spherical rigid shell.

1.5 Normal Modes of a Uniformly Rotating Fluid in a Rigid Spherical Shell Container

The Earth's core is a thick nearly spherical rotating fluid shell, therefore, the inertial modes are most likely excited in this body. In fact, except for the toroidal modes, the solutions of the Poincaré equation are associated with the impermeability boundary conditions on the inner and outer surfaces of the container. This overconstrained boundary conditions makes the hyperbolic equation to be mathematically ill-posed. Ill-posed here means that the existence of the analytical solutions depends on the geometry of the container. The

problem admits analytical solutions in a sphere but not in a spherical shell.

Longuet-Higgins (1964, 1965) considered the container to be a thin spherical shell and was able to determine the free oscillations of the rotating fluid in the spherical shell, by neglecting radial motions, so that the governing equation reduced to Laplace's tidal equation. He showed that, there are no general explicit solutions available for Poincaré equation in shell geometry and the success in determining the free oscillation modes depends on possibility of separation of the variables.

Stewartson (1969) studied the perturbations of the solutions found by Longuet-Higgins that arise when the thickness of the shell is allowed to increase from zero. They found that the non-integrable singularity, in the pressure, appears in the equation when the characteristic cones of the hyperbolic equation touch the inner boundary of the shell. Stewartson (1971, 1972) used ray theory to study the propagation of characteristics and thus get information about probable *pathological* character of inviscid solutions and low-frequency modes trapped in the equatorial region of a very thin shell. They found that the periodic patterns depend on the excitation frequency and also on the number of reflections on the shell walls.

Henderson (1996) described the problem of the spherically rotating fluid shell in a *weak*[1] form as a variational principle. He used finite element method and placed the mesh elements along the characteristics surfaces and found the approximate solutions for Poincaré model in the shell. These solutions were merely continuous and neither smooth nor differentiable.

Rieutord (1987, 1991) (see also, Rieutord, 1997), used an iterative procedure based on the incomplete Arnoldi-Chebyshev method to numerically solved the equation of motion for a spherical shell. They added the viscous term to the model and showed that inertial modes in a spherical shell are determined by a web of rays that reflect at the boundaries[2].

---

[1]The term ,*Weakness*, used to indicate the sudden change in the normal component of the pressure gradient and in the tangential component of the velocity along a characteristic line.

[2]Kinetic energy is not evenly distributed in the volume of the shell but concentrated on conical surfaces which have some thickness however. The intersection of these *surfaces* with a meridional section forms the

They showed that the web of rays depends on viscosity and the pattern of rays bifurcates as viscosity tends to zero and no asymptotic smooth solution exists for the limit of zero viscosity. The different scales which occur in a solution are related to the appearance of many internal layers which are resulted from singularities of the boundary layers. These singularities are like the ones arising at the critical latitude (see Kerswell, 1995). Shear layers were studied previously by Stewartson (1957) on the basic setup of coaxial rotating disks, and by Kerswell (1995) and Hollerbach (1995) by connecting them to the problem of precession of fluids. Despite the fact that these inertial layers to play a minor role in the linear theory, they are important when nonlinear effects are considered (Le Bars, 2015).

Dintrans (1999) concluded that individual eigenmodes do not follow any precise asymptotic law as viscosity tends to zero; only statistical properties of these modes satisfy some simple rules (scalings) [1].

In spite of their considerable progress in the Poincaré problem, all the above mentioned attempts were a partial answer to the question of the nature of the spectrum of normal modes in a rotating shell of inviscid fluid. Progress toward more realistic Earth models (including minor effects of ellipticity, inhomogeneity and elasticity) requires better understanding of this basic model. In this thesis we will show that we have found numerical solutions for the inviscid fluid shell by directly solving the momentum and the continuity equations.

1.6 Normal Modes of a Realistic Earth Model

The above mentioned models are too simplified to be able to completely describe the complex behavior of the real Earth. Even so, they allow us to approximately model the Earth's free wobble/nutation, elliptical instability, geodynamo and other naturally occurring phenomena. First of all, the boundaries of the Earth's fluid core are not rigid, instead,

---

web of rays.

[1]This problem is in fact related to another eigenvalue problem in physics, namely quantum chaos. In semi-classical systems, quantum chaos appears when the wave function and its associated energy eigenvalue strongly depend on a control parameter of the system. For this system, changing the control parameter result in a chaotic evaluation of the energy eigenvalues of the system.

they are comprised of a deformable solid mantle as well as an inner core. Secondly, the effect of self-gravitation of the Earth is not completely negligible. Moreover, the Earth is not homogeneous and its properties vary with depth. Therefore, realistic theoretical calculations must accurately take into account (1) the elastic-gravitational behavior of the mantle and inner core, (2) the compressibility and density distribution of the outer fluid core, (3) gravitational and pressure interactions in ICB and core-mantle boundaries (CMB), and finally (4) non-neutral stratification in the fluid OC.

By modifying the Earth model to include a fluid OC, a deformable mantle (MT) and a solid IC, important contributions were made to the theory of the free oscillations (Lamb, 1895; Jeffreys, 1948, 1949). Jeffreys (1957) considered Earth model with radially stratified elastic mantle and homogeneous incompressible liquid OC, and calculated the frequency of the Earth's nutation modes. Molodensky (1961) (see also Molodensky, 2004) added the effects of core compressibility in his calculations and considered the known elastic properties of the mantle. Alterman (1974), and Toomre (1974) reviewed the history of the nearly diurnal wobble problem and modified Lamb's notation slightly by developing a special method for harmonic analysis. Shen (1976) extended the theory by adding non-neutral stratification in the liquid core. Their extension to Molodonsky's (1961) theory relied principally upon a truncated surface spherical harmonic representation of the response of the fluid core. Generally speaking, these studies rely on the Liouville equations, that are Euler's equations which are modified to allow for deformation and internal flow.

Using the linear momentum description (LMD), Smith (1974) derived the elastic-gravitational normal modes theory. In this theory, the variation in self-gravitation and the deformation in the solid Earth are expressed in the spheroidal and toroidal representation. Also, the effects of rotation and ellipticity are treated explicitly. Wahr (1981) used by Smith's formulation to study the effects of the Earth's rotation and ellipticity on the body tides. Smylie and Rochester (1981) derived equations of the core dynamics by finding an alternative scalar second order partial differential equation (The subseismic PDE). Dehant (1990) used

Wahr's numeric code and allowed material anelasticity in the equations of motion.

Wu and Rochester (1990) showed that the dynamics of the inviscid liquid core can be described precisely by two scalar second order PDEs with scalar potentials, the Two Potential Description of the core dynamics. Rochester (1993) proposed a non-orthogonal coordinate system, named the *Clairaut* coordinate system. Then, they modified field variables and removed derivatives of material properties across elliptical boundaries. The *subseismic description* of core dynamics is used Smylie et al. (1992) to study the Earth's wobble/nutation modes. The effect of the viscosity of fluid core is also studied in some recent works by Greiner-Mai et al. (2000); Guo (2004), and Lubkov (2007).

Seyed-Mahmoud (1994) introduced three-potential descriptions (3PD) of the core by using a set of three scalar PDEs in three potentials as independent variables, which exactly describe the linearized dynamics of the inviscid liquid core. The variational principle of free oscillations in a rotating, inviscid, and elliptically stratified fluid outer core is developed byXU et al. (2004), and Rogister (2004). Seyed-Mahmoud (2006),(also Seyed-Mahmoud, 2007) implemented the Galerkin method to find the normal modes of a rotating spherical liquid core for a realistic core model. Taking advantage of the Clairaut coordinate system and considering first order terms in ellipticity, Seyed-Mahmoud and Moradi (2014) also studied inertial modes of an elliptical Earth model. Recently, using the same coordinate system Rochester et al. (2014) built a new mathematical formulation and included second order terms in the ellipticity to described the Earth's wobble/nutation modes.

1.7 Outlines

In this thesis we first give the theoretical derivation of the partial differential equations (PDEs) governing the inertial modes of free oscillations of a realistic Earth model. We will then use a Galerkin method to solve these equations for the frequencies and eigenfunctions of the inertial modes of several core models.

In chapter 2, using the conventional approach of spheroidal/toroidal representation of

vector displacement fields, and following Rochester formulation (lecture notes provided by my supervisor), we derive PDEs and the BCs governing the free oscillations of the self-gravitating, spherical, rotating Earth model. In section 2.5 we make the assumption that the core is homogeneous and incompressible in order to numerically solve the governing equations for a spherical shell. We use a Galerkin method and FORTRAN programming to numerically solve for some of the low order (wavenumber 0 and 1) inertial modes of (a) a homogeneous and incompressible core model, and (b) a more realistic core model which is compressible and stratified. To validate our approach, we compare the frequencies and the displacement and pressure patterns for these modes to those of a fluid sphere for which analytical solutions exists.

In chapter 4, we extend our model to include the effects of elasticity, incompressibility and inhomogeneity. We show that the divergence theorem may be used to (a) remove the dependence of the equations on the gradient of the density, which is poorly constrained within Earth, and (b) to take advantage of the *natural* nature of the boundary conditions. In chapter 5, we expand our equations to include the first order effect of ellipticity in the Earth model. In order to minimize the effects of derivatives on material properties, a (non-orthogonal) Clairaut coordinate system (Jeffreys, 1942; Kopal, 1980; Seyed-Mahmoud, 2006) is used. Finally, our conclusions are presented in chapter 6, and we discuss our results and compare them with previously obtained results.

Chapter 2

Normal Modes of an Incompressible Fluid Core Model

2.1 Hydrostatic Earth Model

Neglecting the effects of thermal convection and magnetic field [1], the reference state of the Earth is considered to be one of *hydrostatic equilibrium*. This reference frame has its origin in the Earth's center and rotates with the constant angular velocity of Ω about a fix axis in space defined by a unit vector $\hat{\mathbf{e}}_3$. In this reference state, the dynamics of the self-gravitating, rotating, spheroidal Earth which is subjected to a small elastic deformation, can be described by, (i) five conservation laws: conservation of mass, momentum, angular momentum, mechanical energy, and gravitational flux; and (ii) a Hook's law. In this chapter we show that to first order in deformation variables, these laws can be expressed by linear PDEs.

2.2 Equations of Motion

2.2.1 Hydrostatic equilibrium

It is convenient to use Earth's properties, (mean radios $R = 6371$ *km*, average density $< \rho >= 5.54$ *g.cm^{-3}*, and speed of rotation $\Omega = 7.292 \times 10^{-5} rad.s^{-1}$), to introduce non-

---

[1]As far as the effect of deformations on the rotation at the Earth is small and can be taken to be isentropic, these assumptions are valid

dimensionalized parameters as,

$$r_{ND} = \frac{r}{R} \quad ; \quad \mathbf{u}_{ND} = \frac{\mathbf{u}}{R} \quad ; \quad \rho_{ND} = \frac{\rho}{<\rho>} \quad ; \quad \nabla_{ND} = R\nabla$$

where r, u and ρ are position of the mass element, displacement vector and density, respectively, that will be explained later. In our notation, for brevity, we drop subscript ND, by keeping in mind that all quantities are dimensionless afterwards. In the equilibrium config-
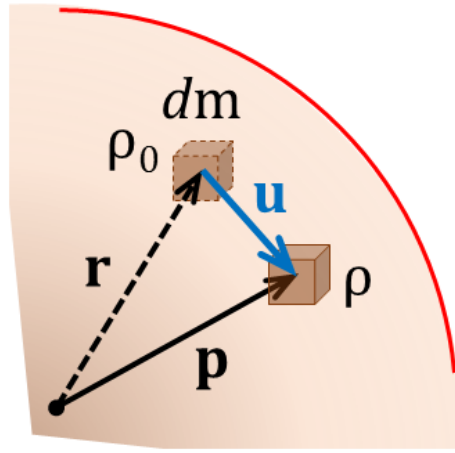
Figure 2.1: A small displacement $\mathbf{u}$ leads the mass element dm to move to the new position, $\mathbf{p} = \mathbf{r} + \mathbf{u}$, and to have the density of $\rho(\mathbf{p}) = \rho_0(\mathbf{r} + \mathbf{u}) + \rho_1(\mathbf{r} + \mathbf{u})$.

uration, the dimensionless mass element dm, at position $\mathbf{r}$ from the origin has the density of $\rho_0(\mathbf{r})$. A small displacement $\mathbf{u} = \mathbf{u}(\mathbf{r},t)$ leads the mass element to move to the new position, $\mathbf{p} = \mathbf{r} + \mathbf{u}$, and to have the density of $\rho(\mathbf{p}) = \rho_0(\mathbf{r} + \mathbf{u}) + \rho_1(\mathbf{r} + \mathbf{u})$, where ρ_1 is Eulerian change in the density at $\mathbf{p}$, due to deformation. To first order in the small quantities, $\mathbf{u}$ and ρ_1, conservation of mass requires that in every point in the volume to have

$$\rho_1 = -\nabla.(\rho_0\mathbf{u}). \tag{2.1}$$

Also, conservation of momentum for every mass element at the displaced position **p** is expressed by the Newton's second law of motion,

$$\frac{d\mathbf{v}}{dt} = \mathbf{F} + \frac{1}{\rho}\nabla.\tilde{\mathbf{T}} \qquad (2.2)$$

In (2.2), **v** is the non-dimensionalized velocity ($\mathbf{v}_{ND} = \mathbf{u}/R\Omega$) of the displaced mass element, dm, relative to the inertial frame, ρ is the dimensionless density of the mass element at the instant of deformation, **F** is a dimensionless long range body force ($\mathbf{F}_{ND} = \mathbf{F}/<\rho>R\Omega^2$), and $\tilde{\mathbf{T}}$ is a stress tensor [1].

We are assuming that there are no external forces (such as gravity forces from the Moon and other external bodies) present. Also we are considering that the reference state is symmetric, i.e., density is a function or r only. Therefore **F** and $\tilde{\mathbf{T}}$ depend on the internal gravity and pressure, respectively. The gravitational force on the non-displaced mass element located at **r**, in the reference frame, is originated from the mass enclosed by **r**. This force can be written as $\mathbf{F} = \nabla V_0(r)$, where $V_0(\mathbf{r})$ is the dimensionless gravitational potential at point **r** in the equilibrium configuration. As indicated, the only stress is due to the pressure, $p_0(r)$, and can be expressed as $\tilde{\mathbf{T}} = -p_0\tilde{\mathbf{1}}$ (where $\tilde{\mathbf{1}}$ is the unit tensor).

On the other hand, the mass element experiences a centripetal acceleration

$$\frac{d\mathbf{v}}{dt} = \Omega\hat{\mathbf{e}}_3 \times (\Omega\hat{\mathbf{e}}_3 \times \mathbf{r}) \qquad (2.3)$$

Therefore the equation (2.2) can be written as

$$\Omega\hat{\mathbf{e}}_3 \times (\Omega\hat{\mathbf{e}}_3 \times \mathbf{r}) = \nabla V_0 - \frac{1}{\rho_0}\nabla p_0 \qquad (2.4)$$

---

[1] Physically stress tensor defines short range surface forces including normal (tensile or compressive) stress and shear stresses.

Defining gravity $\mathbf{g}_0$ as a result of gravitational and centrifugal acceleration

$$\mathbf{g}_0 = \nabla(V_0 + \frac{1}{2}|\Omega\hat{\mathbf{e}}_3 \times \mathbf{r}|^2) \tag{2.5}$$

(2.4) result in basic equation of hydrostatic equilibrium

$$\nabla p_0 = \rho_0 \mathbf{g}_0 \tag{2.6}$$

in which, $\mathbf{g}_0$ is the dimensionless gravity ($\mathbf{g}_{0ND} = \frac{\mathbf{g}_0}{4R\Omega^2}$). Expression (2.6) implies

$$\nabla \times \mathbf{g}_0 = 0. \tag{2.7}$$

Equations (2.7) and (2.6) basically show that everywhere in the interior and surface of a fluid in hydrostatic equilibrium, gravity equipotentals coincide with the surfaces of equal pressure (isobars) and equal density (isopycnics).

2.2.2 Deformation from hydrostatic equilibrium

In the deformed Earth, dm acquires an additional stress, $\tilde{\mathbf{S}}$, which is due to the deformation during the displacement.

Suppose two neighboring mass elements at locations x_i and $x_i + dx_i$ experience a displacement u_i and $u_i + \frac{\partial u_i}{\partial x_j}dx_j$, respectively. Therefore, in the Cartesian coordinate system the distance between these two mass elements changes from $\sqrt{dx_i dx_i}$, before deformation, to

$$\sqrt{(dx_i + \frac{\partial u_i}{\partial x_j}dx_j)(dx_i + \frac{\partial u_i}{\partial x_k}dx_k)},$$

after displacement. So, to the first order in u_i, square of the distance separating the two mass elements becomes

$$2\frac{\partial u_i}{\partial x_j}dx_j dx_i = 2\left(dx_j\hat{\mathbf{e}}_j\right) \cdot \left(\hat{\mathbf{e}}_j\frac{\partial u_i}{\partial x_j}\hat{\mathbf{e}}_i\right) \cdot \left(dx_i\hat{\mathbf{e}}_i\right) \tag{2.8}$$

The middle term in the right hand side of the (2.8) is deformation dyadic

$$\nabla \mathbf{u} = \hat{\mathbf{e}}_j \frac{\partial u_i}{\partial x_j} \hat{\mathbf{e}}_i, \tag{2.9}$$

and means that deformation takes place when (2.9) is nonzero. Hence, a pure translation or a pure rigid rotation of matter will not cause a change in the distance between neighbouring mass elements. From (2.8) it can be seen that only symmetric part of $\nabla \mathbf{u}$ contributes to deformation[1],

$$\tilde{\mathbf{e}} = \frac{1}{2} \left[\nabla \mathbf{u} + (\nabla \mathbf{u})^T \right] \tag{2.10}$$

which called strain tensor.

Elastic behavior of a perfectly elastic and isotropic matter (i.e. that its elastic properties at a point are the same in all directions) is perfectly represented by the most general form of Hooke's law, conversations of the angular momentum and energy, as a linear relation between stress tensor, $\tilde{\mathbf{S}}$, and strain, $\tilde{\mathbf{e}}$.

$$\tilde{\mathbf{S}} = \rho_0(\alpha^2 - 2\beta^2)(\nabla.\mathbf{u})\,\tilde{\mathbf{1}} + 2\rho_0\beta^2\,\tilde{\mathbf{e}}, \tag{2.11}$$

where α and β are dimensionless speeds of propagation of the compressional and shear waves in the Earth, respectively ($\alpha_{ND} = \alpha/R\Omega$, $\beta_{ND} = \beta/R\Omega$). $\tilde{\mathbf{1}}$ and $\tilde{\mathbf{e}}$ are the *unit* and *strain* tensors, where in the spherical polar coordinate system are given by the following matrices

$$\tilde{\mathbf{1}} = \begin{bmatrix} \hat{\mathbf{r}}\hat{\mathbf{r}} & 0 & 0 \\ 0 & \hat{\theta}\hat{\theta} & 0 \\ 0 & 0 & \hat{\phi}\hat{\phi} \end{bmatrix} \qquad \tilde{\mathbf{e}} = \begin{bmatrix} e_{rr} & e_{r\theta} & e_{r\phi} \\ e_{\theta r} & e_{\theta\theta} & e_{\theta\phi} \\ e_{\phi r} & e_{\phi\theta} & e_{\phi\phi} \end{bmatrix}. \tag{2.12}$$

---

[1] ij'th component of $\nabla \mathbf{u}^T$ is ji'th component of $\nabla \mathbf{u}$

In (2.12),

$$
\begin{aligned}
e_{rr} &= \frac{\partial u_r}{\partial r} \\
2e_{r\theta} = 2e_{\theta r} &= \frac{\partial u_\theta}{\partial r} - \frac{u_\theta}{r} + \frac{1}{r}\frac{\partial u_r}{\partial \theta} \\
2e_{r\phi} = 2e_{\phi r} &= \frac{\partial u_\phi}{\partial r} - \frac{u_\phi}{r} + \frac{1}{r\sin\theta}\frac{\partial u_r}{\partial \phi} \\
e_{\theta\theta} &= \left[\frac{u_r}{r} + \frac{1}{r}\frac{\partial u_\theta}{\partial \theta}\right] \\
2e_{\theta\phi} = 2e_{\phi\theta} &= \frac{1}{r}\frac{\partial u_\phi}{\partial \theta} - \frac{u_\phi\cot\theta}{r} + \frac{1}{r\sin\theta}\frac{\partial u_\theta}{\partial \phi} \\
e_{\phi\phi} &= \left[\frac{1}{r\sin\theta}\frac{\partial u_\phi}{\partial \phi} + \frac{u_r}{r} + \frac{u_\theta\cot\theta}{r}\right]
\end{aligned}
\tag{2.13}
$$

Physically, the terms $\rho_0(\alpha^2 - 2\beta^2)$ and $2\rho_0\beta^2$ in equation (2.11), are measure of the incompressibility (pressure deformation) and rigidity (shear deformation) of an elastic material. It should be mentioned that, by definition, a fluid has no rigidity, i.e. can not be twisted. Therefore, shear waves do not travel in the Earth's fluid core; $\beta = 0$.

Eventually, the total stress on the disturbed mass element at the displaced position, $\mathbf{p}$, is

$$
\tilde{\mathbf{T}} = -p_0(\mathbf{r})\mathbf{1} + \tilde{\mathbf{S}}.
\tag{2.14}
$$

In the deformed Earth, moreover, the total force on the mass element is resulted from both gradient of the gravitational flux and its perturbation. The total gravitational potential experienced by the disturbed mass element at $\mathbf{p}$ is $V_0(\mathbf{p}) + V_1(\mathbf{p})$, where, V_1 is the Eulerian change in the gravitational potential due to the displacement field, $\mathbf{u}$. The net body force on the disturbed mass element, dm, evaluated at $\mathbf{p}$ is

$$
\mathbf{F} = \nabla V_0 + \nabla V_1.
\tag{2.15}
$$

18

2.2.3   Rigid rotational oscillations

Suppose the displacement, $\mathbf{u}$, experienced by the mass element, dm, undergo a small oscillation in time with the frequency of ω, and write

$$\mathbf{u}(\mathbf{r},t) = Re[\mathbf{u}(\mathbf{r})e^{i\omega t}]. \tag{2.16}$$

The acceleration of the mass element, dm, at $\mathbf{p}$, relative to the inertial frame, is combination of the translational, Coriolis and centrifugal accelerations and is expressed by the Lagrangian formulation as

$$\frac{d\mathbf{v}}{dt} = \frac{d^2\mathbf{p}}{dt^2} = -\sigma^2\mathbf{u} + i\sigma\hat{\mathbf{e}}_3 \times \mathbf{u} + \frac{1}{4}\hat{\mathbf{e}}_3 \times (\hat{\mathbf{e}}_3 \times \mathbf{p}). \tag{2.17}$$

where $\sigma = \dfrac{\omega}{2\Omega}$, is non-dimensionalized frequency of the oscillation. Substituting (2.15) and (2.17), the equation of motion, (2.2), at the disturbed position, $\mathbf{p}$, can be written as

$$-\sigma^2\mathbf{u} + i\sigma\hat{\mathbf{e}}_3 \times \mathbf{u} = \mathbf{g}_0 + \nabla V_1 + \frac{1}{\rho}\nabla.\tilde{\mathbf{T}}, \tag{2.18}$$

in which $\mathbf{g}_0$, dimensionless gravity, is defined similar to (2.5) as a result of the gravitational and centrifugal accelerations at $\mathbf{p}$

$$\mathbf{g}_0 = \nabla V_0 - \frac{1}{4}\hat{\mathbf{e}}_3 \times (\hat{\mathbf{e}}_3 \times \mathbf{p}) = \nabla(V_0 + \frac{1}{2}|\hat{\mathbf{e}}_3 \times \mathbf{r}|^2) = \left[-g_0(r) + \frac{2}{3}r\right]\hat{\mathbf{r}},. \tag{2.19}$$

in which

$$g_0(r) = -\frac{dV_0}{dr} = G\frac{M(r)}{r^2} \tag{2.20}$$

is dimensionless gravitational acceleration[1]. From (2.20)

$$\frac{dg_0}{dr} = -\frac{2g_0(r)}{r} + 4\pi G \rho_0(r) \tag{2.21}$$

All quantities on the right hand side (RHS) of the equation (2.18) are evaluated at the disturbed position, $\mathbf{p}$. To first order in $\mathbf{u}$, these quantities can be evaluated with respect to the coordinates of $\mathbf{r}$, using the following Taylor expansions

$$\nabla_{\mathbf{p}} = \nabla_{\mathbf{r}} - (\nabla \mathbf{u}).\nabla_{\mathbf{r}} \tag{2.22}$$

$$\psi(\mathbf{p}) = \psi(\mathbf{r}) + \mathbf{u}.\nabla\psi. \tag{2.23}$$

Operating (2.22) and (2.23) on the (2.14), we obtain

$$\nabla.\tilde{\mathbf{T}} = -\nabla p_0 + (\nabla \mathbf{u}).(\nabla p_0) + \nabla.\tilde{\mathbf{S}}. \tag{2.24}$$

Also operating (2.22), To first order in $\mathbf{u}$,(2.19) can be evaluated at $\mathbf{r}$ as

$$\mathbf{g}_0(\mathbf{p}) = \mathbf{g}_0(\mathbf{r}) + \mathbf{u}.\nabla\mathbf{g}_0(\mathbf{r}). \tag{2.25}$$

Using (2.1) and (2.23), the density of the disturbed mass element can be evaluated at $\mathbf{r}$ as

$$\rho(\mathbf{p}) = \rho_0(\mathbf{r}) + \mathbf{u}.\nabla\rho_0 + \rho_1 \mathbf{r} = \rho_0(\mathbf{r}) - \rho_0\nabla.\mathbf{u}. \tag{2.26}$$

Multiplying (2.18)by ρ (from (2.26)), and substituting (2.24) and (2.25), we get

$$\left(\rho_0(\mathbf{r}) - \rho_0\nabla.\mathbf{u}\right)\left(\sigma^2\mathbf{u} - i\sigma\hat{\mathbf{e}}_3 \times \mathbf{u} + \mathbf{g}_0 + \mathbf{u}.\nabla\mathbf{g}_0 + \nabla V_1\right) - \nabla p_0 + (\nabla\mathbf{u}).(\nabla p_0) + \nabla.\tilde{\mathbf{S}} = 0. \tag{2.27}$$

---

[1]Recall that the parameters g_0, G, ρ and M are non-dimensionalized as $G = G/\Omega^2$, $g_0 = g_0/(r\Omega^2)$, $\rho = \rho/<\rho>$ and $M = M/(r^3 <\rho>)$, respectively.

Dropping the terms of higher than the first order in $\mathbf{u}$ and V_1, and using (2.6), the equation of motion evaluated at $\mathbf{r}$ becomes

$$\sigma^2 \mathbf{u} - i\sigma \hat{\mathbf{e}}_3 \times \mathbf{u} - \mathbf{g}_0 \nabla.\mathbf{u} + \nabla(\mathbf{u}.\mathbf{g}_0) + \nabla V_1 + \frac{1}{\rho_0}\left(\nabla.\tilde{\mathbf{S}}\right) = 0, \qquad (2.28)$$

in which we used (2.7) to simplify the third term as

$$\mathbf{u}.\nabla \mathbf{g}_0 + (\nabla \mathbf{u}).\mathbf{g}_0 = \nabla(\mathbf{u}.\mathbf{g}_0). \qquad (2.29)$$

2.3   Poission's Equation

Conservation of the gravitational flux through the Earth evaluated at $\mathbf{p}$ is

$$\nabla^2 V = -4\pi G\rho. \qquad (2.30)$$

where G is non-dimensionalized gravitational constant ($G_{ND} = G < \rho > /(R\Omega)^2$). Using (2.1), (2.23), and the fact that the equation (2.30) is valid in the equilibrium configuration at r (i.e. $\nabla^2 V_0 = -4\pi G\rho_0$), The Poisson's equation (2.30) can be evaluated at $\mathbf{p}$ as

$$\nabla^2 V_1 = -4\pi G\nabla(\rho_0 \mathbf{u}). \qquad (2.31)$$

The PDEs (2.28) and (2.31) are governing the small periodic oscillations of a spherically-symmetric isotropic elastic rotating Earth model, slightly disturbed from hydrostatic equilibrium. These equations involve all five conservation laws. Complete solutions of these equations require implementing of the correct boundary conditions. Note that the response of the real Earth to the stress is not perfectly elastic which means that any free oscillation is damping in time. This feature cause the parameters to be function of frequency. However, at this point we shall not consider the effect of anelasticity. Besides, in the equations we derived the effect of the viscosity is ignored.

2.4 Boundary Conditions at the Interfaces

The boundaries are referred to the surfaces where one or more of the material properties (such as ρ_0, α and β) are discontinuous. In the spherically symmetric Earth in hydrostatic equilibrium, these surfaces are spheres of the equipotentials of $V_0(\mathbf{r})$. Suppose the unit normal vector on the equilibrium boundary at $\mathbf{r}$, to be $\hat{\mathbf{n}}$, and on the deformed boundary at $\mathbf{p}$, to be $\hat{\mathbf{N}}$. We also denote Δ to refer to the difference between the outer and inner parts of the boundary.

Conservation of the mass requires a continuity of displacement, $\mathbf{u}$, at the deformed boundary $\mathbf{p}$ in a solid-solid interfaces. to first order in $\mathbf{u}$, this kinematic boundary condition at the equilibrium boundary can be regarded as

$$\boxed{\Delta \mathbf{u} = 0}.\tag{2.32}$$

However, at a solid-fluid interface, for an inviscid fluid, in the absence of viscosity, there is no friction between fluid layers to prevent tangential slip. Therefore, only the normal component of the $\mathbf{u}$ is required to be continuous at the deformed boundary.
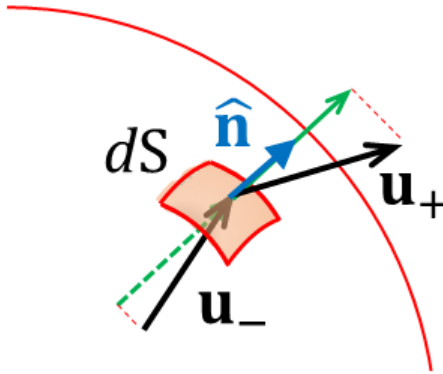
Figure 2.2: The normal component of the $\mathbf{u}$ is required to be continuous at the solid-fluid boundary.

$$\Delta(\hat{\mathbf{N}}.\mathbf{u}) = 0.\tag{2.33}$$

Again, neglecting the quantities higher than the first order in the $\mathbf{u}$, the kinematic boundary condition at a solid/fluid interface can be evaluated at the equilibrium boundary as

$$\boxed{\Delta(\hat{\mathbf{n}}.\mathbf{u}) = 0}. \tag{2.34}$$

The next is the dynamic boundary conditions. Newton's third law for the short range force across the deformed boundary results in

$$\Delta(\hat{\mathbf{N}}.\mathbf{T}) = 0. \tag{2.35}$$

The equilibrium boundary is an isobar, $\rho_o(\mathbf{r}_+) = \rho_o(\mathbf{r}_-)$. Therefore, using (2.14), to the first order in $\mathbf{u}$, (2.35) reduces to

$$\boxed{\Delta(\hat{\mathbf{n}}.\mathbf{S}) = 0}, \tag{2.36}$$

evaluated at the equilibrium boundary.

We also need to establish a boundary condition on the gravitational field. The body forces depend on the derivatives of an Eulerian change in the gravitational potential, ∇V_1. Therefore, ∇V_1 must exist in the boundary which requires V_1 to be continuous at the deformed boundary. Sine V_1 is evaluated at the equilibrium position, then,

$$\boxed{\Delta V_1 = 0}. \tag{2.37}$$

Last boundary condition is resulted from the Poisson's equation, (2.31), which can be written as

$$\nabla.(\nabla V_1 - 4\pi G \rho_0 \mathbf{u}) = 0. \tag{2.38}$$

To extract the boundary condition on the gravitational flux, we consider a small cylindrical surface with the following characteristics: (1) An infinitely small side area, and (2) the upper and lower surfaces normal to the deformed boundary (see Figure 2.3). Applying the

23
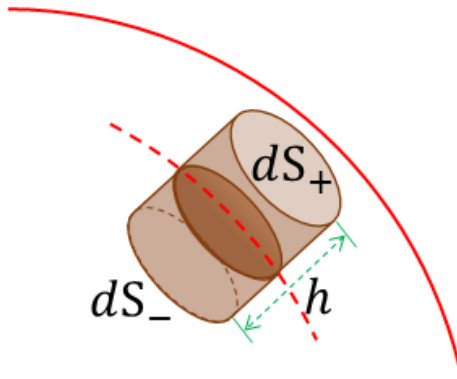
Figure 2.3: A small cylindrical Gaussian surface with an infinitely small side area ($h \to 0$), and the bellow and above surfaces normal to the deformed boundary.

divergence theorem on the (2.38) in this surface, results in

$$\hat{\mathbf{N}}.[\nabla V_1 - 4\pi G\rho_0\mathbf{u}]_+ - \hat{\mathbf{N}}.[\nabla V_1 - 4\pi G\rho_0\mathbf{u}]_- = 0. \tag{2.39}$$

to first order in $\mathbf{u}$ and V_1, (2.39) reduces to

$$\boxed{\Delta[\mathbf{n}.(\nabla V_1 - 4\pi G\rho_0\mathbf{u})] = 0}. \tag{2.40}$$

In summary, the boundary conditions of (2.32) [or (2.34)], (2.36), (2.37) and (2.39) are essential to calculate the solutions of the (2.28) and (2.31) across a surfaces of discontinuity in any material properties.

2.5 The Poincaré Earth Model

2.5.1 Single scalar equation representation

For an incompressible inviscid fluid, PDEs (2.28) and (2.31) reduce to equation of the motion (Greenspan, 1968),

$$\sigma^2\mathbf{u} - i\sigma\hat{\mathbf{e}}_3 \times \mathbf{u} + \nabla P = 0, \tag{2.41}$$

and continuity equation,

$$\nabla.\mathbf{u} = 0, \tag{2.42}$$

where **u** and P are respectively dimensionless displacement vector field and pressure, and have wave-like time dependence with frequency of ω, ($\sigma = \omega/2\Omega$). Note that the dimensionless pressure in (2.41) is ($P_{ND} = P/\rho$). Solutions of the equations (2.41) and (2.42) are subject to inviscid impermeability boundary condition

$$\mathbf{n}.\mathbf{u} = 0. \tag{2.43}$$

In terms of the pressure, equations (2.41) and (2.42) reduce to a boundary value so-called Poincaré equation,

$$\nabla^2 P - \frac{1}{\sigma^2}\left(\hat{\mathbf{e}}_3.\nabla\right)^2 P = 0. \tag{2.44}$$

$$-\sigma^2\hat{\mathbf{n}}.\nabla P + (\hat{\mathbf{n}}.\hat{\mathbf{e}}_3)(\hat{\mathbf{e}}_3.\nabla P) + i\sigma(\hat{\mathbf{e}}_3 \times \hat{\mathbf{n}}).\nabla P = 0 \tag{2.45}$$

for $\sigma \leq 1$. This equation is hyperbolic (Greenspan, 1964) and since pressure perturbations for contained fluids must meet impermeability boundary conditions, the problem is mathematically ill-posed.

For some containers (such as full sphere or cylinder) the Poincaré equation is separable and admits analytical solutions, while, for most of the other geometries (such as spherical shell) above mentioned property implies the solutions of the problem to be ill-posed, i.e. the boundary conditions become over constrained and solutions of the equations can not be uniquely determined in these geometries . In these cases, the determinant of the matrix of coefficients becomes unstable with respect to the frequency and forbids the existence of eigenvalues and eigenmodes. Considering viscosity (Rieutord, 1995) and compressibility (Seyed-Mahmoud, 2007) may regularize the singularities.

2.5.2 Four equation description

Instead of solving the second order hyperbolic equations of (2.44) and (2.45), in the next chapter, we use Galerkin method to directly solve system of linear equations (2.41) and (2.42). We will show that, this approach may remove part of the singularity of the problem

25

and result in the convergence of matrix of coefficients for most of the inertial modes. Also, implementation of a Galerkin allows us to apply divergence theorem to make boundary conditions to be satisfied *naturally*. This condition may also remove the singularities that arise from impermeability BCs in the Poincaré method.

From (2.41), equation (2.42) can be written as

$$\nabla.\left(-i\sigma\hat{\mathbf{e}}_3 \times \mathbf{u} + \nabla P\right) = 0 \tag{2.46}$$

Therefore, the dynamics of our Earth model is described by the set of four scalar second-order PDEs, three components(2.44) and a (2.46), along with the corresponding boundary condition (2.43). These PDEs governing the four dependent variables (the three components of $\mathbf{u}$, and the P. For the sake of brevity, we write these dependent variables as the column matrix, $\Psi = [\Psi_1, \Psi_2, \Psi_3, \Psi_4]^T$.

Also, we define coefficient matrices $\mathbf{K}$ and $\mathbf{B}$ to represent three scalar components of PDEs (2.43) and (2.46) and BC (2.43), respectively.

$$\mathbf{K}\Psi = 0 \quad ; \quad \mathbf{B}\Psi = 0 \tag{2.47}$$

It the next chapter we will show that, without involving in the complexity of the real equations, this notation permits us to simply show the basics of the Galerkin method that we use to obtain approximate solutions $\overline{\Psi}$ of PDEs and BCs governing Earth dynamic.

Chapter 3

Galerkin Method and Integration of the Governing Equations

In this chapter we introduce the Galerkin method to numerically solve these PDEs for the normal modes of the Earth. The Galerkin method is the equivalent of the method of variational principles. It is a numerical method for converting a continuous differential equations to a discrete problem and then applying some constraints to characterize the space with a finite set of basis functions.

The formulation we will use in this chapter is pretty much routine and was used by many other authors (see for example Smith, 1974; Rieutord, 1995), however the uniqueness of this study is in the implementation of the Galerkin method for solving the equations.

3.1   Spheroidal and Toroidal Vector Fields

The objectives are this work is to first solve for the eigenfrequencies and the displacement and pressure eigenfunctions of the inertial modes of the rotating fluid body. Mathematically, any continuous function can be represented as an infinite sum of independent terms. For example, Taylor expansion represents a function as an infinite sum of the values that calculated from the derivatives of the function at certain point (Thomas and Finney, 1992). In the spherical coordinate system, it is more convenient to factor dependent variables into a radial (r-dependent part) and a spherical part (depending on θ and ϕ). Solutions of spherical parts can be then written in terms of the spherical harmonics. We also represent the vector displacement, $\mathbf{u}$, by its radial $\hat{\mathbf{r}}$, transverse spheroidal ∇Y_n^m, and toroidal $\mathbf{r} \times \nabla Y_n^m$

components. We will show that this representation allow us to use the properties of the spherical harmonics (section A.1) to separated our vector equation into three linear scalar PDEs. Therefore, non-dimensionalized solutions (displacement vector $\mathbf{u}$ and pressure P) of (2.41) and (2.46) have the form

$$\mathbf{u} = \sum_{n=0}^{\infty} \sum_{m=-n}^{n} \left[\hat{\mathbf{r}} U_n^m(r) + r V_n^m(r) \nabla - W_n^m(r) \mathbf{r} \times \nabla \right] Y_n^m(\theta, \phi) \tag{3.1}$$

and

$$P = \sum_{n=0}^{\infty} \sum_{m=-n}^{n} X_n^m(r) Y_n^m(\theta, \phi), \tag{3.2}$$

where $Y_n^m(\theta, \phi)$ are the spherical harmonics of degree n and azimutal order m. In the spherical polar coordinate, components of $\mathbf{u}$ in (3.1) are

$$
\begin{aligned}
u_r &= \sum_{n=0}^{\infty} \sum_{m=-n}^{n} U_n^m(r) Y_n^m(\theta, \phi) \\
u_\theta &= \sum_{n=0}^{\infty} \sum_{m=-n}^{n} \left[V_n^m(r) \frac{\partial}{\partial \theta} + im \frac{W_n^m(r)}{\sin \theta} \right] Y_n^m(\theta, \phi) \\
u_\phi &= \sum_{n=0}^{\infty} \sum_{m=-n}^{n} \left[im \frac{V_n^m(r)}{\sin \theta} - W_n^m(r) \frac{\partial}{\partial \theta} \right] Y_n^m(\theta, \phi).
\end{aligned}
\tag{3.3}
$$

We can write radial parts of (3.2) and (3.3) in terms of linear combination of Legendre functions of degree l

$$
\begin{aligned}
U_n^m(r) &= \sum_{l=0}^{\infty} U_{n,l}^m P_l(x) \\
V_n^m(r) &= \sum_{l=0}^{\infty} V_{n,l}^m P_l(x) \\
W_n^m(r) &= \sum_{l=0}^{\infty} W_{n,l}^m P_l(x) \\
X_n^m(r) &= \sum_{l=0}^{\infty} X_{n,l}^m P_l(x)
\end{aligned}
\tag{3.4}
$$

in which $U_{n,l}^m$, $V_{n,l}^m$, $W_{n,l}^m$ and $X_{n,l}^m$ are all constants that will be defined by solutions of PDEs. Parameter x is the dimensionless distance that has been modified to satisfy $x \in [-1, +1]$.

Where $x = -1$ corresponds to $r = 0$, and $x = 1$ to $r = R$ [1].

3.2   The Galerkin Method

Assume Ψ to be the exact solutions of the set of PDEs (like (2.47)). In general the Galerkin method indicates that $\overline{\Psi}$ is also the acceptable approximate solution of those equations if for any arbitrary weight function $\phi^\top$, we can write

$$\int \phi^\top \tilde{\mathbf{K}} \overline{\Psi} \, dV = 0, \tag{3.5}$$

We consider $\Phi^\top = \Psi^{*\top} = [\mathbf{u}^*(r, \theta, \phi), P^*(r, \theta, \phi)]^\top$ and define F as,

$$F = \sum_{n,l}^{N,L} \sum_{q,j}^{N,L} \int \Phi^*_{q,j} \tilde{\mathbf{K}} \Psi_{n,l} \, dV, \tag{3.6}$$

where, similar to (3.2) and (3.4), j, q and k indicate radial, spherical and azimuthal parts, respectively. Condition (3.5) requires,

$$\frac{\partial F}{\partial U^*_{q,j}} = 0 \quad ; \quad \frac{\partial F}{\partial V^*_{q,j}} = 0 \quad ; \quad \frac{\partial F}{\partial W^*_{q,j}} = 0 \quad ; \quad \frac{\partial F}{\partial X^*_{q,j}} = 0 \tag{3.7}$$

This condition result in $N \times L$ linear equations for each component, which in total gives $4 \times N \times L$ linear equations that must be solved for $4 \times N \times L$ unknowns.

3.3   Integrational Form of the Governing PDEs

Plugging equations (2.41) and (2.46) into the Galerkin integral, (3.5), we obtain

$$\int \mathbf{u}^* . \left[\sigma^2 \mathbf{u} - i\sigma \hat{\mathbf{e}}_3 \times \mathbf{u} + \nabla P \right] dV = 0 \tag{3.8}$$

---

[1] For each layer, x is defined as $x = (2r - LB - HB)/(HB - LB)$, where LB and HB are lower and higher boundaries of each layer, respectively. For example for innercore with radius of $a = 1221.5$ km, $HB = a$ and $LB = 0$, therefore, $r \in [0, a] \rightarrow x \in [-1, 1]$.

$$\int P^* \nabla. \left(-i\sigma\hat{\mathbf{e}}_3 \times \mathbf{u} + \nabla P \right) dV = 0 \tag{3.9}$$

Now we can apply the divergence theorem on gradient terms to remove derivatives and write (3.8) as

$$\int \left\{ \mathbf{u}^*. \left(\sigma^2\mathbf{u} - i\sigma\hat{\mathbf{e}}_3 \times \mathbf{u} \right) - (\nabla.\mathbf{u}^*)P \right\} dV + \int_S \left\{ \hat{\mathbf{n}}.\mathbf{u}^* P \right\} dS = 0 \tag{3.10}$$

Also, (3.9) can be simplified as

$$\int \nabla P^*. \left(-i\sigma\hat{\mathbf{e}}_3 \times \mathbf{u} + \nabla P \right) dV - \int_S P^*\hat{\mathbf{n}}. \left(-i\sigma\hat{\mathbf{e}}_3 \times \mathbf{u} + \nabla P \right) dS = 0 \tag{3.11}$$

We follow Rochester (lecture notes provided by my supervisor) and write spheroidal and
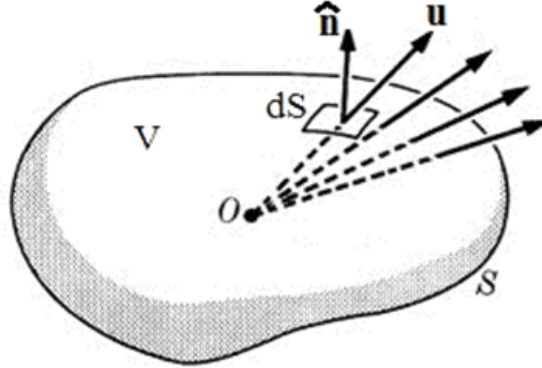
Figure 3.1: Divergence theorem is used in equations (3.10) and (3.11) to reduce the order of the equations by one, and to make impermeability boundary condition to be satisfied naturally.

toroidal components of the $\hat{\mathbf{e}}_3 \times \mathbf{u}$ term in equations (3.10) and (3.11) as

$$\begin{aligned}
\hat{\mathbf{e}}_3 \times \mathbf{u} &= -\sin\theta\, u_\phi \hat{\mathbf{r}} - \cos\theta\, u_\phi \hat{\theta} + (\sin\theta\, u_r + \cos\theta\, u_\theta)\hat{\phi} \\
&= \sum_{n}^{\infty} \sum_{m=-n}^{n} [D_n^m \hat{\mathbf{r}} + rE_n^m \nabla_r - F_n^m \mathbf{r} \times \nabla]Y_n^m,
\end{aligned} \tag{3.12}$$

where

$$D_n^m = -imV_n^m + W_n^m \sin\theta \frac{\partial}{\partial\theta}$$

$$n(n+1)E_n^m = -im(U_n^m + V_n^m) + W_n^m[n(n+1)\cos\theta + \sin\theta\frac{\partial}{\partial\theta}] \tag{3.13}$$

$$n(n+1)F_n^m = [2U_n^m - n(n+1)V_n^m]\cos\theta + (U_n^m - V_n^m)\sin\theta\frac{\partial}{\partial\theta} - imW_n^m$$

In (3.13) we used recurrence relations for spherical harmonic functions and their derivatives section A.1.

Similarly, the term $\nabla.\mathbf{u}^*$ is

$$\nabla.\mathbf{u}^* = \sum_{q}^{\infty} \sum_{k=-q}^{q} \left[\frac{dU_q^k}{dr} + \frac{2U_q^k - q(q+1)V_q^k}{r} \right] Y_q^k \tag{3.14}$$

3.3.1 Implementation of Galerkin method on the equation of motion

Substituting (3.2), (3.3), (3.12) and (3.14) in to the equations (3.10) and (3.11) result in

$$
\begin{aligned}
&\int \sum_n \sum_m \sum_q \sum_k \left\{ \left[U_q^{k*}\hat{\mathbf{r}} + \left(V_q^{k*}\frac{\partial}{\partial\theta} - ik\frac{W_q^{k*}}{\sin\theta} \right)\hat{\theta} - \left(ik\frac{V_q^{k*}}{\sin\theta} + W_q^{k*}\frac{\partial}{\partial\theta} \right)\hat{\phi} \right] Y_q^{k*} \right. \\
&\times \left[\sigma^2 \left[U_n^m Y_n^m \hat{\mathbf{r}} + \left(V_n^m\frac{\partial}{\partial\theta} + im\frac{W_n^m}{\sin\theta} \right)Y_n^m\hat{\theta} + \left(im\frac{V_n^m}{\sin\theta} - W_n^m\frac{\partial}{\partial\theta} \right)Y_n^m\hat{\phi} \right] \right. \\
&\left. - i\sigma \left[D_n^m Y_n^m \hat{\mathbf{r}} + \left((E_n^m\frac{\partial}{\partial\theta} + im\frac{F_n^m}{\sin\theta} \right)Y_n^m\hat{\theta} + \left(im\frac{E_n^m}{\sin\theta} - F_n^m\frac{\partial}{\partial\theta} \right)Y_n^m\hat{\phi} \right] \right. \\
&\left. \left. - \left[\frac{dU_q^{k*}}{dr} + \frac{2U_q^{k*} - q(q+1)V_q^{k*}}{r} \right] Y_q^{k*} \left[X_n^m Y_n^m \right] \right] \right\} dV \tag{3.15} \\
&+ \int_S \sum_n \sum_q \sum_m \left\{ U_q^{k*} Y_q^{k*} \left[X_n^m Y_n^m \right] \right\} dS = 0
\end{aligned}
$$

Expanding (3.15), substituting Y_n^m from (A.10) and integrating over ϕ using (A.12) result in

$$
\begin{aligned}
\int \sum_n \sum_q \sum_m &\left\{ \sigma^2 \left[U_q^{m*} U_n^m P_q^m P_n^m + \left(V_q^{m*} V_n^m + W_q^{m*} W_n^m \right) \left[\frac{\partial P_q^m}{\partial \theta} \frac{\partial P_n^m}{\partial \theta} + \frac{m^2}{\sin^2 \theta} P_q^m P_n^m \right] \right. \right. \\
&\left. + im \left(V_q^{m*} W_n^m - W_q^{m*} V_n^m \right) \left[\frac{P_q^m}{\sin \theta} \frac{\partial P_n^m}{\partial \theta} + \frac{\partial P_q^m}{\partial \theta} \frac{P_n^m}{\sin \theta} \right] \right] \\
&- i\sigma \left[U_q^{m*} D_n^m P_q^m P_n^m + \left(V_q^{m*} E_n^m + W_q^{m*} F_n^m \right) \left[\frac{\partial P_q^m}{\partial \theta} \frac{\partial P_n^m}{\partial \theta} + \frac{m^2}{\sin^2 \theta} P_q^m P_n^m \right] \right. \\
&\left. + im \left(V_q^{m*} F_n^m - W_q^{m*} E_n^m \right) \left[\frac{P_q^m}{\sin \theta} \frac{\partial P_n^m}{\partial \theta} + \frac{\partial P_q^m}{\partial \theta} \frac{P_n^m}{\sin \theta} \right] \right] \\
&\left. - \left[\frac{dU_q^{m*}}{dr} + \frac{2U_q^{m*} - q(q+1)V_q^{m*}}{r} \right] P_q^m \left[X_n^m P_n^m \right] \right\} r^2 dr \, \sin \theta d\theta \\
+ \int_S \sum_n \sum_q \sum_m &\left\{ U_q^{m*} P_q^m X_n^m P_n^m \right\} r^2 \, \sin \theta d\theta = 0
\end{aligned}
$$

$$(3.16)$$

Using recurrence formulas (A.4) and (A.5), equations (3.16) becomes simplified to

$$
\begin{aligned}
\int \sum_n \sum_q \sum_m &\left\{ \sigma^2 \left[U_q^{m*} U_n^m P_q^m P_n^m + \left(V_q^{m*} V_n^m + W_q^{m*} W_n^m \right) n(n+1) P_q^m P_n^m \right] \right. \\
&- i\sigma \left[U_q^{m*} D_n^m P_q^m P_n^m + \left(V_q^{m*} E_n^m + W_q^{m*} F_n^m \right) n(n+1) P_q^m P_n^m \right] \\
&\left. - \left[\frac{dU_q^{m*}}{dr} + \frac{2U_q^{m*} - q(q+1)V_q^{m*}}{r} \right] P_q^m \left[X_n^m P_n^m \right] \right\} r^2 dr \, \sin \theta d\theta \\
+ \int_S \sum_n \sum_q \sum_m &\left\{ U_q^{m*} P_q^m X_n^m P_n^m \right\} r^2 \, \sin \theta d\theta = 0
\end{aligned}
$$

$$(3.17)$$

By rearrangement of the terms in (3.17), we get

$$
\begin{aligned}
\int \sum_n \sum_q \sum_m \Bigg\{ & U_q^{m*} P_q^m \left(\sigma^2 U_n^m P_n^m - i\sigma D_n^m P_n^m \right) - \left[\frac{dU_q^{m*}}{dr} + \frac{2U_q^{m*}}{r} \right] P_q^m X_n^m P_n^m \\
& + V_q^{m*} P_q^m n(n+1) \left(\sigma^2 V_n^m P_n^m - i\sigma E_n^m P_n^m + \frac{X_n^m}{r} P_n^m \right) \\
& + W_q^{m*} P_q^m n(n+1) \left(\sigma^2 W_n^m P_n^m - i\sigma F_n^m P_n^m \right) \Bigg\} r^2 dr \ \sin\theta d\theta \\
& + \int_S \sum_n \sum_q \sum_m \left\{ U_q^{m*} P_q^m X_n^m P_n^m \right\} r^2 \ \sin\theta d\theta = 0
\end{aligned}
\tag{3.18}
$$

Plugging (3.13) into (3.18), the Glerkin integrals of Poincaré equation becomes

$$
\begin{aligned}
\sum_n \sum_q \sum_m \int \Bigg(& U_q^{m*} P_q^m \left[\sigma^2 U_n^m - \sigma m V_n^m - i\sigma W_n^m \sin\theta \frac{\partial}{\partial\theta} \right] P_n^m \\
& - \left[\frac{dU_q^{m*}}{dr} + \frac{2U_q^{m*}}{r} \right] P_q^m X_n^m P_n^m \\
& + V_q^{m*} P_q^m \left[-\sigma m U_n^m P_n^m + V_n^m \left(n(n+1)\sigma^2 - \sigma m \right) P_n^m \right. \\
& + W_n^m \left[n(n+1)\sigma\cos\theta + \sigma\sin\theta \frac{\partial}{\partial\theta} \right] P_n^m + n(n+1)\frac{X_n^m}{r} \Bigg] \\
& + W_q^{m*} P_q^m \left[-U_n^m \left[2\sigma\cos\theta + \sigma\sin\theta \frac{\partial}{\partial\theta} \right] P_n^m \right. \\
& + V_n^m \left[\sigma n(n+1)\cos\theta + \sigma\sin\theta \frac{\partial}{\partial\theta} \right] P_n^m \\
& + W_n^m \left[n(n+1)\sigma^2 - \sigma m \right] P_n^m \Bigg] \Bigg) r^2 dr \ \sin\theta d\theta \\
& + \sum_n \sum_q \sum_m \int_S \left\{ U_q^{m*} P_q^m X_n^m P_n^m \right\} r^2 \ \sin\theta d\theta = 0
\end{aligned}
\tag{3.19}
$$

With the same approach incompressibility condition, (3.11), can be written as

$$
\sum_n \sum_q \sum_m \int \left(\frac{\partial X_q^{m*}}{\partial x} \left[-\sigma m V_n^m - i\sigma W_n^m \sin\theta \frac{\partial}{\partial\theta} + \frac{\partial X_n^m}{\partial r} \right] \right.
$$

$$
+ \frac{X_q^{m*}}{x} \left[-\sigma m U_n^m - \sigma m V_n^m - W_n^m \left(-n(n+1)\sigma\cos\theta - \sigma\sin\theta\frac{\partial}{\partial\theta} \right) \right.
$$

$$
\left. \left. + n(n+1)\frac{X_n^m}{x} \right] \right) P_n^m P_q^m \ r^2 dr \ \sin\theta d\theta \tag{3.20}
$$

$$
- \sum_n \sum_q \sum_m \int_S \left\{ U_q^{m*} P_q^m \left[-\sigma m V_n^m - i\sigma W_n^m \sin\theta\frac{\partial}{\partial\theta} + \frac{\partial X_n^m}{\partial r} P_n^m \right] \right\} r^2 \ \sin\theta d\theta = 0
$$

where, as we mentioned before, $Y_n^m(\theta,\phi)$ are the spherical harmonics of degree n and order m, and $U_n^m(r)$, $V_n^m(r)$, $W_n^m(r)$, and $X_n^m(r)$ are functions of r only. Because of the symmetry around $\hat{\mathbf{e}}_3$ it can be seen that in (3.19) and (3.20), equations with different order m are decoupled, While, rotation causes terms of degree n to form a coupled chain (appears in the form of sin and cos functions).

Invoking the linear independence of the P_n^m and use of (3.7) condition in the next chapter we will introduce numerical method to solve PDEs (3.19) and (3.20).

3.4 Implementation of Boundary Conditions

Integral equations (3.19) and (3.20) are linear PDEs that governing Earth's normal modes. Complete solution of these PDEs requires adding the boundary conditions to the integrals, both at the inner-core boundary (ICB) and core-mantle boundary(CMB).

3.4.1 Regularity of dependent variables at $\mathbf{r} = 0$

To guarantee that the solutions are finite at $r = 0$ we follow Seyed-Mahmoud (Seyed-Mahmoud et al., 2015) and make derivatives of radial terms (Legendre expansions) to van-

ish at the center of the Earth. Suppose in general we have such an expression.

$$F(x) = \sum_n c_n P_n(x) = \sum_n c_n P_n(x) = c_0 + c_1 r + c_2 P_2(x) + \cdots + c_N P_N(x) \qquad (3.21)$$

where $x \in [-1, +1]$ and c_n are constants. We set $P_0(x) = 1$ and $P_1(x) = x$. The boundary condition at $r = 0$ requires.

$$F'(x) = c_1 + c_2 P_2'(x) + \cdots + c_N P_N'(x) = 0$$
$$\therefore \quad c_1 = -c_2 P_2'(x) - \cdots - c_N P_N'(x) \qquad (3.22)$$

Substituting (3.22) into (3.21) result in

$$F(x) = c_0 + \left(-c_2 P_2'(r) - \cdots - c_N P_N'(r) \right) r + c_2 P_2(r) + \cdots + c_N P_N$$
$$= c_0 + \sum_{n=2} c_n \left(P_n(r) - r P_n'(r) \right) \qquad (3.23)$$

Using (3.23) in a spherical container, grantees that our results will remain finite in the limit of $r \to 0$.

3.4.2 At solid-fluid boundary

Both at the ICB and CMB, shear stress vanishes due to fluidity of the outer core. The normal displacement, normal component of the stress, gravitational potential perturbation and its gradient are continuous. Therefore implementing the Galerkins' method on BCs from section 2.4 result is following boundary equations

$$\Delta(\hat{\mathbf{n}}.\mathbf{u}) = 0$$
$$\therefore \quad \int_S \sum_n \sum_q \sum_m U_q^{m*} P_q^m \left(U_n^m P_n^m \Big|_- - U_n^m P_n^m \Big|_+ \right) r^2 \sin\theta \, d\theta = 0 \qquad (3.24)$$

Where $-$ and $+$ refer to upper part and lower part of the boundaries, respectively.

Chapter 4

Numerical integration of the PDEs

In this chapter, we describe the method that we use to integrate the Galerkin equations we derived in chapter 3. We first, validate our numerical method by computing the eigenfrequencies and the eigenfunctions of an incompressible, homogeneous fluid which completely fills a rotating spherical cavity which described by so-called Poincaré equation (2.44) and the accompanying impermeability boundary condition (2.45) for which analytical solutions exists. We show that the computed frequencies (given to 3 decimal points) and the pattern of the eigenfunctions are identical to their analytically computed counterparts. In subsection 4.2.2, our numerical result for frequencies and displacement eigenvectors and pressure eigenvalues of the inertial modes of spherical shell container with rigid boundaries are given.

4.1   Coefficient Matrix

We are interested to study the normal modes of the Earth with azimuthal order of 0 and 1 which are associated with Earth's length of day and wobble/nutation modes, respectively. We consider finite number of basis functions for integration but increase the number as appropriate to make sure the results are converged. We set L truncation for radial and N for azimuthal expansions and apply the Galerkin method. L and N are then increased independently until convergence is achieved. The equations (3.19) and (3.20) form a $(4NL \times 4NL)$

matrix, by setting the trial functions, (3.4) as

$$
\begin{aligned}
U(r) &= \sum_{n=1}^{N} U_n^m(r) = \sum_{n=1}^{N} \left(\sum_{l=1}^{L} U_{n,l}^m \, P_l(x) \right) Y_n^m = \sum_{n=1}^{N} \sum_{l=1}^{L} a_{L(n-1)+l} P_l(x) Y_n^m(\theta, \phi) \\
V(r) &= \sum_{n=1}^{N} V_n^m(r) = \sum_{n=1}^{N} \left(\sum_{l=1}^{L} V_{n,l}^m \, P_l(x) \right) Y_n^m = \sum_{n=1}^{N} \sum_{l=1}^{L} a_{L(N+n-1)+l} P_l(x) Y_n^m(\theta, \phi) \\
W(r) &= \sum_{n=1}^{N} W_n^m(r) = \sum_{n=1}^{N} \left(\sum_{l=1}^{L} W_{n,l}^m \, P_l(x) \right) Y_n^m = \sum_{n=1}^{N} \sum_{l=1}^{L} a_{L(2N+n-1)+l} P_l(x) Y_n^m(\theta, \phi) \\
X(r) &= \sum_{n=1}^{N} X_n^m(r) = \sum_{n=1}^{N} \left(\sum_{l=1}^{L} X_{n,l}^m \, P_l(x) \right) Y_n^m = \sum_{n=1}^{N} \sum_{l=1}^{L} a_{L(3N+n-1)+l} P_l(x) Y_n^m(\theta, \phi)
\end{aligned}
\tag{4.1}
$$

where m is either 0 or 1.

4.1.1 Integration with respect to θ

We take advantage of the orthogonality property of the associated Legendre polynomials in which $\int P_n^m(x) P_q^m(x) \, dx \propto \delta_{n,q}$. Using following relations, we can simplify integration over θ.

$$
\cos\theta P_n^m = \frac{n+m}{2n+1} P_{n-1}^m + \frac{n-m+1}{2n+1} P_{n+1}^m
\tag{4.2}
$$

$$
\sin\theta \frac{\partial P_n^m}{\partial \theta} = \frac{n(n-m+1)}{2n+1} P_{n+1}^m - \frac{(n+1)(n+m)}{2n+1} P_{n-1}^m
\tag{4.3}
$$

$$
P_2 P_n^m = \frac{3}{2} \frac{(n+m)(n+m-1)}{(2n+1)(2n-1)} P_{n-2}^m + \frac{n(n+1)-3m^2}{(2n+3)(2n-1)} P_n^m + \frac{3}{2} \frac{(n+2-m)(n-m+1)}{(2n+1)(2n+3)} P_{n+2}^m
\tag{4.4}
$$

$$P_2 \cos\theta P_n^m = \frac{3(n+m)(n+m-1)(n+m-2)}{2(2n+1)(2n-1)(2n-3)} P_{n-3}^m$$
$$+ \left[\frac{3(n+m)(n+m-1)(n-m-1)}{2(2n+1)(2n-1)(2n-3)} + \frac{(n(n+1)-3m^2)(n+m)}{(2n+3)(2n-1)(2n+1)} \right] P_{n-1}^m$$
$$+ \left[\frac{(n(n+1)-3m^2)(n-m+1)}{(2n+3)(2n-1)(2n+1)} + \frac{3(n+2-m)(n-m+1)(n+m+2)}{2(2n+1)(2n+3)(2n+5)} \right] P_{n+1}^m$$
$$+ \frac{3(n+2-m)(n-m+1)(n-m+3)}{2(2n+1)(2n+3)(2n+5)} P_{n+3}^m$$

$$(4.5)$$

$$P_2 \sin\theta \frac{\partial P_n^m}{\partial\theta} = -\frac{(n+1)(n+m)}{2n+1} \frac{3}{2} \frac{(n+m-1)(n+m-2)}{(2n-1)(2n-3)} P_{n-3}^m$$
$$+ \left[-\frac{(n+1)(n+m)}{2n+1} \frac{(n-1)(n)-3m^2}{(2n-1)(2n-3)} + \frac{n(n-m+1)}{2n+1} \frac{3}{2} \frac{(n+m+1)(n+m)}{(2n+3)(2n+1)} \right] P_{n-1}^m$$
$$+ \left[-\frac{(n+1)(n+m)}{2n+1} \frac{3}{2} \frac{(n-m-1)(n-m)}{(2n-1)(2n+1)} + \frac{n(n-m+1)}{2n+1} \frac{(n+1)(n+2)-3m^2}{(2n+5)(2n+1)} \right] P_{n+1}^m$$
$$+ \frac{n(n-m+1)}{2n+1} \frac{3}{2} \frac{(n-m+1)(n-m+2)}{(2n+3)(2n+5)} P_{n+3}^m$$

$$(4.6)$$

$$P_2^1 \frac{\partial P_n^m}{\partial\theta} = \frac{3(n+1)(n+m)(n+m-1)}{(2n+1)(2n-1)} P_{n-2}^m + \frac{3n(n+1)-9m^2}{(2n+3)(2n-1)} P_n^m$$
$$- \frac{3n(n+2-m)(n-m+1)}{(2n+1)(2n+3)} P_{n+2}^m$$

$$(4.7)$$

We developed FORTRAN subroutines to integrate the equations with respect to θ.

4.1.2 Integration with respect to *r*

We use FORTRAN subroutine from Numerical Precipices (see Seyed-Mahmoud, 1994) to produce Legendre polynomials and their derivatives as a trial function for *r* dependency. Next, we use the orthogonality properties to simplify the integrals. Finally, we use *IMSL* (IMSL, 1989) subroutine to integrate equations with respect to *r*.

4.2   Eigenfrequencies and Eigenfunctions of the Normal Modes

Once we integrate over volume and surface boundaries of the Earth, we have 4*NL* linear equations in 4*NL* unknowns. This system of equations can be presented in matrix form as

a $4NL \times 4NL$ matrix of coefficients governing $4NL$ variables, $a_{n,l}$,

$$
\begin{matrix}
U_{1,1} & U_{1,2} & \cdots & U_{1,L} & U_{2,1} & \cdots & U_{N,L} & V_{1,1} & \cdots & V_{N,L} \cdots & X_{N,L}
\end{matrix}
$$

$$
\begin{pmatrix}
 & & & & & & & & \\
 & & & & & & & & \\
 & & & & & & & & \\
 & & & \text{(3.19)} & - & \text{(3.20)} & & & \\
 & & & & & & & & \\
 & & & & & & & & \\
 & & & & & & & & \\
 & & & & & & & &
\end{pmatrix}
\begin{pmatrix}
a_1 \\
a_2 \\
\vdots \\
a_L \\
a_{L+1} \\
\vdots \\
a_{NL} \\
a_{NL+1} \\
\vdots \\
a_{2NL} \\
\vdots \\
a_{4NL}
\end{pmatrix}
= 0
$$

The eigenfrequencies of the Earth's inertial modes are the eigenvalues of this matrix (σ), which correspond to the zeros of the determinant. N_{min} and L_{min} are minimum numbers of iterations required for converged results in radial and azimuthal terms, respectively. Using (3.2) and (3.3), we calculate the displacement eigenvectors, **u**, and eigenvalues of pressure, P and compare them with those for a fluid sphere for which analytical solutions exists.

4.2.1 Norman Modes of the Poincaré Earth Model

In the first stage, we check the validity of our numerical approach, by computing some of the low order ($m = 0$ and $m = 1$) inertial modes of the Poincaré Earth model for a spherical container. We check the convergence of the results by using different number of terms L_{min} and N_{min}. The criteria we use to check the convergence of the frequencies is that, for

a given N_{min}, we increase L_{min} until the modal *frequency* of interest shows convergence (do not change by increasing N and L). We then fix L_{min} and increase N_{min} till the value of a *frequency* reconverges. Such a stable frequency (for any $N > N_{min}$ and $L > L_{min}$) is identified temporarily as a modal frequency. We will then plot the displacement patterns to make sure that the identified frequency indeed corresponds to a model frequency.

We search the entire range of frequencies, $-1 < \sigma < 1$, (for $m = 0$ and $m = 1$ modes) for full-spherical Earth model. We use increment of 10^{-5} to minimize the possibility of over stepping a frequency. To present the modes, we use the same notation that was defined by Greenspan (1968) in which for the (n, k, m) mode, n and m refer to the degree (meridional) and the order (azimuthal) dependence, respectively, and $k = 1, \ldots, n - |m|$. Because of the truncation, we expect a number of spurious frequencies to appear in the computed frequency spectrum, arising from zeros of the determinant of the coefficients matrix.

In Table 4.1 the non-dimensional eigenfrequencies that we calculated for a spherical model are given. The frequencies obtained using our model converged, to 3 decimal points, to the exact analytic solutions of Poincaré equations and displacement patterns of the identified modes are identical to those of the Poincaré model. This indicates the reliability of our numerical approach.

4.2.2 Normal Modes of the Uniformly Rotating Spherical Fluid Shell

We now use our approach to calculate the normal modes of the uniformly rotating incompressible fluid contained within a rigid spherical shell proportional to the Earth's fluid core. Note that, unlike the spherical case, no general analytical solutions exist for the inertial modes of a fluid shell of zero viscosity. This is due to the hyperbolic nature of the Poincaré equation, (Rieutord, 1997).

We use the same criteria described in previous section, and search in the range of $\sigma \in (-1, 1)$ for modal frequencies of the spherical shell. We expect that these frequencies are in the vicinity of the frequencies of the spherical model. Table 4.2 shows some of the

Table 4.1: Convergence pattern for some of the frequencies with $m = 1$ modes. The exact frequencies for the Poincaré model are shown in column 2.

Mode	Poincaré	(N=4, L=6)	(N=4, L=7)	σ (N=4, L=8)	(N=5, L=7)	(N=5, L=8)
(2,1,1)	0.500	0.500	0.500	0.500	0.500	0.500
(3,1,1)	-0.088	-0.088	-0.088	-0.088	-0.088	-0.088
(3,2,1)	0.755	0.755	0.755	0.755	0.755	0.755
(4,1,1)	-0.410	-0.410	-0.410	-0.410	-0.410	-0.410
(4,2,1)	0.306	0.306	0.306	0.306	0.306	0.306
(4,3,1)	0.854	0.854	0.854	0.854	0.854	0.854
(5,1,1)	-0.592	–	–	–	-0.592	-0.592
(5,2,1)	-0.034	-0.052	-0.052	-0.053	-0.034	-0.034
(5,3,1)	0.523	0.521	0.529	0.534	0.523	0.523
(5,4,1)	0.903	0.884	0.893	0.900	0.903	0.903
(6,1,1)	-0.702	–	–	-0.688	-0.702	-0.702
(6,2,1)	-0.269	–	–	-0.262	-0.269	-0.269
(6,3,1)	0.220	–	–	0.282	0.220	0.220
(6,4,1)	0.653	–	–	0.587	0.653	0.653
(6,5,1)	0.931	–	–	0.941	0.931	0.931

frequencies we have computed for a spherical shell model for the $m = 0$ and $m = 1$ modes. The counterpart frequencies for the Poincaré model is also shown in the table (column 3).

Seyed-Mahmoud et al., (2006, 2007) used the so-called 3PD approach (Seyed-Mahmoud, 1994) to compute the frequencies of the rotating compressible and stratified fluid spherical shell with rigid boundaries. The authors could not get the converged frequencies for some of the modes and they reported the range of fluctuations (in the third decimal place) about respective mean frequencies. The authors also could not get converged frequencies for some other modes, for example (3,1,1), (3,2,1), (4,1,1), (5,1,1), (5,2,1), (5,3,1) and (5,4,1) modes.

The 3PD equations contain the Poincaré operator, therefore the ill-poseness of the problem may still manifest itself in their approach. This is probably the reason that authors did not get convergence results for some of the modes. They argue that because of the geometry of the displacement eigenfunctions of these modes near inner core boundary, they may

Table 4.2: Some frequencies of the wavenumbers $m = 0$ and $m = 1$ inertial modes of a uniformly rotating spherical shell models. The exact frequencies for the Poincaré model is also shown in column 3.

Mode	σ_{shell}	$\sigma_{Poincare}$	Mode	σ_{shell}	$\sigma_{Poincare}$
(3,1,0)	0.456	0.447	(4,2,1)	0.303	0.306
(4,1,0)	0.663	0.655	(4,3,1)	0.860	0.854
(5,2,0)	0.750	0.765	(5,1,1)	-0.586	-0.592
(6,2,0)	0.842	0.830	(5,2,1)	0.024	0.034
(2,1,1)	0.500	0.500	(5,3,1)	0.571	0.523
(3,1,1)	-0.068	-0.088	(5,4,1)	0.916	0.903
(3,2,1)	0.673	0.755	(6.1.1)	-0.696	-0.702
(4,1,1)	-0.402	-0.410			

Table 4.3: The convergence pattern for the frequency of the (7,5,1) mode of a spherical fluid shell

L_{min}	$\sigma(N_{min} = 8)$	N_{min}	$\sigma(L_{min} = 14)$
10	0.743	8	0.743
11	0.743	9	0.744
12	0.743	10	0.745
14	0.743	10	0.744
16	0.744	12	0.744
18	0.744	13	0.744

not satisfy boundary conditions. Therefore, they concluded that these modes may not have counterparts in the spherical shell.

Our results show that many of these frequencies indeed converge and the displacement vectors curve near the ICB to satisfy the BC there. Tables 4.3 and 4.4 show the convergence pattern for (7,5,1) and (5,4,1) modes. Notice that these mode were considered as non converged modes by Seyed-Mahmoud et al., (2006 ; 2007).

In Figures 4.1 we plotted the displacement eigenvectors, **u**, and pressure eigenfunction contours, P, for the (4,2,1) mode of a full sphere and spherical shell model. The displacement patterns calculated in meridional plane, $\phi = 0$, and plotted using *TecPlot* 10.0 Software. In the pressure contours, red indicate the higher pressure and blue is the indicator of the lower pressure.

Table 4.4: The convergence pattern for the frequency of the (5,4,1) mode of a spherical fluid shell

L_{min}	$\sigma(N_{min}=8)$	N_{min}	$\sigma(L_{min}=14)$
10	0.940	7	0.934
11	0.940	8	0.941
12	0.940	9	0.940
13	0.940	10	0.940
14	0.940	11	0.940

The displacement vectors in a sphere are not nearly parallel to the inner core boundary, where the inner core boundary would be in a shell. The displacement patterns (position and orientation of the cells) is regular and imitate the displacement pattern of (4,2,1) mode of the Poincaré model.

In figure 4.2, we show the meridional displacement vectors and the pressure eigenfunction contours for some the wave numbers $m = 0$ and $m = 1$, inertial modes of a full-sphere(left) and their counterparts for a spherical shell (right).
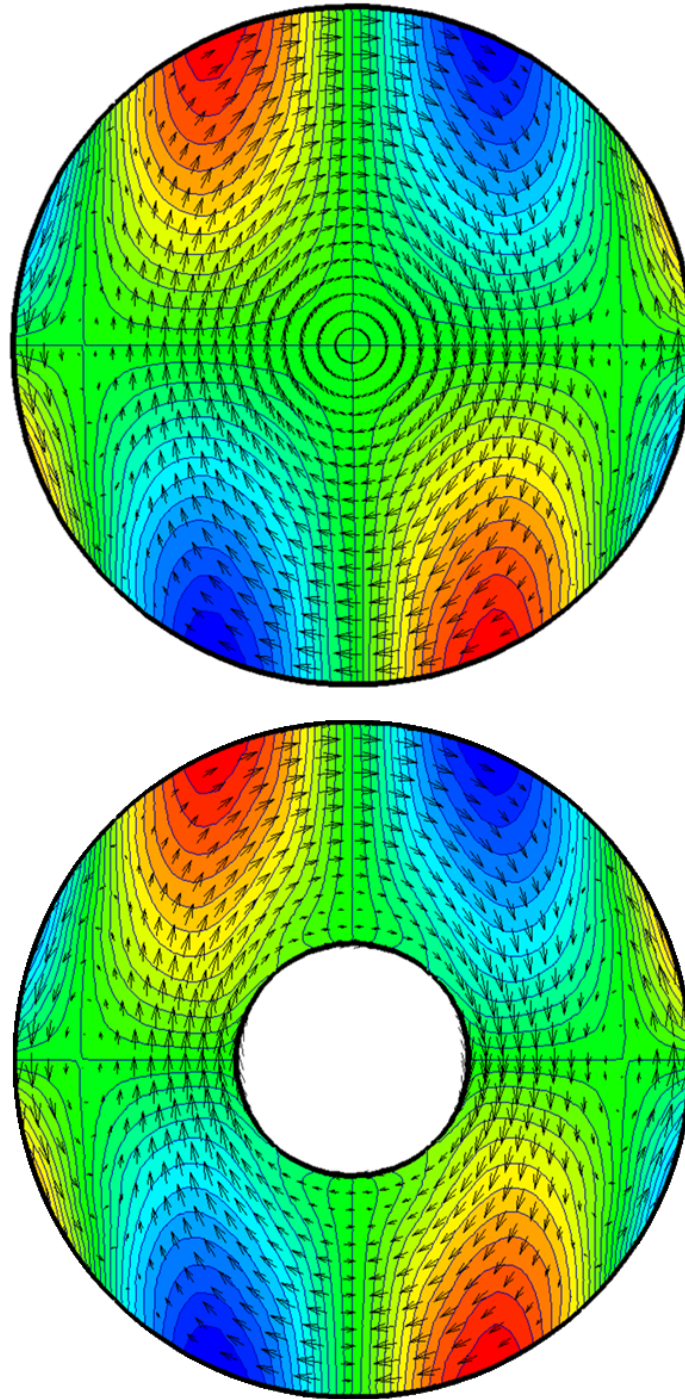
Figure 4.1: The displacement eigenvectors **u** in a meridional plane, $\phi = 0$, for the (4,2,1) mode of rotating incompressible fluid in the full-sphere and spherical shell container with rigid boundaries. The non-dimensional pressure eigenfunctions are superimposed as contours. Note that the displacement patterns for this mode in the shell they rearrange themselves to satisfy the impermeability BC.
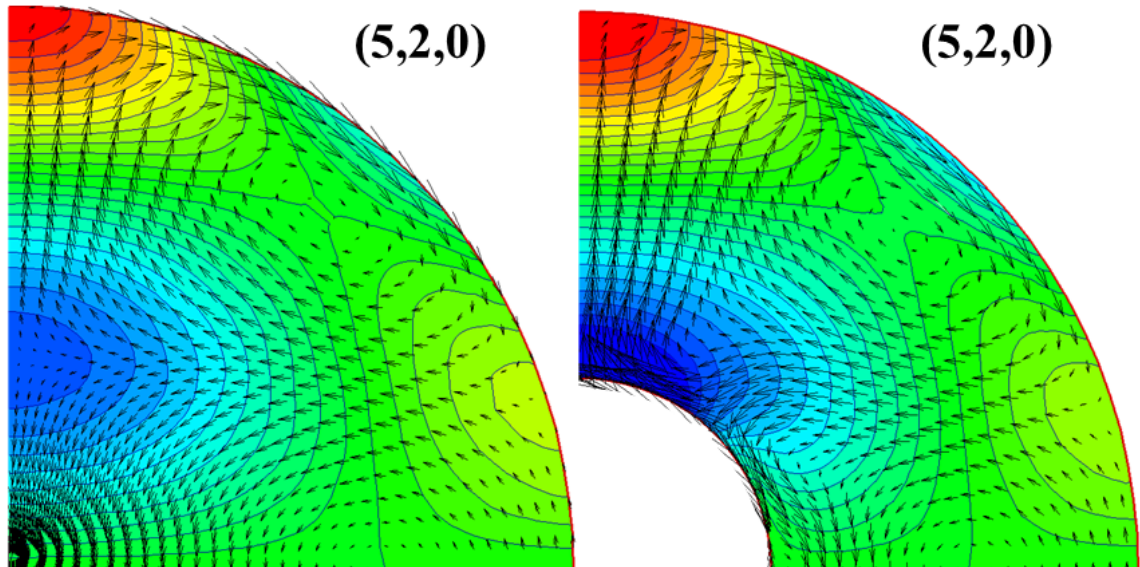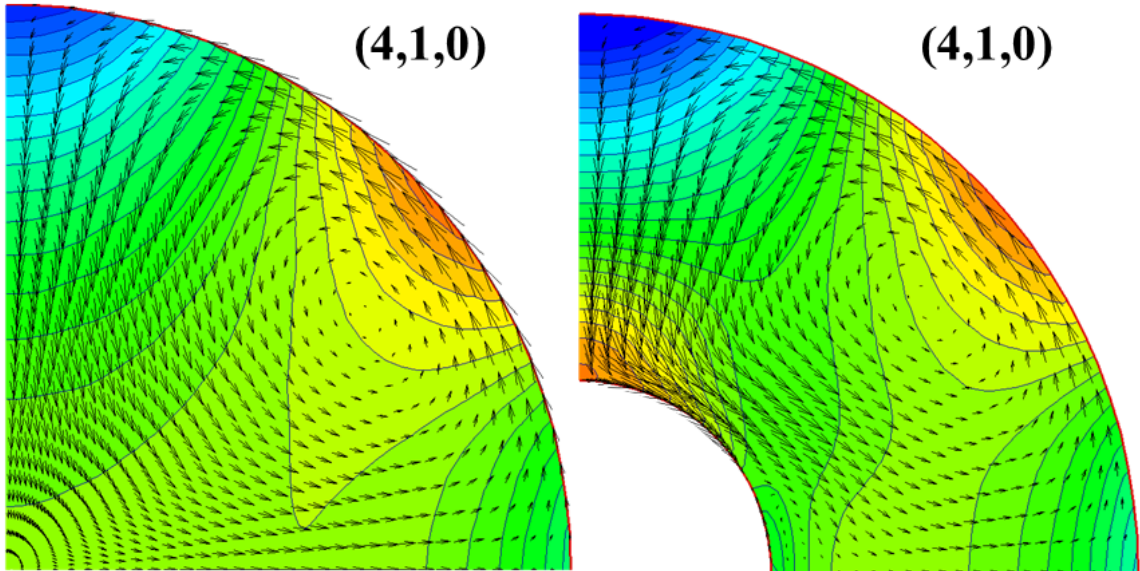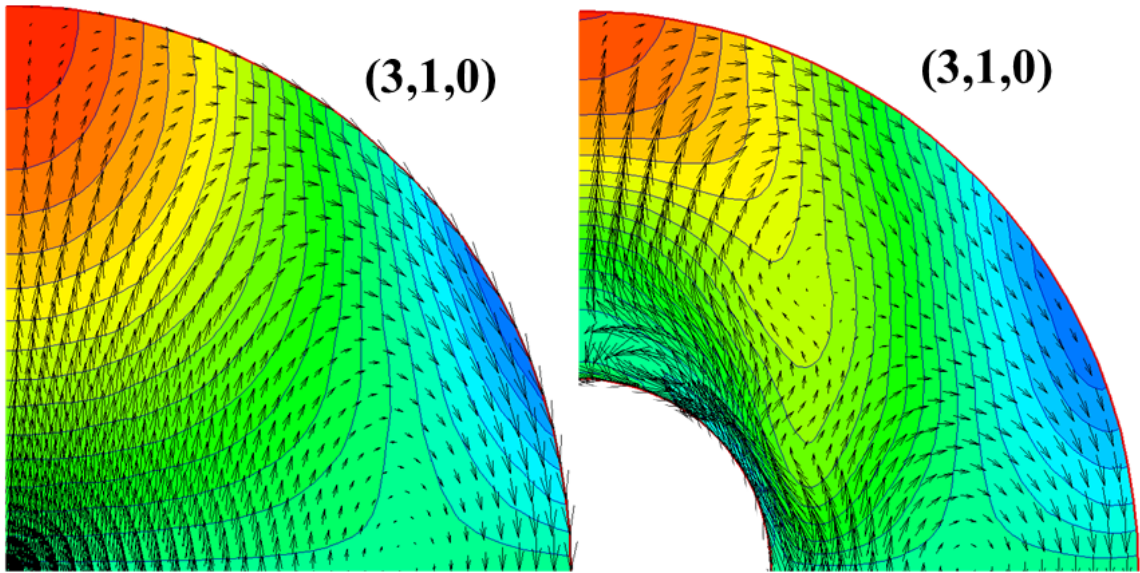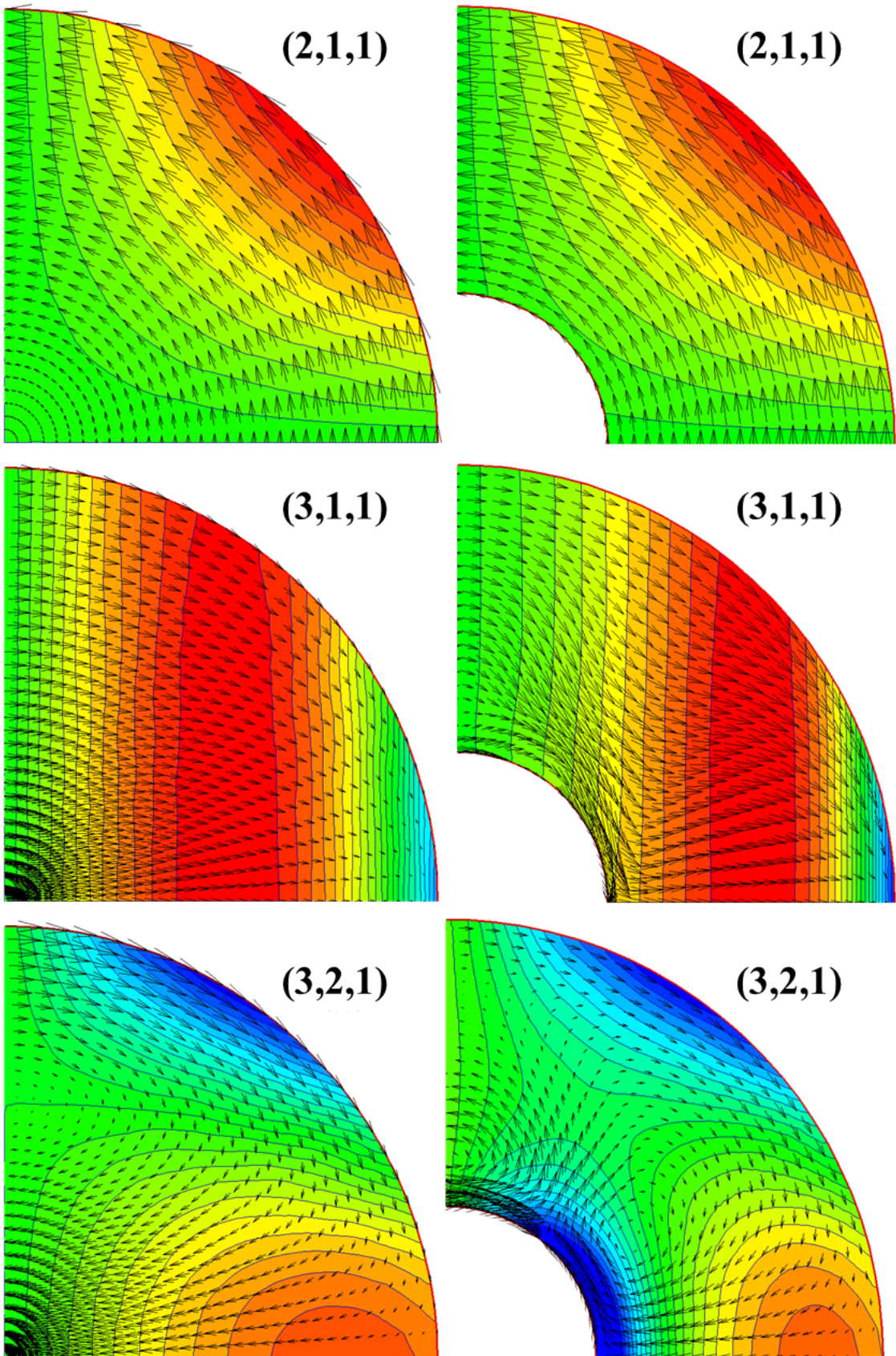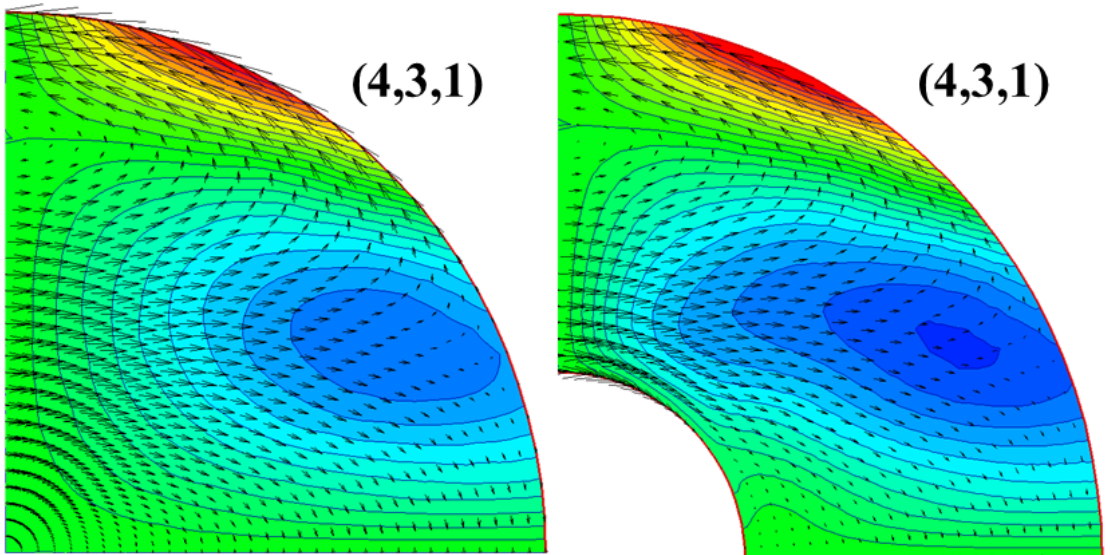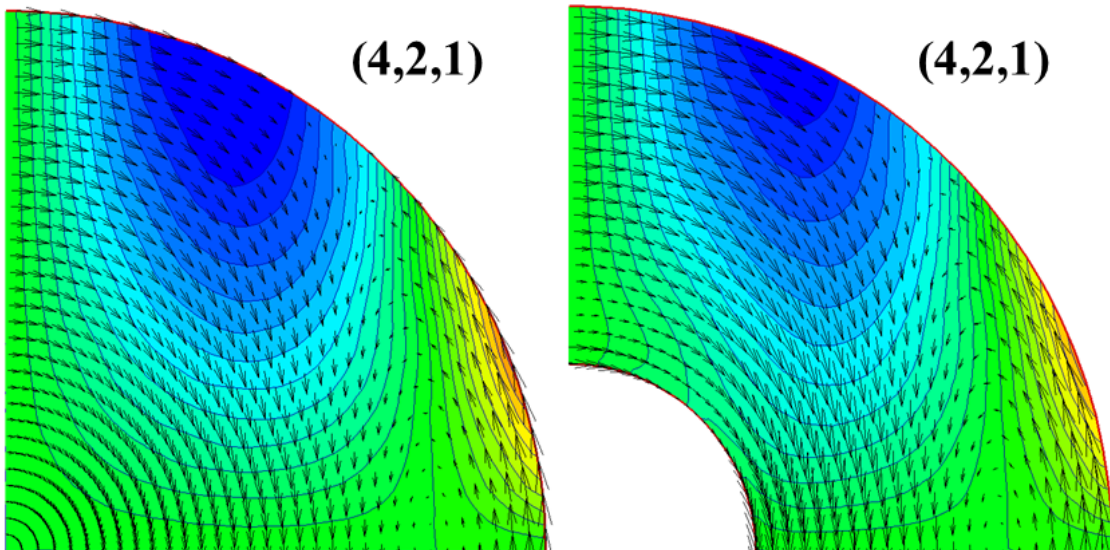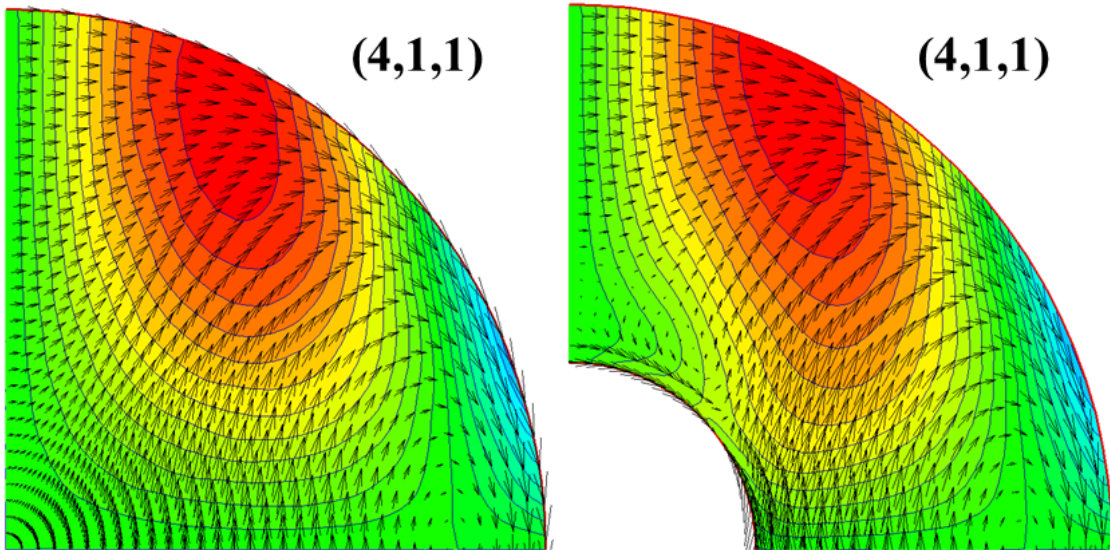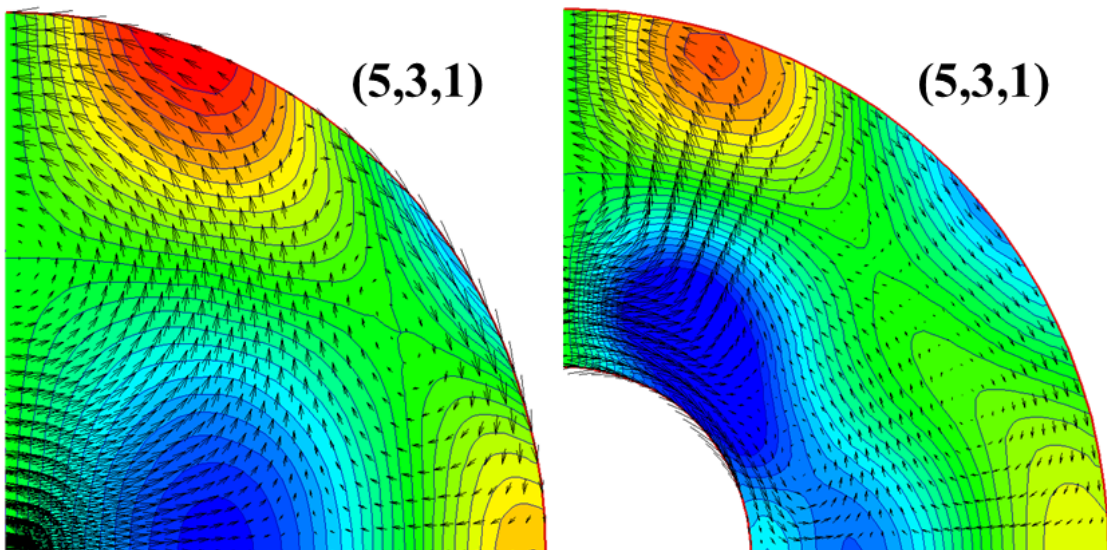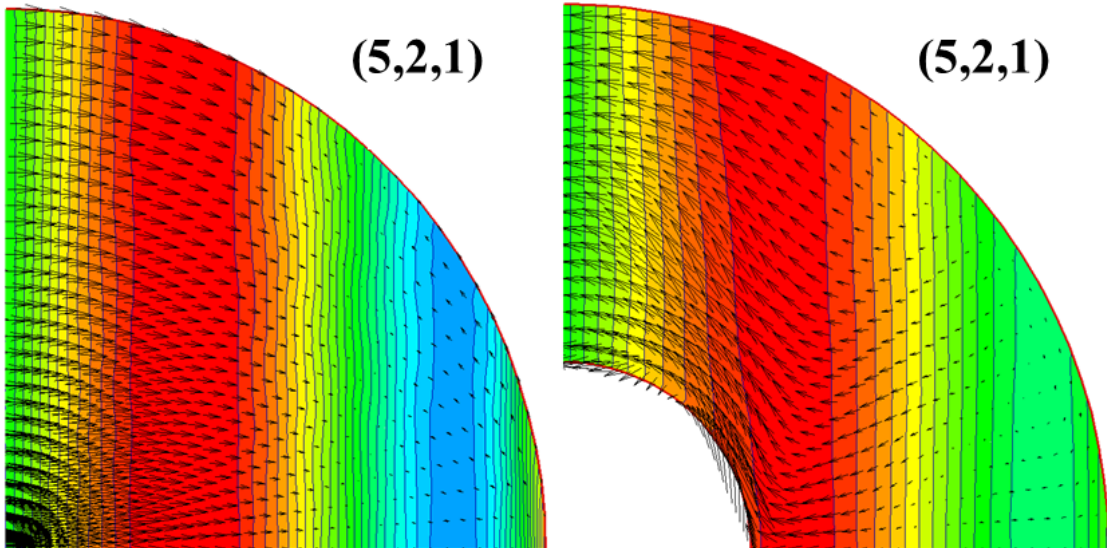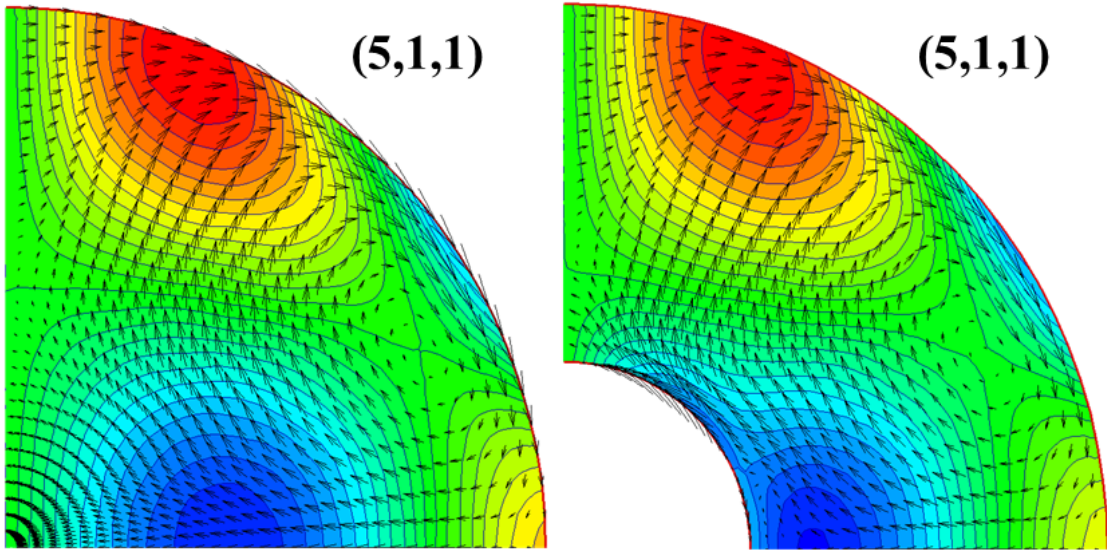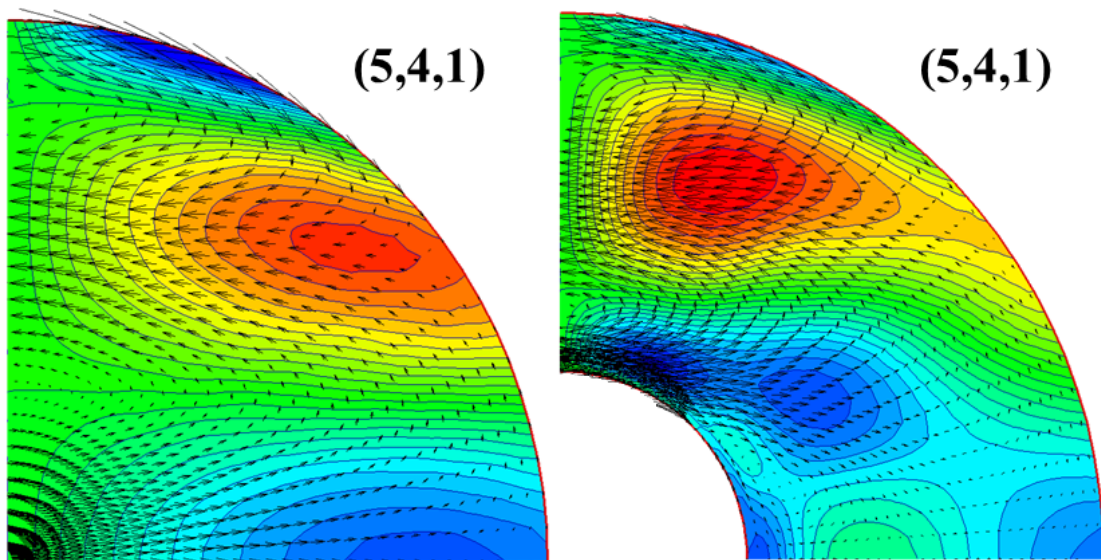
Figure 4.2: The displacement eigenvectors **u** in a meridional plane, $\phi = 0$, for some of the low order, azimuthal wavenumbers, $m = 0$ and $m = 1$, of rotating incompressible fluid in the full-sphere and spherical shell containers with rigid boundaries. non-dimensional pressure eigenfunctions are superimposed as contours. Note that in both we have numerically solved the momentum and the continuity equations for both geometries. The displacement patterns for a sphere are identical to those for a Poincaré model and those for a shell closely match those of a sphere.

Chapter 5

PDEs Governing the Free Oscillations of a Compressible Earth Model

In this chapter, we follow the methodology we explained in chapter 3 and chapter 4, to compute the eigenfrequencies and eigenfunctions of a compressible, stratified fluid which completely fills a rotating spherical cavity (described by set of equations (2.28) and (2.31)).

5.1   Galerkin Formulation of the Momentum Equation

We assume that non-dimensionalized solutions (displacement vector $\mathbf{u}$ and perturbation in the gravitational potential V_1) of the equations (2.28) and (2.31) are (3.4) and (3.2), respectively, except in (3.2) P is replaced by V_1. The terms $\hat{\mathbf{e}}_3 \times \mathbf{u}$ and $\nabla.\mathbf{u}$ in the equation (2.28) were derived as (3.12) and (3.14), respectively. For a rotating Earth, the non-dimensionalized gravity, $\mathbf{g}_0$ is a result of (dimensionless) gravitational and centrifugal accelerations and is define as (Rochester and Crossley, 2009).

$$\mathbf{g}_0 = \nabla(V_0 + \frac{1}{2}|\hat{\mathbf{e}}_3 \times \mathbf{r}|^2) = \left[-g_0(r) + \frac{2}{3}r\right]\hat{\mathbf{r}}, \tag{5.1}$$

where $g_0 = -\nabla V_0 = GM(r)/r^2$, is dimensionless gravitational acceleration[1]. Using (5.1), the fourth and fifth terms in the LHS of (2.28) can be combined as

$$\nabla_x(V_1 + u.\mathbf{g}_0) = \sum\sum\left[G_n^m\hat{\mathbf{r}} + rH_n^m\nabla\right]Y_n^m. \tag{5.2}$$

---

[1]The parameters g_0, G, ρ and M are non-dimensionalized as $G = G/\Omega^2$, $g_0 = g_0/(r\Omega^2)$, $\rho = \rho/<\rho>$ and $M = M/(r^3 <\rho>)$, respectively.

in which G_n^m and H_n^m are

$$G_n^m = \frac{\partial X_n^m}{\partial r} - \frac{\partial U_n^m}{\partial r} g_0 + U_n^m \frac{2g_0}{r} - 4\pi G \rho_0 U_n^m + \frac{2}{3} r \frac{\partial U_n^m}{\partial r} + \frac{2}{3} U_n^m$$

$$H_n^m = \frac{1}{r} \left(X_n^m - U_n^m g_0 + \frac{2}{3} U_n^m r \right)$$

(5.3)

where we used the conservation of the gravitational flux on V_0. The term $\nabla.\tilde{\mathbf{S}}$ in (2.28) is given by (2.11). In the Earth's fluid core $\beta = 0$ and thus (2.11) reduces to

$$\frac{1}{\rho_0} \nabla_x.\tilde{\mathbf{S}} = \frac{1}{\rho_0} \nabla.\left[\rho_0 \alpha^2 (\nabla.u) \, \tilde{\mathbf{1}} \right] = \frac{1}{\rho_0} \nabla \left[\rho_0 \alpha^2 (\nabla.u) \right] = \frac{1}{\rho_0} \frac{d\rho}{dr} \alpha^2 \left[\frac{dU_n^m}{dr} \right.$$

$$\left. + \frac{2U_n^m - n(n+1)V_n^m}{r} \right] Y_n^m \hat{\mathbf{r}} + \nabla \left[\alpha^2 \left[\frac{dU_n^m}{dr} + \frac{2U_n^m - n(n+1)V_n^m}{r} \right] Y_n^m \right].$$

(5.4)

Substituting the terms (3.12), (3.14), (5.2) and (5.4), into the (2.28) and plugging into the Galerkin integral, (3.5), and using divergence theorem, we get

$$\int \sum_n \sum_q \sum_k \left\{ \left[U_q^{k*} \hat{\mathbf{r}} + \left(V_q^{k*} \frac{\partial}{\partial \theta} - ik \frac{W_q^{k*}}{\sin\theta} \right) \hat{\theta} + \left(-ik \frac{V_q^{k*}}{\sin\theta} - W_q^{k*} \frac{\partial}{\partial \theta} \right) \hat{\phi} \right] Y_q^{k*} . \right.$$

$$\left[\sigma^2 \left[U_n^m \hat{\mathbf{r}} + \left(V_n^m \frac{\partial}{\partial \theta} + im \frac{W_n^m}{\sin\theta} \right) \hat{\theta} + \left(im \frac{V_n^m}{\sin\theta} - W_n^m \frac{\partial}{\partial \theta} \right) \hat{\phi} \right] Y_n^m \right.$$

$$- 2i\sigma \left[D_n^m Y_n^m \hat{\mathbf{r}} + \left(E_n^m \frac{\partial}{\partial \theta} + im \frac{F_n^m}{\sin\theta} \right) Y_n^m \hat{\theta} + \left(im \frac{E_n^m}{\sin\theta} - F_n^m \frac{\partial}{\partial \theta} \right) Y_n^m \hat{\phi} \right]$$

$$+ \left[g_0(r) - \frac{2}{3} r + \frac{1}{\rho_0} \frac{d\rho}{dr} (\alpha^2 - 2\beta^2) \right] \left[\frac{dU_n^m}{dr} + \frac{2U_n^m - n(n+1)V_n^m}{r} \right] Y_n^m \hat{\mathbf{r}}$$

$$\left. + \left[A_n^m Y_n^m \hat{\mathbf{r}} + \left(B_n^m \frac{\partial}{\partial \theta} + im \frac{C_n^m}{\sin\theta} \right) Y_n^m \hat{\theta} + \left(im \frac{B_n^m}{\sin\theta} - C_n^m \frac{\partial}{\partial \theta} \right) Y_n^m \hat{\phi} \right] \right]$$

$$- \left[\frac{dU_q^{k*}}{dr} + \frac{2U_q^{k*} - q(q+1)V_q^{k*}}{r} \right] Y_q^{k*} \left[\left[X_n^m - g_0 U_n^m + \frac{2}{3} r U_n^m \right] Y_n^m \right.$$

$$\left. + (\alpha^2 - 2\beta^2) \left[\frac{dU_n^m}{dr} + \frac{2U_n^m - n(n+1)V_n^m}{r} \right] Y_n^m \right] \right\} dV + \int_S \sum_n \sum_q \left\{ U_q^{k*} Y_q^{k*} \right.$$

$$\left[X_n^m - g_0 U_n^m + \frac{2}{3} r U_n^m + (\alpha^2 - 2\beta^2) \left[\frac{dU_n^m}{dr} + \frac{2U_n^m - n(n+1)V_n^m}{r} \right] \right] Y_n^m \right\} dS = 0$$

(5.5)

Recall that the equations with different order m are decoupled, and hence we dropped the summation over m. By substituting Y_n^m from (A.10), integrating over ϕ, rearranging, using recurrence formulas (A.4) and (A.5), and finally implementing (3.7); (5.5) is simplified into the following three linear integral equations

$$
\begin{aligned}
\sum_n \sum_q \int & \left\{ U_q^{m*} P_q^m \left(\sigma^2 U_n^m P_n^m - 2\sigma m V_n^m P_n^m + 2\sigma W_n^m \sin\theta \frac{\partial}{\partial\theta} P_n^m + \left[g_0(r) - \frac{2}{3}r \right. \right. \right. \\
& + \frac{1}{\rho_0} \frac{d\rho}{dr} \alpha^2 \left] \left[\frac{dU_n^m}{dr} + \frac{2U_n^m - n(n+1)V_n^m}{r} \right] P_n^m \right) - \left[\frac{dU_q^{m*}}{dr} + \frac{2U_q^{m*}}{r} \right] P_q^m \left[\left[X_n^m \right. \right. \right. \\
& - g_0 U_n^m + \frac{2}{3} r U_n^m \left] P_n^m + \alpha^2 \left[\frac{dU_n^m}{dr} + \frac{2U_n^m - n(n+1)V_n^m}{r} \right] P_n^m \right] \right\} r^2 dr \, \sin\theta d\theta \\
& + \int_S U_q^{m*} P_q^m \left[X_n^m - \left(g_0 - \frac{2r}{3} \right) U_n^m + \alpha^2 \left[\frac{dU_n^m}{dr} + \frac{2U_n^m - n(n+1)V_n^m}{r} \right] \right] P_n^m \right\} dS = 0
\end{aligned}
\tag{5.6}
$$

$$
\begin{aligned}
\int \sum_n \sum_q V_q^{m*} P_q^m & \left\{ \left(\sigma^2 n(n+1) V_n^m - 2\sigma m U_n^m - 2\sigma m V_n^m + 2\sigma W_n^m n(n+1) \cos\theta \right) P_n^m \right. \\
& + 2\sigma W_n^m \sin\theta \frac{\partial P_n^m}{\partial\theta} + n(n+1) \left[\frac{X_n^m}{r} - g_0 \frac{U_n^m}{r} + \frac{2}{3} U_n^m \right] P_n^m \\
& + n(n+1) \frac{\alpha^2}{r} \left[\frac{dU_n^m}{dr} + \frac{2U_n^m - n(n+1)V_n^m}{r} \right] P_n^m \right\} r^2 dr \, \sin\theta d\theta = 0
\end{aligned}
\tag{5.7}
$$

and,

$$
\begin{aligned}
\sum_n \sum_q \int W_q^{m*} P_q^m & \left\{ n(n+1)\sigma^2 W_n^m P_n^m - 2\sigma \left[2U_n^m - n(n+1)V_n^m \right] \cos\theta P_n^m \right. \\
& - 2i\sigma(U_n^m - V_n^m) \sin\theta \frac{\partial}{\partial\theta} P_n^m - 2\sigma m W_n^m P_n^m \right\} r^2 dr \, \sin\theta d\theta = 0.
\end{aligned}
\tag{5.8}
$$

In (5.6)-(5.8), we apply π degree phase shift to the variables W_n^m and W_q^m as $W_n^m \to -iW_n^m$ and $W_q^{m*} \to +iW_q^{m*}$. This phase shift make all variables to be real.

5.2 Galerkin Formulation of the Poisson's Equation

Applying the Galerkin method and the divergence theorem on the scalar equation (2.31)), and then using (A.10), (A.12), (A.4) and (A.5) to integrate over ϕ we get

$$
\begin{aligned}
\int \sum_n \sum_q &\left\{ \frac{\partial X_q^{m*}}{\partial r} \frac{\partial X_n^m}{\partial r} P_q^m P_n^m + \frac{n(n+1)}{r^2} X_q^{m*} X_n^m P_q^m P_n^m \right. \\
&\left. - 4\pi G \rho_0 \frac{\partial X_q^{m*}}{\partial r} U_n^m P_q^m P_n^m - 4\pi G \rho_0 \frac{n(n+1)}{r} X_q^{m*} V_n^m P_q^m P_n^m \right\} r^2 \, dr \, \sin\theta d\theta \qquad (5.9) \\
&- \int_S \sum_n \sum_q X_q^{m*} P_q^m \left(\frac{\partial X_n^m}{\partial r} P_n^m - 4\pi G \rho_0 U_n^m P_n^m \right) r^2 \, \sin\theta d\theta = 0
\end{aligned}
$$

Integral equations (5.6)-(5.8), and (5.9) are four linear PDEs that governing normal modes of stratified fluid core. Complete solution of these PDEs requires adding appropriate boundary conditions to the integrals.

5.3 The Governing Boundary Conditions

In addition to the boundary conditions we derived for incompressible fluid in section 3.4, compressibility imposes additional boundary conditions as following. Both in the ICB and CMB, the shear stress vanishes. The normal displacement, normal stress, gravitational potential perturbation and its gradient are continuous. Therefore implementing the Galerkins's method on BCs from section 2.4 result into the following boundary equations

$$
(\hat{\mathbf{n}}.\mathbf{u}) = 0 \ \therefore \ \int_S \sum_n \sum_q U_q^{m*} P_q^m \left(U_n^m P_n^m \Big|_S \right) r^2 \sin\theta \, d\theta = 0 \qquad (5.10)
$$

Where S refer to *ICB* and *CMB*. Outside the fluid core the perturbation in gravitational potential, V_1, must satisfy Laplace's equation [1] and remain finite when $r \to \infty$. General solutions for Laplace's equation in spherical coordinate can be written in terms of the spherical

---

[1] Outside of the fluid core in the rigid mantle, there is no change in the density and, therefore, Poission's equation, (2.30), reduces to Laplace's equation.

harmonics as

$$V_1(r > R) = \sum_{n=0}^{\infty} \frac{a_n^m}{r^{n+1}} Y_n^m(\theta, \phi) \tag{5.11}$$

At the surface of the Earth, $r = R$, both V_1 and $\hat{\mathbf{n}}.\nabla V_1$ should be continues. Thus from (3.2) and (A.13) for continuity of V_1 we can write,

$$\sum_{n=0}^{\infty} X_n^m(R) Y_n^m(\theta, \phi) = \sum_{n=0}^{\infty} \frac{a_n^m}{R^{n+1}} Y_n^m(\theta, \phi) \tag{5.12}$$

Continuity of $\hat{\mathbf{r}}.\nabla V_1$ requires that

$$\sum_{n=0}^{\infty} X_n^m(R)' Y_n^m(\theta, \phi) = \sum_{n=0}^{\infty} -(n+1) \frac{a_n^m}{R^{n+2}} Y_n^m(\theta, \phi) \tag{5.13}$$

where $X_n^m(R)'$ denotes to $\left. \dfrac{dX_n^m(r)}{dr} \right|_R$. Finally, combining (5.12) and (5.13), and using orthogonality properties of spherical harmonics we get the final boundary condition for V_1.

$$\sum_{n=0}^{\infty} \left[\frac{dX_n^m}{dr} + n(n+1) \frac{X_n^m}{r} \right]_{r=R} Y_n^m = 0 \tag{5.14}$$

Note the equation (5.14) is written entirely in terms of the variables inside the fluid core. Applying Galerkin's method, equation (5.14) gives the BC for V_1 on the surface of the Earth as

$$\int_S \sum_n \sum_q X_q^{m*} P_q^m \left(\frac{dX_n^m}{dr} + n(n+1) \frac{X_n^m}{r} \right) P_n^m r^2 \sin\theta \, d\theta = 0 \tag{5.15}$$

5.4 Removing Surface Integrals from Galerkin Integrals

We use the same weight functions for boundary equations that we used for governing PDEs. Better to say: using (5.6) and (5.9), (5.10)-(5.14) are written as:

$$
\begin{aligned}
&\sum_n \sum_q \int \left\{ U_q^{m*} P_q^m \left(\sigma^2 U_n^m P_n^m - 2\sigma m V_n^m P_n^m + 2\sigma W_n^m \sin\theta \frac{\partial}{\partial\theta} P_n^m \right. \right. \\
&+ \frac{2\beta^2}{\rho_0} \frac{d\rho}{dr} \frac{dU_n^m}{dr} P_n^m + 4\beta \frac{d\beta}{dr} \frac{dU_n^m}{dr} P_n^m + 2\beta^2 \frac{d^2 U_n^m}{dr^2} P_n^m \\
&- n(n+1)\frac{\beta^2}{r}\left[\frac{dV_n^m}{dr} + \frac{1}{r}\left(U_n^m - 3V_n^m\right)\right]P_n^m + \frac{4\beta^2}{r}\left[\frac{dU_n^m}{dr} - \frac{U_n^m}{r}\right]P_n^m \\
&+ \left[g_0(r) - \frac{2}{3}r + \frac{1}{\rho_0}\frac{d\rho}{dr}(\alpha^2 - 2\beta^2)\right]\left[\frac{dU_n^m}{dr} + \frac{2U_n^m - n(n+1)V_n^m}{r}\right]P_n^m \right) \\
&- \left[\frac{dU_q^{m*}}{dr} + \frac{2U_q^{m*}}{r}\right]P_q^m \left[\left[X_n^m - g_0 U_n^m + \frac{2}{3}rU_n^m\right]P_n^m + (\alpha^2 - 2\beta^2)\left[\frac{dU_n^m}{dr}\right.\right. \\
&\left.\left.+ \frac{2U_n^m - n(n+1)V_n^m}{r}\right]P_n^m \right] \right\} r^2 dr \, \sin\theta d\theta + \int_S U_q^{m*} P_q^m \left[X_n^m \right. \\
&\left.\left. - g_0 U_n^m + \frac{2}{3}rU_n^m + (\alpha^2 - 2\beta^2)\left[\frac{dU_n^m}{dr} + \frac{2U_n^m - n(n+1)V_n^m}{r}\right]\right]P_n^m\right\} r^2 \, \sin\theta d\theta = 0
\end{aligned}
\tag{5.16}
$$

$$
\begin{aligned}
&\int \sum_n \sum_q \left(V_q^{m*} P_q^m \left\{ \sigma^2 n(n+1)V_n^m - 2\sigma m U_n)^m - 2\sigma m V_n^m + 2\sigma W_n^m n(n+1)\cos\theta \right) P_n^m \right. \\
&+ 2\sigma W_n^m \sin\theta \frac{\partial P_n^m}{\partial\theta} + n(n+1)\frac{1}{\rho_0}\frac{d\rho}{dr}\beta^2\left[\frac{dV_n^m}{dr} + \frac{U_n^m - V_n^m}{r}\right]P_n^m \\
&+ n(n+1)\beta^2 \frac{d}{dr}\left(\frac{dV_n^m}{dr} + \frac{U_n^m - V_n^m}{r}\right)P_n^m + 2n(n+1)\beta\frac{d\beta}{dr}\left(\frac{dV_n^m}{dr} + \frac{U_n^m - V_n^m}{r}\right)P_n^m \\
&+ n(n+1)\frac{3\beta^2}{r}\left[\frac{dV_n^m}{dr} + \frac{U_n^m - V_n^m}{r}\right]P_n^m + n(n+1)\frac{2\beta^2}{r^2}\left[U_n^m - \left(n(n+1)-1\right)V_n^m\right]P_n^m \\
&+ n(n+1)\left[\frac{X_n^m}{r} - g_0\frac{U_n^m}{r} + \frac{2}{3}U_n^m\right]P_n^m + n(n+1)\frac{(\alpha^2 - 2\beta^2)}{r}\left[\frac{dU_n^m}{dr} + \frac{2U_n^m - n(n+1)V_n^m}{r}\right]P_n^m \\
&\left. \right\} r^2 dr \, \sin\theta d\theta = 0
\end{aligned}
\tag{5.17}
$$

$$\int \sum_n \sum_q W_q^{m*} P_q^m \left\{ n(n+1)\sigma^2 W_n^m P_n^m - 2\sigma \left[2U_n^m - n(n+1)V_n^m \right] \cos\theta P_n^m \right.$$

$$- 2i\sigma(U_n^m - V_n^m)\sin\theta \frac{\partial}{\partial\theta} P_n^m - 2\sigma m W_n^m P_n^m + n(n+1)\frac{1}{\rho_0}\frac{d\rho}{dr}\beta^2 \left[\frac{dW_n^m}{dr} - \frac{W_n^m}{r} \right] P_n^m$$

$$+ 2n(n+1)\beta\frac{d\beta}{dr}\left(\frac{dW_n^m}{dr} - \frac{W_n^m}{r} \right)P_n^m + n(n+1)\beta^2\frac{d}{dr}\left(\frac{dW_n^m}{dr} - \frac{W_n^m}{r} \right)P_n^m$$

$$\left. + n(n+1)\frac{3\beta^2}{r}\left[\frac{dW_n^m}{dr} - \frac{W_n^m}{r} \right]P_n^m - n(n+1)\frac{\beta^2}{r^2}\left[n(n+1) - 2 \right]W_n^m P_n^m \right\} r^2 dr \, \sin\theta d\theta = 0$$

$$(5.18)$$

$$\int \sum_n \sum_q \left\{ \frac{\partial X_q^{m*}}{\partial r}\frac{\partial X_n^m}{\partial r}P_q^m P_n^m + \frac{n(n+1)}{r^2}X_q^{m*}X_n^m P_q^m P_n^m \right.$$

$$\left. - 4\pi G\rho_0 \frac{\partial X_q^{m*}}{\partial r}U_n^m P_q^m P_n^m - 4\pi G\rho_0 \frac{n(n+1)}{r}X_q^{m*}V_n^m P_q^m P_n^m \right\} r^2 \, dr \, \sin\theta d\theta \quad (5.19)$$

$$- \int_S \sum_n \sum_q X_q^{m*}P_q^m \left(\frac{\partial X_n^m}{\partial r}P_n^m - 4\pi G\rho_0 U_n^m P_n^m \right) \, r^2 \, \sin\theta d\theta = 0$$

Note that in (5.16) and (5.19) surface integrals are evaluated using the material properties corresponding to the associated side of the boundary.

5.5 Material Properties of the Earth Model

In this thesis the material properties and position of the boundaries are taken from the Preliminary Reference Earth Model (PREM). PREM is a spherical non-rotating Earth model that first constructed by Dziewonski and Anderson (1981), by inverting a huge amount of the seismological data (including the speed of body waves and frequencies of normal modes). PREM satisfies the fundamental properties of the Earth such as the mean radios, $R = 6371$ km and the average mass, $M = 5.974 \times 10^{24}4$ kg. In PREM the Earth is divided into the 13 concentric spherical layers, and the material properties (density and speed of the P and S waves) in each layer are functions of radius (which are represented by polynomials).

For the case of spherical fluid core, when the IC is ignored, we modify the density profile to satisfy a specified stratification. the core properties ρ and α are modified as necessary

Table 5.1: Convergence pattern for some of the frequencies with $m = 1$ modes for stratified earth model. Values in the brackets are the number of truncations (N, L). The exact frequencies for the Poincaré model are shown in column 2. The non-dimensionalized eigenfrequencies of the neutrally stratified fluid core model obtained using 3PD (Seyed-Mahmoud, 2007) are shown in column 3 (we refer them as SM).

					σ			
Mode	Poincaré	SM	(4,7)	(4,8)	(6,9)	(6,11)	(8,11)	(8,13)
(2,1,1)	0.500	0.500	0.500	0.500	0.500	0.500	0.500	0.500
(3,1,1)	-0.088	–	-0.080	-0.115	-0.113	0.112	0.112	0.112
(3,2,1)	0.755	0.748	–	0.751	0.753	0.754	0.752	0.753
(4,1,1)	-0.410	–	–	-0.438	-0.436	-0.439	0.432	-0.432
(4,2,1)	0.306	0.310		–	0.320	0.320	0.319	0.319
(4,3,1)	0.854	0.849	0.826	0.843	0.852	0.853	0.853	0.853
(5,1,1)	-0.592	-0.598	-0.611	-0.613	-0.616	-0.608	-0.609	-0.609
(5,2,1)	-0.034	–	-0.050	-0.051	-0.061	-0.530	-0.053	-0.053
(5,3,1)	0.523	–	0.532	0.531	0.535	0.531	0.531	0.531
(5,4,1)	0.903	0.928	0.906	0.903	0.906	0.904	0.904	0.904

Seyed-Mahmoud (1994).

5.6 Numerical Integration of the PDEs

We follow the same steps we introduced in section 4.1to form the coefficients matrix, and solve for eigenfrequencies and displacement eigenvectors of stratified core Model.

In Table 5.1 the non-dimensional eigenfrequencies of stratified Earth model are given. We could get converged results for all the modes that we searched for them. However, for stratified model convergence requires more number of terms in the iteration chain than for the Poincaré model. The frequencies obtained using our model are converging to the values in the vicinity of the analytic solutions of the Poincaré equation, and displacement patterns of the identified modes are match to those of the Poincaré model (see Figure A.1). In Table 5.1 (column 3) we also show the numerical results for neutrally stratified fluid core obtained by Seyed-Mahmoud (2007) using 3PD.

From the results it can be seen that all the models show similar trend. For instance in all compared models (2,1,1) mode is not affected by stratification, while (4,2,1) mode has

largest deviation from Poincaré model. This result shows that the effects of the density stratification is most likely related to the displacement eigenfunctions of the modes. For (2,1,1) mode the flow is solenoidal then the frequency of the mode is not affected by density stratification. The modes that displacement goes through the center of the Earth in Poincaré model are influenced more by the density stratification.

Chapter 6

Governing Equations of an Elliptical Earth Model

In the chapter 2 PDEs governing free oscillations of the spherically symmetric Earth model were given. In chapter 3 and chapter 5, we introduced a Galerkin method to integrate these equations numerically for an incompressible and a compressible spherical models, respectively. In this chapter, we expand these PDEs to take into account the effects of ellipticity. We will then use a non-orthogonal (Clairaut) coordinate system to reduce the effects of the derivatives of the material properties which are poorly constrained in existing Earth models.

6.1   Clairaut Coordinate System

To introduce the effects of ellipticity of the Earth in our governing PDEs (2.28) and (2.31), we consider the surface of the reference (hydrostatic equilibrium) Earth model to be an oblate spheroid with a small deviation from spherical Earth. Therefore, we can use a first order theory to described this surface as,

$$r = r_0 \left[1 - \frac{2}{3} \varepsilon(r_0) P_2(\cos \theta_0) \right] \tag{6.1}$$

where ε is the *ellipticity* of the spheroid and r_0, is mean (equivoluminal) radius of this surface. $P_2(\cos)$ is second degree Legendre polynomial (Roberts, 1963; Rochester and Crossley, 2009; Rochester et al., 2014).
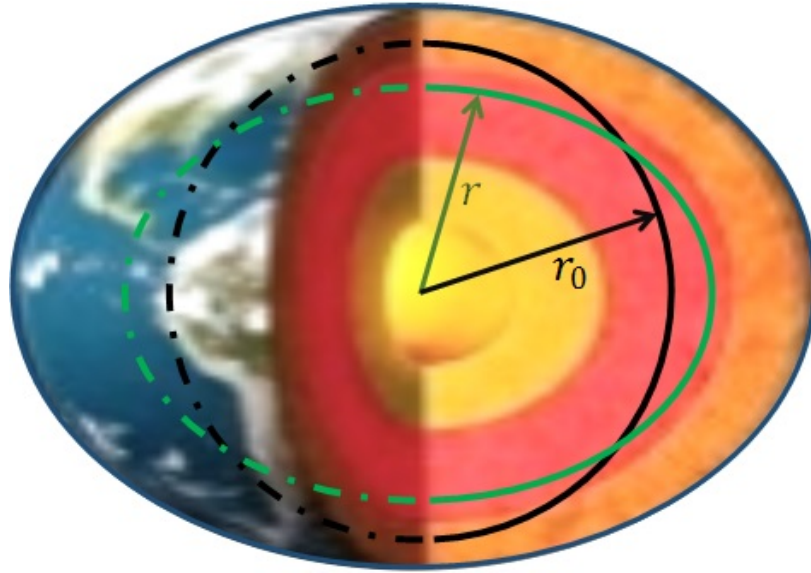
Figure 6.1: Cross sectional area bounded by an equipotential surface of the (a) elliptical Earth model with radius r described by eq. (6.1) and (b) equivoluminetric spherical Earth model with radius r_0.

We use the Clairaut coordinate system in which we adopt r_0, the mean radius of isopycnics, as a radial coordinate in the hydrostatic Earth model. Then, to first order in ellipticity the following transformation rules are used to convert any function from spherical coordinate (r, θ, ϕ) to Clairaut coordinates (r_0, θ_0, ϕ).

$$r = r_0 \left[1 - \frac{2}{3}\varepsilon P_2 \right]$$

$$\hat{\mathbf{n}} = \hat{\mathbf{r}} + \frac{2}{3}\varepsilon P_2^1 \hat{\theta}$$

$$\frac{1}{r} = \frac{1}{r_0} \left[1 + \frac{2}{3}\varepsilon P_2 \right]$$

$$\theta = \theta_0$$

$$\frac{\partial}{\partial \theta_0} = \frac{2}{3} r_0 \varepsilon P_2^1 \frac{\partial}{\partial r_0} + \frac{\partial}{\partial \theta_0}$$

$$dV = r_0^2 \left[1 - \frac{2}{3}(3\varepsilon + r_0 \varepsilon') P_2 \right] dr_0 \, \sin\theta_0 \, d\theta_0 \, d\phi$$

$$\frac{\partial}{\partial r} = \left[1 + \frac{2}{3}(\varepsilon + r_0 \varepsilon') P_2 \right] \frac{\partial}{\partial r_0}$$

$$\frac{\partial^2}{\partial r^2} = \left[\frac{4}{3}\varepsilon' P_2 \frac{\partial}{\partial r_0} + \left[1 + \frac{4}{3}(\varepsilon + r_0 \varepsilon') P_2 \right] \frac{\partial^2}{\partial r_0^2} \right]$$

$$\frac{1}{r}dV = \left[1 - \frac{2}{3}(2\epsilon + r_0\epsilon')P_2\right]r_0 \, dr_0 \, \sin\theta_0 d\theta_0 \, d\phi$$

$$\frac{1}{r^2}dV = \left[1 - \frac{2}{3}(\epsilon + r_0\epsilon')P_2\right] dr_0 \, \sin\theta_0 d\theta_0 \, d\phi$$

$$\frac{dr_0}{dr}dV = \left[1 - \frac{4}{3}\epsilon P_2\right]r_0^2 \, dr_0 \, \sin\theta_0 d\theta_0 \, d\phi \qquad (6.2)$$

$$\left(\frac{dr_0}{dr}\right)^2 dV = r_0^2\left[1 - \frac{2}{3}(\epsilon - r_0\epsilon')P_2\right] dr_0 \, \sin\theta_0 d\theta_0 \, d\phi$$

$$\frac{1}{r}\frac{dr_0}{dr}dV = \left[1 - \frac{2}{3}\epsilon P_2\right]r_0 \, dr_0 \, \sin\theta_0 d\theta_0 \, d\phi$$

Where ϵ' is derivative of ellipticity, $\epsilon(r_0)$, with respect to the r_0, mean radius of equipotential surface, and $P_2^1 = dP_2/d\theta_0$.

Implementing the above-mentioned transformations, the governing PDEs for spherical Earth model, transform to the elliptical Earth model.

6.2   PDEs Governing the Free Oscillations of an Elliptical Earth Model

We use the Galerkin method in a same way that we used in chapter 3 to solve the governing PDEs of rotating spherical Earth model, PDEs (2.28) and (2.31), and BCs section 2.4. Material properties still given by PREM as a function of r_0. Also, we expand field variables, three components of $\mathbf{u}$ and a V_1, as functions of r_0 exactly as before,

$$\mathbf{u} = \sum_{n=0}^{\infty}\left[\hat{\mathbf{r}}U_n^m(r_0) + r_0V_n^m(r_0)\nabla - W_n^m(r_0)r_0\hat{\mathbf{r}}\times\nabla\right]Y_n^m(\theta_0,\phi), \qquad (6.3)$$

$$V_1 = \sum_{n=0}^{\infty}X_n^m(r_0)Y_n^m(\theta_0,\phi). \qquad (6.4)$$

Similar to (3.8) and (3.9), application of the Galerkin method on the governing PDEs and using divergance theorem result in

$$
\int \left\{ \mathbf{u}^* \cdot \left(\sigma^2 \mathbf{u} - 2i\sigma \hat{\mathbf{e}}_3 \times \mathbf{u} - \mathbf{g}_0 (\nabla . \mathbf{u}) + (\alpha^2 - 2\beta^2)(\nabla . \mathbf{u}) \frac{1}{\rho_0} \frac{d\rho_0}{dr} \hat{\mathbf{r}} + \frac{1}{\rho_0} \nabla . \left[2\rho_0 \beta^2 \, \mathbf{e} \right] \right) \right.
$$

$$
\left. - (\nabla . \mathbf{u}^*) \left(V_1 + \mathbf{u} . \mathbf{g}_0 + (\alpha^2 - 2\beta^2) \nabla . \mathbf{u} \right) \right\} dV
$$

$$
+ \int_S \left\{ \hat{\mathbf{n}} . \mathbf{u}^* \left(V_1 + \mathbf{u} . \mathbf{g}_0 + (\alpha^2 - 2\beta^2)(\nabla . \mathbf{u}) \right) \right\} dS = 0
$$

$$(6.5)$$

$$
\int \nabla V_1^* . \left(\nabla V_1 - 4\pi G \rho_0 \mathbf{u} \right) dV - \int_S V_1^* \left(\hat{\mathbf{n}} . \nabla V_1 - 4\pi G \rho_0 \hat{\mathbf{n}} . \mathbf{u} \right) dS = 0 \qquad (6.6)
$$

All quantities in the (6.5) and (6.6), evaluated at elliptical surface r. Unit normal vector to this surface to first order in ellipticity is $\hat{\mathbf{n}} = \dfrac{\nabla r_0}{|\nabla r_0|} = \hat{\mathbf{r}} + \dfrac{2}{3} \varepsilon P_2^1 \hat{\theta}$. Using (6.2), we proceed to replace these terms by quantities evaluated at r_0.

6.3 Equation of Motion in the Clairaut Coordinate System

With the same approach explained in chapter 4, we expand the terms in the equations (6.5) in terms or radial and polar parts and are mapped to Clairaut coordinate system using (6.2). Term $\hat{\mathbf{e}}_3 \times \mathbf{u}$ is described by (3.12) in which D_n^m, E_n^m and F_n^m are calculated in new coordinate system as

$$
D_n^m = - im V_n^m + W_n^m \sin \theta_0 \left[\frac{2}{3} r_0 \varepsilon P_2^1 \frac{\partial}{\partial r_0} + \frac{\partial}{\partial \theta_0} \right]
$$

$$
n(n+1) E_n^m = - im (U_n^m + V_n^m)
$$

$$
+ W_n^m \left[n(n+1) \cos \theta_0 + \sin \theta_0 \left[\frac{2}{3} r_0 \varepsilon P_2^1 \frac{\partial}{\partial r_0} + \frac{\partial}{\partial \theta_0} \right] \right] \qquad (6.7)
$$

$$
n(n+1) F_n^m = \left[2 U_n^m - n(n+1) V_n^m \right] \cos \theta_0
$$

$$
+ (U_n^m - V_n^m) \sin \theta_0 \left[\frac{2}{3} r_0 \varepsilon P_2^1 \frac{\partial}{\partial r_0} + \frac{\partial}{\partial \theta_0} \right] - im W_n^m
$$

It will ease further simplifications of the integrating, if we multiplying dV to the coefficient. Therefore,

$$
\begin{aligned}
D_n^m \; dV =& r_0^2 \left[1 - \frac{2}{3}(3\varepsilon + r_0\varepsilon')P_2 \right] \times \\
& \left[-imV_n^m + W_n^m \sin\theta_0 \left[\frac{2}{3}r_0\varepsilon P_2^1 \frac{\partial}{\partial r_0} + \frac{\partial}{\partial \theta_0} \right] \right] dr_0 \; \sin\theta_0 d\theta_0 d\phi \\
E_n^m \; dV =& \frac{1}{n(n+1)} r_0^2 \left[1 - \frac{2}{3}(3\varepsilon + r_0\varepsilon')P_2 \right] \times \left[-im(U_n^m + V_n^m) \right. \\
& \left. + W_n^m \left[n(n+1)\cos\theta_0 + \sin\theta_0 \left[\frac{2}{3}r_0\varepsilon P_2^1 \frac{\partial}{\partial r_0} + \frac{\partial}{\partial \theta_0} \right] \right] \right] dr_0 \; \sin\theta_0 d\theta_0 \; d\phi \\
F_n^m \; dV =& \frac{1}{n(n+1)} r_0^2 \left[1 - \frac{2}{3}(3\varepsilon + r_0\varepsilon')P_2 \right] \times \left[-\left[2U_n^m + n(n+1)V_n^m \right] \cos\theta_0 \right. \\
& \left. - V_n^m \sin\theta_0 \left[\frac{2}{3}r_0\varepsilon P_2^1 \frac{\partial}{\partial r_0} + \frac{\partial}{\partial \theta_0} \right] - imW_n^m \right] dr_0 \; \sin\theta_0 d\theta_0 \; d\phi
\end{aligned}
$$

(6.8)

To first order in ellipticity and **u** the coefficients (6.8) reduce to

$$
\begin{aligned}
D_n^m \, dV =& r_0^2 \Bigg[-imV_n^m + \frac{2}{3}imV_n^m(3\varepsilon + r_0\varepsilon')P_2 + W_n^m \sin\theta_0 \frac{\partial}{\partial\theta_0} \\
&+ \frac{2}{3}r_0 W_n^m \sin\theta_0\varepsilon P_2^1 \frac{\partial}{\partial r_0} - \frac{2}{3}W_n^m(3\varepsilon + r_0\varepsilon')P_2 \sin\theta_0 \frac{\partial}{\partial\theta_0} \Bigg] dr_0 \ \sin\theta_0 d\theta_0 d\phi \\
E_n^m \, dV =& r_0^2 \Bigg[-\frac{im}{n(n+1)}U_n^m - \frac{im}{n(n+1)}V_n^m + \frac{2im}{3n(n+1)}U_n^m(3\varepsilon + r_0\varepsilon')P_2 + \\
&\frac{2im}{3n(n+1)}V_n^m(3\varepsilon + r_0\varepsilon')P_2 + W_n^m \cos\theta_0 + \frac{W_n^m}{n(n+1)}\sin\theta_0 \frac{\partial}{\partial\theta_0} \\
&+ \frac{2}{3}r_0\frac{W_n^m}{n(n+1)}\sin\theta_0\varepsilon P_2^1 \frac{\partial}{\partial r_0} - \frac{2}{3}W_n^m(3\varepsilon + r_0\varepsilon')P_2 \cos\theta_0 \\
&- \frac{2W_n^m}{3n(n+1)}(3\varepsilon + r_0\varepsilon')P_2 \sin\theta_0 \frac{\partial}{\partial\theta_0} \Bigg] dr_0 \ \sin\theta_0 d\theta_0 \ d\phi \\
F_n^m \, dV =& r_0^2 \Bigg[-\frac{2U_n^m}{n(n+1)}\cos\theta_0 + \frac{4U_n^m}{3n(n+1)}(3\varepsilon + r_0\varepsilon')P_2 \cos\theta_0 \\
&- V_n^m \cos\theta_0 + \frac{2}{3}V_n^m(3\varepsilon + r_0\varepsilon')P_2 \cos\theta_0 - \frac{V_n^m}{n(n+1)}\sin\theta_0 \frac{\partial}{\partial\theta_0} \\
&- \frac{2}{3}r_0\frac{V_n^m}{n(n+1)}\sin\theta_0\varepsilon P_2^1 \frac{\partial}{\partial r_0} + \frac{2V_n^m}{3n(n+1)}(3\varepsilon + r_0\varepsilon')P_2 \sin\theta_0 \frac{\partial}{\partial\theta_0} \\
&- \frac{imW_n^m}{n(n+1)} + \frac{2imW_n^m}{3n(n+1)}(3\varepsilon + r_0\varepsilon')P_2 \Bigg] dr_0 \ \sin\theta_0 d\theta_0 \ d\phi
\end{aligned}
\tag{6.9}
$$

Similarly, $\nabla . \mathbf{u}$ becomes,

$$
\nabla . \mathbf{u} = \sum \sum \left[\left[1 + \frac{2}{3}(\varepsilon + r_0\varepsilon')P_2 \right] \frac{\partial U_n^m}{\partial r_0} + \frac{2U_n^m - n(n+1)V_n^m}{r_0}\left[1 + \frac{2}{3}\varepsilon P_2 \right] \right] Y_n^m \tag{6.10}
$$

To first order in the ellipticity and displacement we get,

$$
\begin{aligned}
\nabla . \mathbf{u} \, dV =& \left[\frac{dU_n^m}{dr_0}\left[1 - \frac{4}{3}\varepsilon P_2 \right] r_0^2 \right. \\
&\left. + \left(2U_n^m - n(n+1)V_n^m \right)r_0\left[1 - \frac{2}{3}(2\varepsilon + r_0\varepsilon')P_2 \right] \right] dr_0 \ \sin\theta_0 d\theta_0 \ d\phi
\end{aligned}
\tag{6.11}
$$

To first order in the ellipticity the Earth the equilibrium dimensionless gravity in the Earth's interior is given by Seyed-Mahmoud and Moradi (2014)

$$\mathbf{g}_0 = -\left\{\left[1 + \frac{2}{3}(\varepsilon + r_0\varepsilon')P_2\right]g_0 - \frac{2}{3}r_0\right\}\hat{\mathbf{r}} - \left\{\frac{2}{3}\varepsilon P_2^1 g_0\right\}\hat{\theta}_0. \tag{6.12}$$

where, as in chapter 3, we used $R\Omega^2$ for nondimensionalizing and $g_0(r_0) = GM_0/r_0^2$ (M_0 is the mass enclosed by r_0).

The term $[\nabla.(2\rho_0\beta^2\,\mathbf{e})]/\rho_0$ can be extended as

$$\nabla.\left(2\rho_0\beta^2\tilde{\mathbf{e}}\right) = \nabla.\left(2\mu\tilde{\mathbf{e}}\right) = \nabla.\left(2\mu\tilde{\mathbf{e}}\right)_r + \nabla.\left(2\mu\tilde{\mathbf{e}}\right)_\theta + \nabla.\left(2\mu\tilde{\mathbf{e}}\right)_\phi$$

$$= \sum\sum\left\{A_n^m Y_n^m\hat{\mathbf{r}} + \left(B_n^m\frac{\partial Y_n^m}{\partial\theta} + imC_n^m\frac{1}{\sin\theta}Y_n^m\right)\hat{\theta} + \left(im\frac{1}{\sin\theta}B_n^m Y_n^m - C_n^m\frac{\partial Y_n^m}{\partial\theta}\right)\hat{\phi}\right\}$$

$$\tag{6.13}$$

In the new coordinate system, coefficients A_n^m, B_n^m and C_n^m are

$$A_n^m = 2\left(\frac{dr_0}{dr}\right)^2\frac{d\beta^2}{dr_0}\frac{dU_n^m}{dr_0} + 2\beta^2\frac{d^2}{dr^2}U_n^m - n(n+1)\beta^2\left[\frac{1}{r}\frac{dr_0}{dr}\frac{dV_n^m}{dr_0}\right.$$

$$\left. + \frac{1}{r^2}\left(U_n^m - 3V_n^m\right)\right] + 4\beta^2\left[\frac{1}{r}\frac{dr_0}{dr}\frac{dU_n^m}{dr_0} - \frac{U_n^m}{r^2}\right]$$

$$B_n^m = \left(\frac{dr_0}{dr}\right)^2\frac{d\beta^2}{dr_0}\frac{dV_n^m}{dr_0} + \beta^2\frac{d^2V_n^m}{dr^2} + \frac{1}{r}\frac{dr_0}{dr}\frac{d\beta^2}{dr_0}\left(U_n^m - V_n^m\right)$$

. $$- \frac{1}{r^2}\beta^2\left(U_n^m - V_n^m\right) + \beta^2\frac{1}{r}\frac{dr_0}{dr}\frac{d\left(U_n^m - V_n^m\right)}{dr_0} + 3\beta^2\left[\frac{1}{r}\frac{dr_0}{dr}\frac{dV_n^m}{dr_0}\right] \tag{6.14}$$

$$+ 3\beta^2\frac{1}{r^2}\left(U_n^m - V_n^m\right) + \frac{2\beta^2}{r^2}\left[U_n^m - \left(n(n+1) - 1\right)V_n^m\right]$$

$$C_n^m = \left(\frac{dr_0}{dr}\right)^2\frac{d\beta^2}{dr_0}\frac{dW_n^m}{dr_0} + \beta^2\frac{d^2W_n^m}{dr^2} - \frac{1}{r}\frac{dr_0}{dr}\frac{d\beta^2}{dr_0}W_n^m + \frac{1}{r^2}\beta^2 W_n^m$$

$$- \beta^2\frac{1}{r}\frac{dr_0}{dr}\frac{dW_n^m}{dr_0} + 3\beta^2\left[\frac{1}{r}\frac{dr_0}{dr}\frac{dW_n^m}{dr_0}\right] - \frac{\beta^2}{r^2}\left[n(n+1) + 1\right]W_n^m$$

Multiplying dV and neglecting the terms higher than the first order in $\mathbf{u}$ and ε we get

$$
\begin{aligned}
A_n^m \, dV = \Bigg\{ & 2r_0^2\Big[1 - \frac{2}{3}(\varepsilon - r_0\varepsilon')P_2\Big]2\beta\frac{d\beta}{dr_0}\frac{dU_n^m}{dr_0} + \frac{8}{3}\beta^2 r_0^2\varepsilon' P_2\frac{\partial U_n^m}{\partial r_0} \\
& + 2\beta^2 r_0^2\Big[1 - \frac{2}{3}(\varepsilon - r_0\varepsilon')P_2\Big]\frac{\partial^2 U_n^m}{\partial r_0^2} - n(n+1)\beta^2\Big[1 - \frac{2}{3}\varepsilon P_2\Big]r_0\frac{dV_n^m}{dr_0} \\
& + 4\beta^2\Big[1 - \frac{2}{3}\varepsilon P_2\Big]r_0\frac{dU_n^m}{dr_0} - 4\beta^2 U_n^m\Big[1 - \frac{2}{3}(\varepsilon + r_0\varepsilon')P_2\Big] \\
& - n(n+1)\beta^2\Big[1 - \frac{2}{3}(\varepsilon + r_0\varepsilon')P_2\Big]\Big(U_n^m - 3V_n^m\Big)\Bigg\} dr_0 \, \sin\theta_0 \, d\theta_0 \, d\phi
\end{aligned}
$$

$$
\begin{aligned}
B_n^m \, dV = \Bigg\{ & r_0^2\Big[1 - \frac{2}{3}(\varepsilon - r_0\varepsilon')P_2\Big]2\beta\frac{d\beta}{dr_0}\frac{dV_n^m}{dr_0} + \frac{4}{3}\beta^2 r_0^2\varepsilon' P_2\frac{\partial V_n^m}{\partial r_0} \\
& + \beta^2 r_0^2\Big[1 - \frac{2}{3}(\varepsilon - r_0\varepsilon')P_2\Big]\frac{\partial^2 V_n^m}{\partial r_0^2} + \Big[1 - \frac{2}{3}\varepsilon P_2\Big]r_0\Big[2\beta\frac{d\beta}{dr_0}\Big(U_n^m - V_n^m\Big) \\
& + \beta^2\frac{d\Big(U_n^m - V_n^m\Big)}{dr_0}\Big] + 3\beta^2\Big[1 - \frac{2}{3}\varepsilon P_2\Big]r_0\frac{dV_n^m}{dr_0} \\
& + 2\beta^2\Big[1 - \frac{2}{3}(\varepsilon + r_0\varepsilon')P_2\Big]\Big[2U_n^m - n(n+1)V_n^m\Big]\Bigg\} dr_0 \, \sin\theta_0 \, d\theta_0 \, d\phi
\end{aligned}
$$

$$
\begin{aligned}
C_n^m \, dV = \Bigg\{ & r_0^2\Big[1 - \frac{2}{3}(\varepsilon - r_0\varepsilon')P_2\Big]2\beta\frac{d\beta}{dr_0}\frac{dW_n^m}{dr_0} + \frac{4}{3}\beta^2 r_0^2\varepsilon' P_2\frac{\partial W_n^m}{\partial r_0} \\
& + \beta^2\Big[1 - \frac{2}{3}(\varepsilon - r_0\varepsilon')P_2\Big]\frac{\partial^2 W_n^m}{\partial r_0^2} - \Big[1 - \frac{2}{3}\varepsilon P_2\Big]r_0\Big[2\beta\frac{d\beta}{dr_0}W_n^m + \beta^2\frac{dW_n^m}{dr_0}\Big] \\
& + 3\beta^2\Big[1 - \frac{2}{3}\varepsilon P_2\Big]r_0\frac{dW_n^m}{dr_0} - \beta^2\Big[1 - \frac{2}{3}(\varepsilon + r_0\varepsilon')P_2\Big]n(n+1)W_n^m\Bigg\} dr_0 \, \sin\theta_0 \, d\theta_0 \, d\phi
\end{aligned}
$$

$$(6.15)$$

Substituting (6.3) and (6.4) into (6.5), integrating over ϕ and simplifying the terms using

(A.4), (A.5) and (A.10) we get

$$
\begin{aligned}
\int \sum_n \sum_q &\left\{ \sigma^2 \left[U_q^m U_n^m P_q^m P_n^m + \left(V_q^m V_n^m + W_q^m W_n^m \right) n(n+1) P_q^m P_n^m \right] \right. \\
&- 2i\sigma \left[U_q^m D_n^m P_q^m P_n^m + \left(V_q^m E_n^m + W_q^m F_n^m \right) n(n+1) P_q^m P_n^m \right] \\
&+ \left[U_q^m A_n^m P_q^m P_n^m + \left(V_q^m B_n^m + W_q^m C_n^m \right) n(n+1) P_q^m P_n^m \right] \\
&+ \left[-\mathbf{g}_0 + \frac{1}{\rho_0} \frac{d\rho_0}{dr} (\alpha^2 - 2\beta^2) \right] U_q^m P_q^m \left[\frac{dU_n^m}{dr} + \frac{2U_n^m - n(n+1)V_n^m}{r} \right] P_n^m \\
&- \left[\frac{dU_q^m}{dr} + \frac{2U_q^m - q(q+1)V_q^m}{r} \right] P_q^m \left[X_n^m P_n^m + \mathbf{u} \cdot \mathbf{g}_0 \right. \\
&+ (\alpha^2 - 2\beta^2) \left[\frac{dU_n^m}{dr} + \frac{2U_n^m - n(n+1)V_n^m}{r} \right] P_n^m \right] \right\} r^2 dr \, \sin\theta_0 d\theta_0 \\
+ \int_S \sum_n \sum_q &\left\{ U_q^m P_q^m \left[X_n^m P_n^m + \mathbf{u} \cdot \mathbf{g}_0 \right. \right. \\
&+ (\alpha^2 - 2\beta^2) \left[\frac{dU_n^m}{dr} + \frac{2U_n^m - n(n+1)V_n^m}{r} \right] P_n^m \right] \right\} r^2 \, \sin\theta_0 d\theta_0 = 0
\end{aligned} \tag{6.16}
$$

where all terms in (6.16) are evaluated at elliptical surface r. We use (6.9), (6.11), (6.12) and (6.15) to substitute for $D_n^m, E_n^m, F_n^m, A_n^m, B_n^m, C_n^m$ and $\mathbf{g}_0$ in terms of r_0 and θ_0. We follow the same steps in chapter 4 to expand and simplify PDEs. Finally, we apply the Galerkin's

conditions (3.7) and relations (A.6) and (A.7) to get three scalar equations [1] as

$$
\int \sum_n \sum_q \left\{ U_q^m \left[\sigma^2 U_n^m r_0^2 - \frac{2}{3}(3\varepsilon + r_0\varepsilon')\sigma^2 U_n^m r_0^2 P_2 - 2\sigma r_0^2 m V_n^m + \frac{4}{3}\sigma r_0^2 m V_n^m (3\varepsilon + r_0\varepsilon')P_2 \right.\right.
$$

$$
- 2\sigma r_0^2 W_n^m \sin\theta_0 \frac{\partial}{\partial\theta_0} + \frac{4}{3}\sigma r_0^2 W_n^m (3\varepsilon + r_0\varepsilon')P_2 \sin\theta_0 \frac{\partial}{\partial\theta_0} + r_0^2 \left[\frac{\partial X_n^m}{\partial r_0} - \frac{4}{3}\left(\frac{\partial X_n^m}{\partial r_0}\varepsilon + X_n^m\varepsilon'\right)P_2 \right]
$$

$$
- \frac{\partial U_n^m}{\partial r_0}\left(g_0 + \frac{2}{3}r_0\right) - U_n^m\left(-\frac{2g_0}{x} - \frac{4g_0}{3r_0}\varepsilon P_2 + 4\pi G\rho_0 + \frac{2}{3}\right)
$$

$$
+ \frac{2}{3}\frac{\partial U_n^m}{\partial r_0}\left(g_0(\varepsilon - r_0\varepsilon') + \frac{4}{3}r_0\varepsilon\right)P_2 + \frac{2}{3}U_n^m\left((-\frac{2g_0}{r_0} - \frac{4g_0}{3r_0}\varepsilon P_2 + 4\pi G\rho_0)(\varepsilon - r_0\varepsilon')\right.
$$

$$
\left.+ \frac{4}{3}(\varepsilon + r_0\varepsilon')\right)P_2 - \frac{2}{3}\left(\frac{\partial V_n^m}{\partial r_0}\varepsilon g_0 - V_n^m\varepsilon\frac{2g_0}{x} + 4\pi G\rho_0 V_n^m\varepsilon + V_n^m\varepsilon' g_0\right)P_2^1 \frac{\partial}{\partial\theta_0}
$$

$$
+ 2m\left(\frac{\partial W_n^m}{\partial r_0}\varepsilon g_0 - W_n^m\varepsilon\frac{2g_0}{x} + 4\pi G\rho_0 W_n^m\varepsilon + W_n^m\varepsilon' g_0\right)\cos\theta_0 \right]
$$

$$
+ \frac{1}{\rho}\frac{d\rho}{dr_0}r_0 \left[\left[1 + \frac{2}{3}(\varepsilon + r_0\varepsilon')P_2\right]\alpha^2 r_0 \frac{dU_n^m}{dr_0} + \left[2 + \frac{4}{3}(\varepsilon + r_0\varepsilon')P_2\right](\alpha^2 - 2\beta^2)U_n^m - \frac{4}{3}\alpha^2 r_0\varepsilon P_2 \frac{dU_n^m}{dr_0} \right.
$$

$$
\left.- \frac{4}{3}(\alpha^2 - 2\beta^2)(2\varepsilon + r_0\varepsilon')U_n^m P_2 - n(n+1)(\alpha^2 - 2\beta^2)V_n^m + \frac{2}{3}n(n+1)(\alpha^2 - 2\beta^2)\varepsilon P_2 V_n^m \right]
$$

$$
+ 2\left[2r_0^2\left[1 - \frac{2}{3}(\varepsilon - r_0\varepsilon')P_2\right]2\beta\frac{d\beta}{dr_0}\frac{dU_n^m}{dr_0} + \frac{8}{3}\beta^2 r_0^2\varepsilon' P_2 \frac{\partial U_n^m}{\partial r_0} + 2\beta^2 r_0^2\left[1 - \frac{2}{3}(\varepsilon - r_0\varepsilon')P_2\right]\frac{\partial^2 U_n^m}{\partial r_0^2} \right.
$$

$$
- n(n+1)\beta^2\left[1 - \frac{2}{3}\varepsilon P_2\right]r_0\frac{dV_n^m}{dr_0} + 4\beta^2\left[1 - \frac{2}{3}\varepsilon P_2\right]r_0\frac{dU_n^m}{dr_0} - 4\beta^2 U_n^m\left[1 - \frac{2}{3}(\varepsilon + r_0\varepsilon')P_2\right]
$$

$$
\left.\left.- n(n+1)\beta^2\left[1 - \frac{2}{3}(\varepsilon + r_0\varepsilon')P_2\right]\left(U_n^m - 3V_n^m\right)\right]\right] P_q^m P_n^m \right\} dr_0 \, \sin\theta_0 \, d\theta_0
$$

$$
+ [cont]
$$

---

[1] The equations are valid for azimutal numbers $m = 0, \pm 1$ that we are interested.

$$
+ \int \left\{ U_q^m \left[g_0 r_0^2 \frac{\partial U_n^m}{\partial r_0} - \frac{2}{3} r_0^3 \frac{\partial U_n^m}{\partial r_0} + 2 g_0 r_0 U_n^m - \frac{4}{3} r_0^2 U_n^m - n(n+1) g_0 r_0 V_n^m \right. \right.
$$

$$
+ \frac{2}{3} n(n+1) r_0^2 V_n^m \Bigg] P_n^m P_q^m + U_q^m \left[-\frac{2}{3} (3\varepsilon + r_0 \varepsilon') g_0 r_0^2 \frac{\partial U_n^m}{\partial r_0} + \frac{4}{9} r_0^3 (3\varepsilon + r_0 \varepsilon') \frac{\partial U_n^m}{\partial r_0} \right.
$$

$$
- \frac{4}{3} (3\varepsilon + r_0 \varepsilon') g_0 r_0^2 \frac{U_n^m}{r_0} + \frac{8}{9} r_0^2 (3\varepsilon + r_0 \varepsilon') U_n^m + \frac{2}{3} n(n+1) g_0 (3\varepsilon + r_0 \varepsilon') r_0 V_n^m
$$

$$
- \frac{4}{9} n(n+1)(3\varepsilon + r_0 \varepsilon') r_0^2 V_n^m + \frac{2}{3} (\varepsilon + r_0 \varepsilon') g_0 r_0^2 \frac{\partial U_n^m}{\partial r_0} + \frac{4}{3} \varepsilon g_0 r_0 U_n^m
$$

$$
- \frac{4}{9} (\varepsilon + r_0 \varepsilon') r_0^3 \frac{\partial U_n^m}{\partial r_0} - \frac{8}{9} \varepsilon r_0^2 U_n^m - \frac{2}{3} n(n+1) \varepsilon g_0 r_0 V_n^m + \frac{4}{9} n(n+1) r_0^2 \varepsilon V_n^m
$$

$$
+ \frac{2}{3} g_0 (\varepsilon + r_0 \varepsilon') r_0^2 \frac{\partial U_n^m}{\partial r_0} + \frac{4}{3} g_0 (\varepsilon + r_0 \varepsilon') r_0 U_n^m - \frac{2}{3} n(n+1) g_0 (\varepsilon + r_0 \varepsilon') r_0 V_n^m \Bigg] P_2 P_n^m P_q^m
$$

$$
- (\alpha^2 - 2\beta^2) \left[\left(r_0^2 \frac{\partial U_n^m}{\partial r_0} \frac{dU_q^m}{dr_0} + 2 r_0 \frac{\partial U_n^m}{\partial r_0} U_q^m + 2 r_0 U_n^m \frac{dU_q^m}{dr_0} + 4 U_n^m U_q^m - n(n+1) r_0 V_n^m \frac{dU_q^m}{dr_0} \right. \right.
$$

$$
- 2 n(n+1) V_n^m U_q^m \Bigg) P_q^m P_n^m + \left(\frac{2}{3} r_0^2 (\varepsilon + r_0 \varepsilon') \frac{\partial U_n^m}{\partial r_0} \frac{dU_q^m}{dr_0} + \frac{4}{3} (\varepsilon + r_0 \varepsilon') r_0 \frac{\partial U_n^m}{\partial r_0} U_q^m \right.
$$

$$
+ \frac{4}{3} r_0 U_n^m \varepsilon \frac{dU_q^m}{dr_0} + \frac{8}{3} \varepsilon U_n^m U_q^m - \frac{2}{3} n(n+1) V_n^m \varepsilon r_0 \frac{dU_q^m}{dr_0} - \frac{4}{3} n(n+1) V_n^m \varepsilon U_q^m
$$

$$
- \frac{4}{3} \varepsilon r_0^2 \frac{\partial U_n^m}{\partial r_0} \frac{dU_q^m}{dr_0} + \frac{4}{3} (2\varepsilon + r_0 \varepsilon') r_0 \frac{\partial U_n^m}{\partial r_0} U_q^m - \frac{8}{3} \varepsilon r_0 U_n^m \frac{dU_q^m}{dr_0} + \frac{8}{3} (2\varepsilon + r_0 \varepsilon') U_n^m U_q^m
$$

$$
+ \frac{4}{3} n(n+1) V_n^m \varepsilon r_0 \frac{dU_q^m}{dr_0} - \frac{4}{3} n(n+1) V_n^m U_q^m (2\varepsilon + r_0 \varepsilon') \right) P_2 P_q^m P_n^m \Bigg] \Bigg\} \, dr_0 \, \sin\theta_0 d\theta_0
$$

$$
+ \int_S \sum_n \sum_q U_q^m (\alpha^2 - 2\beta^2) \left(\frac{\partial U_n^m}{\partial r_0} + \frac{2}{3} (\varepsilon + r_0 \varepsilon') \frac{\partial U_n^m}{\partial r_0} P_2 + \frac{2 U_n^m}{r_0} + \frac{4}{3} \frac{U_n^m}{r_0} \varepsilon P_2 \right.
$$

$$
- n(n+1) \frac{1}{r_0} V_n^m - \frac{2}{3} n(n+1) \varepsilon \frac{1}{r_0} V_n^m P_2 \right) P_q^m P_n^m \, r_0^2 \sin\theta_0 d\theta_0 = 0
$$

$$
\tag{6.17}
$$

$$\int \sum_n \sum_q \left\{ \sigma^2 V_q^m V_n^m r_0^2 - \frac{2}{3}\sigma^2 V_q^m V_n^m r_0^2 (3\varepsilon + r_0\varepsilon')P_2 + 2\sigma V_q^m r_0^2 \left[-\frac{m}{n(n+1)}U_n^m \right.\right.$$

$$-\frac{m}{n(n+1)}V_n^m + \frac{2m}{3n(n+1)}U_n^m(3\varepsilon + r_0\varepsilon')P_2 + \frac{2m}{3n(n+1)}V_n^m(3\varepsilon + r_0\varepsilon')P_2 - W_n^m\cos\theta_0$$

$$\left. -\frac{W_n^m}{n(n+1)}\sin\theta_0\frac{\partial}{\partial\theta_0} + \frac{2}{3}W_n^m(3\varepsilon + r_0\varepsilon')P_2\cos\theta_0 + \frac{2W_n^m}{3n(n+1)}(3\varepsilon + r_0\varepsilon')P_2\sin\theta_0\frac{\partial}{\partial\theta_0} \right]$$

$$+V_q^m r_0\left[X_n^m - \frac{2}{3}X_n^m(2\varepsilon + r_0\varepsilon')P_2 - U_n^m\left(g_0 + \frac{2}{3}r_0\right) + \frac{2}{3}U_n^m\left(g_0\varepsilon + \frac{2}{3}r_0(2\varepsilon + r_0\varepsilon')\right)P_2 \right.$$

$$\left. -\frac{2}{3}V_n^m\varepsilon g_0 P_2^1\frac{\partial}{\partial\theta_0} + 2mW_n^m\varepsilon g_0\cos\theta_0 \right] + V_q^m\frac{1}{\rho}\frac{d\rho}{dr_0}r_0\left[\beta^2 r_0\frac{dV_n^m}{dr_0} - \beta^2 V_n^m - \frac{2}{3}\beta^2 r_0\frac{dV_n^m}{dr_0}(\varepsilon - r_0\varepsilon')P_2 \right.$$

$$\left. +\frac{2}{3}V_n^m\beta^2\varepsilon P_2 + \beta^2 U_n^m - \frac{2}{3}U_n^m\beta^2\varepsilon P_2 \right] + 2V_q^m\left[r_0^2\left[1 - \frac{2}{3}(\varepsilon - r_0\varepsilon')P_2 \right]2\beta\frac{d\beta}{dr_0}\frac{dV_n^m}{dr_0} \right.$$

$$+\frac{4}{3}\beta^2 r_0^2\varepsilon' P_2\frac{\partial V_n^m}{\partial r_0} + \beta^2 r_0^2\left[1 - \frac{2}{3}(\varepsilon - r_0\varepsilon')P_2 \right]\frac{\partial^2 V_n^m}{\partial r_0^2} + \left[1 - \frac{2}{3}\varepsilon P_2 \right]r_0\left[2\beta\frac{d\beta}{dr_0}\left(U_n^m - V_n^m\right) \right.$$

$$\left. +\beta^2\frac{d\left(U_n^m - V_n^m\right)}{dr_0} \right] + 3\beta^2\left[1 - \frac{2}{3}\varepsilon P_2 \right]r_0\frac{dV_n^m}{dr_0} + 2\beta^2\left[1 - \frac{2}{3}(\varepsilon + r_0\varepsilon')P_2 \right]\left[2U_n^m \right.$$

$$\left.\left.\left. -n(n+1)V_n^m \right] \right] \right\}n(n+1)P_q^m P_n^m + \left\{ \left(4\varepsilon g_0 r_0^2\frac{\partial U_n^m}{\partial r_0}V_q^m + 8\varepsilon g_0 r_0 U_n^m V_q^m \right.\right.$$

$$\left. -4n(n+1)\varepsilon g_0 r_0 V_n^m V_q^m \right)P_2 P_n^m P_q^m + \left(-\frac{2}{3}\varepsilon g_0 r_0^2\frac{\partial U_n^m}{\partial r_0}V_q^m - \frac{4}{3}\varepsilon g_0 r_0 U_n^m V_q^m \right.$$

$$\left. +\frac{2}{3}n(n+1)\varepsilon g_0 r_0 V_n^m V_q^m \right)P_2^1 P_q^m\frac{dP_n^m}{d\theta_0} - (\alpha^2 - 2\beta^2)\left[q(q+1)\left(-r_0 V_q^m\frac{\partial U_n^m}{\partial r_0} - 2V_q^m U_n^m \right.\right.$$

$$\left. +n(n+1)V_q^m V_n^m \right)P_q^m P_n^m + \left(\frac{2}{3}q(q+1)V_q^m\left(\varepsilon r_0\frac{\partial U_n^m}{\partial r_0} + 2(\varepsilon + r_0\varepsilon')U_n^m\right) \right.$$

$$\left.\left.\left.\left. -\frac{2}{3}q(q+1)n(n+1)(\varepsilon + r_0\varepsilon')V_n^m V_q^m \right)P_2 P_q^m P_n^m \right] \right\}dr_0\ \sin\theta_0 d\theta_0$$

$$+\int_S \sum_n \sum_q (\alpha^2 - 2\beta^2)\left(\frac{\partial U_n^m}{\partial r_0} + \frac{2U_n^m}{r_0} \right.$$

$$\left. -n(n+1)\frac{1}{r_0}V_n^m \right)\left[-\frac{2}{3}P_2^1\frac{dP_n^m}{d\theta_0} + 4P_2 P_q^m \right]\varepsilon V_q^m P_q^m\ r_0^2\sin\theta_0 d\theta_0 = 0$$

$$(6.18)$$

$$\int \sum_n \sum_q \left\{ \left[-\sigma^2 W_q^m W_n^m r_0^2 + \frac{2}{3}\sigma^2 W_q^m W_n^m r_0^2 (3\varepsilon + r_0\varepsilon')P_2 - 2\sigma W_q^m r_0^2 \left[-\frac{2U_n^m}{n(n+1)}\cos\theta_0 \right. \right.\right.$$

$$+ \frac{4U_n^m}{3n(n+1)}(3\varepsilon + r_0\varepsilon')P_2\cos\theta_0 - V_n^m\cos\theta_0 + \frac{2}{3}V_n^m(3\varepsilon + r_0\varepsilon')P_2\cos\theta_0$$

$$- \frac{V_n^m}{n(n+1)}\sin\theta_0\frac{\partial}{\partial\theta_0} + \frac{2V_n^m}{3n(n+1)}(3\varepsilon + r_0\varepsilon')P_2\sin\theta_0\frac{\partial}{\partial\theta_0} - \frac{mW_n^m}{n(n+1)}$$

$$+ \frac{2mW_n^m}{3n(n+1)}(3\varepsilon + r_0\varepsilon')P_2 \right] - W_q^m\frac{1}{\rho}\frac{d\rho}{dr_0}r_0 \left[\beta^2 r_0\frac{dW_n^m}{dr_0} - \beta^2 W_n^m - \frac{2}{3}\beta^2 r_0\frac{dW_n^m}{dr_0}(\varepsilon - r_0\varepsilon')P_2 \right.$$

$$+ \frac{2}{3}\beta^2 W_n^m\varepsilon P_2 \right] - 4W_q^m \left[r_0^2 \left[1 - \frac{2}{3}(\varepsilon - r_0\varepsilon')P_2 \right]\beta\frac{d\beta}{dr_0}\frac{dW_n^m}{dr_0} + \frac{4}{3}\beta^2 r_0^2\varepsilon' P_2\frac{\partial W_n^m}{\partial r_0} \right.$$

$$+ \beta^2 \left[1 - \frac{2}{3}(\varepsilon - r_0\varepsilon')P_2 \right]\frac{\partial^2 W_n^m}{\partial r_0^2} - \left[1 - \frac{2}{3}\varepsilon P_2 \right]r_0 \left[2\beta\frac{d\beta}{dr_0}W_n^m + \beta^2\frac{dW_n^m}{dr_0} \right]$$

$$+ 3\beta^2 \left[1 - \frac{2}{3}\varepsilon P_2 \right]r_0\frac{dW_n^m}{dr_0} - \beta^2 \left[1 - \frac{2}{3}(\varepsilon + r_0\varepsilon')P_2 \right]n(n+1)W_n^m \right] \right] n(n+1)P_q^m P_n^m$$

$$+ \varepsilon g_0 \left(2mr_0^2 W_q^m\frac{\partial U_n^m}{\partial r_0} + 4mr_0 U_n^m W_q^m - 2mn(n+1)r_0 V_n^m W_q^m \right)\cos\theta_0 P_q^m P_n^m \right\} dr_0 \ \sin\theta_0 \ d\theta_0$$

$$+ \int_S \sum_n \sum_q (\alpha^2 - 2\beta^2)\left(\frac{\partial U_n^m}{\partial r_0} + \frac{2U_n^m}{r_0} - n(n+1)\frac{1}{r_0}V_n^m \right)2mW_q^m\varepsilon\cos\theta_0 P_q^m P_n^m \ r_0^2\sin\theta_0 d\theta_0 = 0$$

$$(6.19)$$

Similarly, using the relations (A.13) and (A.14), the Poisson's equation (6.6), result in

$$\int \sum_n \sum_q \left\{ X_q^m P_q^m \left(\left[1 - \frac{2}{3}(\varepsilon - r_0\varepsilon')P_2 \right]r_0^2\frac{\partial^2 X_n^m}{\partial r_0^2} + 2\left[1 - \frac{2}{3}\varepsilon P_2 \right]r_0\frac{\partial X_n^m}{\partial r_0} \right)P_n^m \right.$$

$$- X_q^m P_q^m n(n+1)X_n^m \left[1 - \frac{2}{3}(\varepsilon + r_0\varepsilon')P_2 \right]P_n^m + 4\pi G\rho_0 U_n^m P_n^m \left[1 - \frac{4}{3}\varepsilon P_2 \right]r_0^2\frac{\partial X_q^m}{\partial r_0}P_q^m$$

$$+ 4\pi G\rho_0 X_q^m r_0 \left[1 - \frac{2}{3}(2\varepsilon + r_0\varepsilon')P_2 \right]V_n^m n(n+1)P_q^m P_n^m \right\} dr_0\sin\theta_0 d\theta_0$$

$$(6.20)$$

$$- \int_S \sum_n \sum_q 4\pi G X_q^m P_q^m\rho_0 \left[U_n^m P_n^m - \frac{2}{3}(3\varepsilon + r_0\varepsilon')P_2 U_n^m P_n^m \right.$$

$$+ \frac{2}{3}\varepsilon V_n^m P_2^1\frac{\partial}{\partial\theta_0}P_n^m - 2imW_n^m\varepsilon\cos\theta_0 P_n^m \right]r_0^2\sin\theta_0 d\theta_0 = 0$$

6.4 Boundary Conditions

We use a similar approach as in chapter 4 and chapter 5, to construct PDEs governing the BC in elliptical interfaces. For geo-centre (3.23) is still valid for elliptical Earth model. At Solid-Solid interfaces

$\Delta \mathbf{u} = 0$

$$
\begin{aligned}
\therefore \int_{S+} \sum_n \sum_q \Bigg\{ & \left(U_n^m U_q^m + \left(V_q^m W_n^m - V_n^m W_q^m \right) imn(n+1) \right) P_n^m P_q^m \\
& - (2\varepsilon + \tfrac{2}{3} r_0 \varepsilon') \left(U_n^m U_q^m + imn(n+1) \left(V_q^m W_n^m - V_n^m W_q^m \right) \right) P_q^m P_2 P_n^m \Bigg\} r_0^2 \sin\theta_0 d\theta_0 \\
= \int_{S-} \sum_n \sum_q \Bigg\{ & \left(U_n^m U_q^m + \left(V_q^m W_n^m - V_n^m W_q^m \right) imn(n+1) \right) P_n^m P_q^m \\
& - (2\varepsilon + \tfrac{2}{3} r_0 \varepsilon') \left(U_n^m U_q^m + imn(n+1) \left(V_q^m W_n^m - V_n^m W_q^m \right) \right) P_q^m P_2 P_n^m \Bigg\} r_0^2 \sin\theta_0 d\theta_0
\end{aligned}
$$

$$(6.21)$$

At Solid/Fluid Boundary

$\Delta(\hat{\mathbf{n}}.\mathbf{u}) = 0$

$$
\begin{aligned}
\therefore \int_{S+} \sum_n \sum_q \Bigg\{ & X_q^m U_n^m P_q^m P_n^m - 2\varepsilon X_q^m V_n^m \cos\theta_0 \sin\theta_0 P_q^m \frac{\partial P_n^m}{\partial\theta_0} - 2\varepsilon im X_q^m W_n^m \cos\theta_0 P_q^m P_n^m \\
& - X_q^m U_n^m (2\varepsilon + \tfrac{2}{3} r_0 \varepsilon') P_2 P_q^m P_n^m \Bigg\} r_0^2 \, dr_0 \, d\theta_0 \, d\phi = \\
= \int_{S-} \sum_n \sum_q \Bigg\{ & X_q^m U_n^m P_q^m P_n^m - 2\varepsilon X_q^m V_n^m \cos\theta_0 \sin\theta_0 P_q^m \frac{\partial P_n^m}{\partial\theta_0} - 2\varepsilon im X_q^m W_n^m \cos\theta_0 P_q^m P_n^m \\
& - X_q^m U_n^m (2\varepsilon + \tfrac{2}{3} r_0 \varepsilon') P_2 P_q^m P_n^m \Bigg\} r_0^2 \, dr_0 \, d\theta_0 \, d\phi
\end{aligned}
$$

$$(6.22)$$

Across all surfaces of discontinuity, dynamic boundary condition $\Delta(\hat{\mathbf{n}}.\mathbf{S}) = 0$ gives following PDE,

$$
\begin{aligned}
\int_{S+} \sum_n \sum_q &\left\{ \left[\begin{array}{l} (\rho_0(\alpha^2 - 2\beta^2) + 2\mu)\dfrac{dU_q^m}{dr}U_n^m + \dfrac{\rho_0(\alpha^2 - 2\beta^2)}{r}\left[2U_q^m - q(q+1)V_q^m\right]U_n^m \\[2mm] +n(n+1)\left(\rho_0\beta^2\left[\dfrac{dV_q^m}{dr} + \dfrac{1}{r}(U_q^m - V_q^m)\right]V_n^m + \rho_0\beta^2\left[\dfrac{dW_q^m}{dr} - \dfrac{W_q^m}{r}\right]W_n^m\right) \\[2mm] +\dfrac{4\varepsilon\mu}{r}\left(\dfrac{n(n+1)}{3} - m^2\right)(V_q^m V_n^m + W_q^m W_n^m) \end{array} \right] P_n^m P_q^m \right. \\[4mm]
&+ \left[\begin{array}{l} -(2\varepsilon + \dfrac{2}{3}r_0\varepsilon')\left(\rho_0\alpha^2\dfrac{dU_q^m}{dr}U_n^m + \dfrac{\rho_0(\alpha^2 - 2\beta^2)}{r}\left[2U_q^m - q(q+1)V_q^m\right]U_n^m \right. \\[2mm] +\rho_0\beta^2\left[\dfrac{dV_q^m}{dr} + \dfrac{1}{r}(U_q^m - V_q^m)\right]V_n^m + \rho_0\beta^2\left[\dfrac{dW_q^m}{dr} - \dfrac{W_q^m}{r}\right]W_n^m\bigg) \\[2mm] +n(n+1)\dfrac{8\varepsilon\mu}{3r}(V_q^m V_n^m + W_q^m W_n^m) \\[2mm] +4\varepsilon V_q^m\left(\rho_0(\alpha^2 - 2\beta^2)\left(\dfrac{dU_n^m}{dr} + \dfrac{2U_n^m - n(n+1)V_n^m}{r}\right)\right. \\[2mm] +\dfrac{2\mu}{r}\left(U_n^m - V_n^m n(n+1) + W_n^m\dfrac{n(n+1)}{2}\right)\bigg) \end{array} \right] P_q^m P_2 P_n^m \\[4mm]
&+ \left[\begin{array}{l} +2im\varepsilon\rho_0\beta^2 U_q^m\left(\dfrac{W_n^m}{r} - \dfrac{\partial W_n^m}{\partial r}\right) + \dfrac{4\varepsilon\mu}{r}im(V_q^m W_n^m - W_q^m V_n^m)\left(2 - n(n+1)\right) \\[2mm] +2\varepsilon im W_q^m\left(\rho_0(\alpha^2 - 2\beta^2)\left(\dfrac{dU_n^m}{dr} + \dfrac{2U_n^m - n(n+1)V_n^m}{r}\right)\right. \\[2mm] +\dfrac{2\mu}{r}\left(U_n^m - V_n^m n(n+1) + W_n^m\dfrac{n(n+1)}{2}\right)\bigg) \end{array} \right] P_q^m \cos\theta_0 P_n^m \\[4mm]
&+ \left[\begin{array}{l} +\dfrac{2}{3}\varepsilon\rho_0\beta^2 U_q^m\left(\dfrac{\partial V_n^m}{\partial r} - \dfrac{V_n^m}{r} + \dfrac{U_n^m}{r}\right) - \dfrac{8\varepsilon\mu}{3r}\left(V_q^m V_n^m + W_q^m W_n^m\right) \\[2mm] -\dfrac{2}{3}\varepsilon V_q^m\left(\rho_0(\alpha^2 - 2\beta^2)\left(\dfrac{dU_n^m}{dr} + \dfrac{2U_n^m - n(n+1)V_n^m}{r}\right)\right. \\[2mm] -\dfrac{2\mu}{3r}\left(U_n^m - V_n^m n(n+1) + W_n^m\dfrac{n(n+1)}{2}\right)\bigg) \end{array} \right] P_q^m P_2^1\dfrac{\partial P_n^m}{\partial\theta_0} \\[4mm]
&\left. -\dfrac{4\varepsilon\mu}{r}im(V_q^m W_n^m - W_q^m V_n^m)P_q^m\sin\theta_0\dfrac{\partial P_n^m}{\partial\theta_0}\right\} r_0^2\sin\theta_0 d\theta_0 = \int_{S-}\sum_n\sum_q\left\{RHS\right\}
\end{aligned}
$$

$$(6.23)$$

Boundary condition on the gravitational field is

$$\Delta[\hat{\mathbf{n}}.(\nabla V_1 - 4\pi G\rho_0 \mathbf{u})] = 0$$

$$\therefore \quad \int_{S+} \sum_n \sum_q \left\{ \left(X_q^m \frac{\partial X_n^m}{\partial r} - 4\pi G\rho_0 X_q^m U_n^m \right) P_q^m P_n^m \right.$$

$$+ \left(\frac{2}{3}\varepsilon X_q^m X_n^m \frac{1}{r} P_q^m + 8\pi G\rho_0 \varepsilon X_q^m V_n^m \right) P_q^m \cos\theta_0 \sin\theta_0 \frac{\partial P_n^m}{\partial \theta_0}$$

$$+ (2\varepsilon + \frac{2}{3}r_0\varepsilon') \left(4\pi G\rho_0 X_q^m U_n^m - X_q^m \frac{\partial X_n^m}{\partial r} \right) P_q^m P_2 P_n^m$$

$$\left. + 8\pi G\rho_0 \varepsilon im X_q^m W_n^m \cos\theta_0 P_q^m P_n^m \right\} r_0^2 \sin\theta_0 d\theta_0 d\phi \qquad (6.24)$$

$$= \int_{S-} \sum_n \sum_q \left\{ \left(X_q^m \frac{\partial X_n^m}{\partial r} - 4\pi G\rho_0 X_q^m U_n^m \right) P_q^m P_n^m \right.$$

$$+ \left(\frac{2}{3}\varepsilon X_q^m X_n^m \frac{1}{r} P_q^m + 8\pi G\rho_0 \varepsilon X_q^m V_n^m \right) P_q^m \cos\theta_0 \sin\theta_0 \frac{\partial P_n^m}{\partial \theta_0}$$

$$+ (2\varepsilon + \frac{2}{3}r_0\varepsilon') \left(4\pi G\rho_0 X_q^m U_n^m - X_q^m \frac{\partial X_n^m}{\partial r} \right) P_q^m P_2 P_n^m$$

$$\left. + 8\pi G\rho_0 \varepsilon im X_q^m W_n^m \cos\theta_0 P_q^m P_n^m \right\} r_0^2 \sin\theta_0 d\theta_0 d\phi$$

Chapter 7

Discussion

In this thesis we first reviewed the theoretical derivation of the partial differential equations (PDEs) governing the free oscillations of a realistic Earth model. The reference state of the Earth is considered to be one of *hydrostatic equilibrium*. This reference frame has its origin in the Earth's center and rotates with the constant angular velocity of Ω about a fix axis in space defined by a unit vector $\hat{\mathbf{e}}_3$. Using the conventional approach of spheroidal and toroidal representation of vector displacement fields, we derive the PDEs and the BCs governing the free oscillations of a self-gravitating, spherical, rotating Earth model.

We used a Galerkin method and FORTRAN programming to numerically solve for some of the low order (wavenumbers 0 and 1) inertial modes of (a) a homogeneous and incompressible core model, and (b) a more realistic, compressible, and stratified core model of spherical and spherical shell geometry. To validate our approach, we compared the frequencies and the displacement and pressure patterns of these modes with those of an incompressible fluid sphere for which analytical solutions exists. We showed that the computed frequencies (given to 3 decimal points) and the patterns of the eigenfunctions are identical to their analytical counterparts. This model is described by so-called *Poincaré* equation and the accompanying incompressibility boundary condition. As it is well-known (Greenspan, 1968), the Poincaré equation is a hyperbolic boundary value PDE which is mathematically ill-posed. For some containers (full sphere and cylinder) the Poincaré equation is separable and has exact analytical solutions while for most of the other geometries (like spherical shell) the solutions of this problem are singular.

In our approach we solved the momentum and the continuity equations and the relevant boundary conditions. In chapter 4 we computed some of low-order inertial modes of this geometry and showed that the results indeed converge.

Previous studies done by Aldridge (1969) and Henderson (1996), used the variational principle for numerical studies of the axisymmetric inertial modes and did not get converged values for most of the modal frequencies. Rieutord (1991, 1997) used iterative technique for a fluid of small viscosity. They showed that as viscosity tends to zero, the frequencies begin to fluctuate about a mean, and there are no solutions at the limit of zero viscosity. Our results seem to contradict Rieutord (1987) conclusion in a sense that we could get the converged values for most of the frequencies that we looked for.

We further computed the inertial modes of a compressible, self gravitating and stratified spherical fluid core. We showed that the divergence theorem may be used to (a) remove the dependence of the equations on the gradient of the density, which is poorly constrained at the boundary interfaces, and (b) to take advantage of the *natural* nature of the boundary conditions.

Finally, we derived integral equations of the Earth model that include the first order effects of ellipticity in the Earth model. In order to minimize the effects of derivatives on material properties, a (non-orthogonal) Clairaut coordinate system (Jeffreys, 1942; Seyed-Mahmoud, 2006) is used.

We have shown that our approach is a novel and reliable technique for the study of the normal modes of a realistic Earth model. Compressibility, elasticity and ellipticity terms are included in our model, though, in this study we have set them to zero to investigate more fundamental problems of the rotating fluids. We have given the necessary equations and expanded them for a Galerkin formulation, to include the effects of elasticity, and the ellipticity of the equipotential surfaces to compute the rotational modes, including those of wobble and nutation for which the observed periods are know, for a realistic Earth model.

Bibliography

A. Aldridge, K.D.and Toomre. Axisymmetric inertial oscillations of a fluid in a rotating spherical container. *Journal of Fluid Mechanics*, 37:307–323, 6 1969. ISSN 1469-7645. doi: 10.1017/S0022112069000565. URL http://journals.cambridge.org/article_S00221112069000565.

K.D. andLumb L.I. Aldridge. Inertial waves identified in the earth's fluid outer core. *Nature*, 325:421–423, 1987.

G.H.and Ewing M. Alsop, L.E.and Sutton. Free oscillations of the earth observed on strain and pendulum seismographs. *Journal of Geophysical Research*, 66(2):631–641, 1961. ISSN 2156-2202. doi: 10.1029/JZ066i002p00631. URL http://dx.doi.org/10.1029/JZ066i002p00631.

H.and Pekeris C.L. Alterman, A.and Jarosch. Oscillations of the earth,. *Proc.Soc.London*, A 252:80–95, 1959.

Y.and Merzer A.M. Alterman, Z.S.and Eyal. On free oscillations of the earth. *Geophysical surveys*, 1(4):409–428, 1974. ISSN 0046-5763. doi: 10.1007/BF01452247. URL http://dx.doi.org/10.1007/BF01452247.

G.E. Backus. The propagation of short elastic surface waves on a slowly rotating earth. *Bulletin of the Seismological Society of America*, 52(4):823–846, 1962. URL http://www.bssaonline.org/content/52/4/823.abstract.

J.C.and LaCoste L.and Munk W.H.and Slichter L.B. Benioff, H.and Harrison. Searching for the earth's free oscillations. *Journal of Geophysical Research*, 64(9):1334–1337, 1959. ISSN 2156-2202. doi: 10.1029/JZ064i009p01334. URL http://dx.doi.org/10.1029/JZ064i009p01334.

A. Bolt, B.A.and Marussi. Eigenvibrations of the earth observed at trieste. *Geophysical Journal of the Royal Astronomical Society*, 6(3):299–311, 1962. ISSN 1365-246X. doi: 10.1111/j.1365-246X.1962.tb00353.x. URL http://dx.doi.org/10.1111/j.1365-246X.1962.tb00353.x.

G.H. Bryan. The waves on a rotating liquid spheroid of finite ellipticity. *Philosophical Transactions of the Royal Society of London A: Mathematical, Physical and Engineering Sciences*, 180:187–219, 1889. ISSN 0264-3820. doi: 10.1098/rsta.1889.0006.

S.C. Chandler. The variation of terrestrial latitudes, by dr.s.c.chandler. *Publications of the Astronomical Society of the Pacific*, 6(36):pp.180–182, 1894. ISSN 00046280. URL http://www.jstor.org/stable/40670335.

D.J. Crossley. The free-oscillation equations at the centre of the earth. *Geophysical Journal of the Royal Astronomical Society*, 41(2):153–163, 1975. ISSN 1365-246X. doi: 10.1111/j.1365-246X.1975.tb04145.x. URL http://dx.doi.org/10.1111/j.1365-246X.1975.tb04145.x.

M.G. Crossley, D.J.and Rochester. Simple core undertones. *Geophysical Journal International*, 60(2):129–161, 1980. doi: 10.1111/j.1365-246X.1980.tb04287.x. URL http://gji.oxfordjournals.org/content/60/2/129.abstract.

F.A. Dahlen. The normal modes of a rotating, elliptical earth. *Geophysical Journal of the Royal Astronomical Society*, 16(4):329–367, 1968. ISSN 1365-246X. doi: 10.1111/j.1365-246X.1968.tb00229.x. URL http://dx.doi.org/10.1111/j.1365-246X.1968.tb00229.x.

V. Dehant. On the nutations of a more realistic earth model. *Geophysical Journal International*, 100(3):477–483, 1990. doi: 10.1111/j.1365-246X.1990.tb00700.x. URL http://gji.oxfordjournals.org/content/100/3/477.abstract.

J.S. Derr. Internal structure of the earth inferred from free oscillations. *Journal of Geophysical Research*, 74(22):5202–5220, 1969. ISSN 2156-2202. doi: 10.1029/JB074i022p05202. URL http://dx.doi.org/10.1029/JB074i022p05202.

M.and Valdettaro L. Dintrans, B.and Rieutord. Gravito-inertial waves in a rotating stratified sphere or spherical shell. *Journal of Fluid Mechanics*, 398:271–297, 11 1999. ISSN 1469-7645. doi: 10.1017/S0022112099006308. URL http://journals.cambridge.org/article_S0022112099006308.

J.and Alsop L.E. Dorman, J.and Ewing. Oscillations of the earth: New core-mantle boundary model based on low-order free vibrations. *Proceedings of the National Academy of Sciences*, 54(2):364–368, 1965. URL http://www.pnas.org/content/54/2/364.short.

A.M. Dziewonski. Upper mantle models from pure-path dispersion data. *Journal of Geophysical Research*, 76(11):2587–2601, 1971. ISSN 2156-2202. doi: 10.1029/JB076i011p02587. URL http://dx.doi.org/10.1029/JB076i011p02587.

D.L. Dziewonski, A.M.and Anderson. Preliminary reference earth model. *Phys.Earth Planet.Inter.*, 25:297–356, 1981.

A.M. Gilbert, F.and Dziewonski. An application of normal mode theory to the retrieval of structural parameters and source mechanisms from seismic spectra. *Philosophical Transactions of the Royal Society of London A: Mathematical, Physical and Engineering Sciences*, 278(1280):187–269, 1975. ISSN 0080-4614. doi: 10.1098/rsta.1975.0025.

H.P. Greenspan. On the transient motion of a contained rotating fluid. *Journal of Fluid Mechanics*, 20:673–696, 12 1964. ISSN 1469-7645. doi: 10.1017/S002211206400146X. URL http://journals.cambridge.org/article_S002211206400146X.

H.P. Greenspan. *The Theory of Rotating Fluids*. Cambridge Monographs on Mechanics and Applied Mathematics. At the University Press, 1968. ISBN 9780962699801. URL `http://books.google.ca/books?id=gtqjx/wuuDMC`.

H. Greiner-Mai, Jochmann. H., and F. Barthelmes. Influence of possible inner-core motions on the polar motion and the gravity field. *Physics of the Earth and Planetary Interiors*, 117(14):81 – 93, 2000. ISSN 0031-9201. doi: http://dx.doi.org/10.1016/S0031-9201(99)00089-8. URL `http://www.sciencedirect.com/science/article/pii/S0031920199000898`.

P.M.and Zhang Z.X.and Ning J.S. Guo, J.Y.and Mathews. Impact of inner core rotation on outer core flow: the role of outer core viscosity. *Geophysical Journal International*, 159 (1):372–389, 2004. ISSN 1365-246X. doi: 10.1111/j.1365-246X.2004.02416.x. URL `http://dx.doi.org/10.1111/j.1365-246X.2004.02416.x`.

G.A. Henderson. Ph.d.thesis: A finite-element method for weak solutions of the poincaré problem. *Ottawa : National Library of Canada=Bibliotheque nationale du Canada, 1997.*, 1996.

M.and Le Gal P. Herreman, W.and Le Bars. On the effects of an imposed magnetic field on the elliptical instability in rotating spheroids. *Physics of Fluids (1994-present)*, 21(4): 046602, 2009. doi: http://dx.doi.org/10.1063/1.3119102. URL `http://scitation.aip.org/content/aip/journal/pof2/21/4/10.1063/1.3119102`.

R.R. Hollerbach, R.and Kerswell. Oscillatory internal shear layers in rotating and precessing flows. *Journal of Fluid Mechanics*, 298:327–339, 9 1995. ISSN 1469-7645. doi: 10.1017/S0022112095003338. URL `http://journals.cambridge.org/article_S0022112095003338`.

W. Hopkins. Researches in physical geology. *Philosophical Transactions of the Royal Society of London*, 129:381–423, 1839. doi: 10.1098/rstl.1839.0022. URL `http://rstl.royalsocietypublishing.org/content/129/381.short`.

S.S. Hough. The oscillations of a rotating ellipsoidal shell containing fluid. *Philosophical Transactions of the Royal Society of London A: Mathematical, Physical and Engineering Sciences*, 186:469–506, 1895. ISSN 0264-3820. doi: 10.1098/rsta.1895.0012.

Inc. IMSL. *User's manual: IMSL MATH/LIBRARY : FORTRAN subroutines for mathematical applications*. Number v.1-4 in International Mathematical and Statistical Libraries Reference Manual. IMSL, Houston, 1989. URL `http://books.google.ca/books?id=x9gnnQEACAAJ`.

H. Jeffreys. A derivation of the tidal equations. *Proceedings of the Royal Society of London. Series A, Mathematical and Physical Sciences*, pages 20–22, 1942.

H. Jeffreys. The earth's core and the lunar nutation. *Geophysical Supplements to the Monthly Notices of the Royal Astronomical Society*, 5(7):282, 1948. doi: 10.1111/j.1365-246X.1948.tb02943.x. URL `http://gsmnras.oxfordjournals.org/content/5/7/282.abstract`.

H. Jeffreys. Dynamic effects of a liquid core. *Monthly Notices of the Royal Astronomical Society*, 109(6):670–687, 1949. doi: 10.1093/mnras/109.6.670. URL `http://mnras. oxfordjournals.org/content/109/6/670.abstract`.

R.O. Jeffreys, H.and Vicente. The theory of nutation and the variation of latitude. *Monthly Notices of the Royal Astronomical Society*, 117(2):142–161, 1957. doi: 10.1093/ mnras/117.2.142. URL `http://mnras.oxfordjournals.org/content/117/2/142. abstract`.

L. Kelvin. Vibrations of a colummar vortex. *Phil.Mag.*, 10:155–168, 1880.

R. R. Kerswell. Tidal excitation of hydromagnetic waves and their damping in the earth. *Journal of Fluid Mechanics*, 274:219–241, 9 1994. ISSN 1469-7645. doi: 10.1017/S0022112094002107. URL `http://journals.cambridge.org/article_ S0022112094002107`.

R.R. Kerswell. The instability of precessing flow. *Geophysical & Astrophysical Fluid Dynamics*, 72(1-4):107–144, 1993. doi: 10.1080/03091929308203609. URL `http: //dx.doi.org/10.1080/03091929308203609`.

R.R. Kerswell. On the internal shear layers spawned by the critical regions in oscillatory ekman boundary layers. *Journal of Fluid Mechanics*, 298:311–325, 9 1995. ISSN 1469-7645. doi: 10.1017/S0022112095003326. URL `http://journals.cambridge.org/ article_S0022112095003326`.

M. D. Kudlick. *On Transient Motions in a Contained, Rotating Fluid*. Massachusetts Institute of Technology, 1966. URL `http://books.google.ca/books?id=N9oIAQAAIAAJ`.

H. Lamb. *Hydrodynamics*. University Press, 1895. URL `http://books.google.ca/ books?id=h-FJAAAAMAAJ`.

D.and Le Gal P. Le Bars, M.and Cbron. Flows driven by libration, precession, and tides. *Annual Review of Fluid Mechanics*, 47(1):163–193, 2015. doi: 10.1146/annurev-fluid-010814-014556. URL `http://dx.doi.org/10.1146/ annurev-fluid-010814-014556`.

I. Lehmann. Publications du bureau central seismologique international. *Ser.A, Trav.Sci. ,*, 14:87–115, 1936.

M.S. Longuet-Higgins. Planetary waves on a rotating sphere. *Proceedings of the Royal Society of London A: Mathematical, Physical and Engineering Sciences*, 279(1379):446–473, 1964. ISSN 0080-4630. doi: 10.1098/rspa.1964.0116.

M.S. Longuet-Higgins. Planetary waves on a rotating sphere.ii. 284(1396):40–68, 1965. doi: 10.1098/rspa.1965.0051.

M. V. Lubkov. Evaluation of outer core viscosity influence on the earth forced nutation. *Odessa Astronomical Publications*, 20:114, 2007.

L. Ian Lumb, Keith D. Aldridge, and Gary A. Henderson. *A Generalized Core Resonance' Phenomenon: Inferences from a Poincar Core Model*, pages 51–68. American Geophysical Union, 1993. ISBN 9781118666739. doi: 10.1029/GM072p0051. URL `http://dx.doi.org/10.1029/GM072p0051`.

M.N. Mamboukou. *The Earth's Slichter modes*. University of Lethbridge, Dept.of Physics and Astronomy, 2013.

Z. Martinec. Free oscillations of the earth. *Travaux géophysiques*, 32(590):117–236, 1987.

B.A.and Herring T.A.and Shapiro I.I. Mathews, P.M.and Buffett. Forced nutations of the earth: Influence of inner core dynamics: 1.theory. *Journal of Geophysical Research: Solid Earth*, 96(B5):8219–8242, 1991. ISSN 2156-2202. doi: 10.1029/90JB01955. URL `http://dx.doi.org/10.1029/90JB01955`.

P. M. Mathews and I. I. Shapiro. Nutations of the earth. *Annual Review of Earth and Planetary Sciences*, 20(1):469–500, 1992. doi: 10.1146/annurev.ea.20.050192.002345. URL `http://dx.doi.org/10.1146/annurev.ea.20.050192.002345`.

P. Melchior and B. Ducarme. Detection of inertial gravity oscillations in the earth's core with a superconducting gravimeter at brussels. *Physics of the Earth and Planetary Interiors*, 42(3):129 – 134, 1986. ISSN 0031-9201. doi: http://dx.doi.org/10.1016/0031-9201(86)90085-3. URL `http://www.sciencedirect.com/science/article/pii/0031920186900853`.

M.S. Molodensky. The theory of nutation and diurnal earth tides. *Comm.Obs.R.Belgique*, 188:25–56, 1961.

S.M. Molodensky. Tides and nutation of the earth: I.models of an earth with an inelastic mantle and homogeneous, inviscid, liquid core. *Solar System Research*, 38(6):476–490, 2004. ISSN 0038-0946. doi: 10.1007/s11208-005-0019-0. URL `http://dx.doi.org/10.1007/s11208-005-0019-0`.

RD. Oldham. The constitution of the interior of the earth as revealed by earthquakes. *NATURE*, 92:684–685, SEP-FEB 1914. ISSN 0028-0836. doi: 10.1038/092684c0.

Y. Pekeris, C.L.and Accad. Dynamics of the liquid core of the earth. *Philosophical Transactions of the Royal Society of London A: Mathematical, Physical and Engineering Sciences*, 273(1233):237–260, 1972. ISSN 0080-4614. doi: 10.1098/rsta.1972.0093.

H. Poincaré. Sur la précession des corps déformables. *Bulletin Astronomique, Serie I*, 27:321–356, 1910.

N.A. Popov. Determination of Diurnal Nutation from Observation of Bright Zenith Stars at Poltava. *SOVIET ASTRONOMY-AJ*, 7:422, December 1963.

L. Rieutord, M.and Valdettaro. Inertial waves in a rotating spherical shell. *Journal of Fluid Mechanics*, 341:77–99, 6 1997. ISSN 1469-7645. doi: 10.1017/S0022112097005491. URL `http://journals.cambridge.org/article_S0022112097005491`.

Michel Rieutord. Linear theory of rotating fluids using spherical harmonics part i: Steady flows. *Geophysical & Astrophysical Fluid Dynamics*, 39(3):163–182, 1987. doi: 10.1080/03091928708208811. URL http://dx.doi.org/10.1080/03091928708208811.

Michel Rieutord. Linear theory of rotating fluids using spherical harmonics part ii, time-periodic flows. *Geophysical & Astrophysical Fluid Dynamics*, 59(1-4):185–208, 1991. doi: 10.1080/03091929108227779. URL http://dx.doi.org/10.1080/03091929108227779.

Michel Rieutord. Inertial modes in the liquid core of the earth. *Physics of the Earth and Planetary Interiors*, 91(13):41 – 46, 1995. ISSN 0031-9201. doi: http://dx.doi.org/10.1016/0031-9201(95)03040-4. URL http://www.sciencedirect.com/science/article/pii/0031920195030404. Study of the Earth's Deep Interior.

P. H. Roberts. On highly rotating polytropes. ii. *apj*, 138:809, October 1963. doi: 10.1086/147687.

E.C. Robertson. *The interior of the earth : an elementary description / by Eugene C.Robertson*. Washington, 1966.

M. G. Rochester and D. J. Crossley. Earth's long-period wobbles: a lagrangean description of the liouville equations. *Geophysical Journal International*, 176(1):40–62, 2009. ISSN 1365-246X. doi: 10.1111/j.1365-246X.2008.03991.x. URL http://dx.doi.org/10.1111/j.1365-246X.2008.03991.x.

M. G. Rochester, D. J. Crossley, and Y. L. Zhang. A new description of earth's wobble modes using clairaut coordinates: 1. theory. *Geophysical Journal International*, 198(3):1848–1877, 2014. doi: 10.1093/gji/ggu226. URL http://gji.oxfordjournals.org/content/198/3/1848.abstract.

O.G.and Smylie D.E. Rochester, M.G.and Jensen. A search for the earth's nearly diurnal free wobble. *Geophysical Journal of the Royal Astronomical Society*, 38(2):349–363, 1974. ISSN 1365-246X. doi: 10.1111/j.1365-246X.1974.tb04127.x. URL http://dx.doi.org/10.1111/j.1365-246X.1974.tb04127.x.

Z.R. Rochester, M.G.and Peng. The slichter modes of the rotating earth: a test of the subseismic approximation. *Geophysical Journal International*, 113(3):575–585, 1993. ISSN 1365-246X. doi: 10.1111/j.1365-246X.1993.tb04653.x. URL http://dx.doi.org/10.1111/j.1365-246X.1993.tb04653.x.

M.G. Rogister, Y.and Rochester. Normal-mode theory of a rotating earth model using a lagrangian perturbation of a spherical model of reference. *Geophysical Journal International*, 159(3):874–908, 2004. ISSN 1365-246X. doi: 10.1111/j.1365-246X.2004.02447.x. URL http://dx.doi.org/10.1111/j.1365-246X.2004.02447.x.

W.and McFadden P.L. Ronald, T.M.and McElhinny. *The Magnetic Field of the Earth: Paleomagnetism, the Core, and the Deep Mantle*. International geophysics series. Academic Press, 1998. ISBN 9780124912465. URL http://books.google.ca/books?id=96APl4nK9lIC.

B. Seyed-Mahmoud. Wobble/nutation of a rotating ellipsoidal earth with liquid outer core: implementation of a new set of equations describing dynamics of rotating fluids. 1994. URL http://research.library.mun.ca/6783/. Bibliography: leaves 66-67.

B. Seyed-Mahmoud and A. Moradi. Dynamics of the earths fluid core: Implementation of a clairaut coordinate system. *Physics of the Earth and Planetary Interiors*, 227(0):61 – 67, 2014. ISSN 0031-9201. doi: http://dx.doi.org/10.1016/j.pepi.2013.11.007. URL http://www.sciencedirect.com/science/article/pii/S0031920113001660.

B. Seyed-Mahmoud, A. Moradi, Z. Kamruzzaman, and H. Naseri. Effects of density stratification on the frequencies of the inertial modes of the earth's fluid core. Submitted to: Geophysical Journal International, GJI-14-0468.R1, 2015.

G.andAldridge K. Seyed-Mahmoud, B.and Henderson. A numerical model for elliptical instability of the earth's fluid outer core. *Physics of the Earth and Planetary Interiors*, 117(14):51 – 61, 2000. ISSN 0031-9201. doi: http://dx.doi.org/10.1016/S0031-9201(99)00086-2. URL http://www.sciencedirect.com/science/article/pii/S0031920199000862.

J.and Seyed-Mahmoud R. Seyed-Mahmoud, B.and Heikoop. Inertial modes of a compressible fluid core model. *Geophysical & Astrophysical Fluid Dynamics*, 101(5-6):489–505, 2007. doi: 10.1080/03091920701523337. URL http://dx.doi.org/10.1080/03091920701523337.

M. Seyed-Mahmoud, B.and Rochester. Dynamics of rotating fluids described by scalar potentials. *Physics of the Earth and Planetary Interiors*, 156(12):143 – 151, 2006. ISSN 0031-9201. doi: http://dx.doi.org/10.1016/j.pepi.2006.02.008. URL http://www.sciencedirect.com/science/article/pii/S0031920106000707.

A.E. Shen, P.Y.and Beck. Determination of surface temperature history from borehole temperature gradients. *Journal of Geophysical Research: Solid Earth*, 88(B9):7485–7493, 1983. ISSN 2156-2202. doi: 10.1029/JB088iB09p07485. URL http://dx.doi.org/10.1029/JB088iB09p07485.

L. Shen, P.Y.and Mansinha. Oscillation, nutation and wobble of an elliptical rotating earth with liquid outer core. *Geophysical Journal International*, 46(2):467–496, 1976. doi: 10.1111/j.1365-246X.1976.tb04167.x. URL http://gji.oxfordjournals.org/content/46/2/467.abstract.

L. Slichter. Fundamental free mode of earth's inner core. *PROCEEDINGS OF THE NATIONAL ACADEMY OF SCIENCES OF THE UNITED STATES OF AMERICA*, 47(2):186–&, 1961. ISSN 0027-8424. doi: 10.1073/pnas.47.2.186.

M.L. Smith. The scalar equations of infinitesimal elastic-gravitational motion for a rotating, slightly elliptical earth. *Geophysical Journal of the Royal Astronomical Society*, 37(3): 491–526, 1974. ISSN 1365-246X. doi: 10.1111/j.1365-246X.1974.tb04099.x. URL `http://dx.doi.org/10.1111/j.1365-246X.1974.tb04099.x`.

M.L. Smith. Translational inner core oscillations of a rotating, slightly elliptical earth. *Journal of Geophysical Research*, 81(17):3055–3065, 1976. ISSN 2156-2202. doi: 10. 1029/JB081i017p03055. URL `http://dx.doi.org/10.1029/JB081i017p03055`.

D. E. Smylie, Xianhua Jiang, B. J. Brennan, and Kachishige Sato. Numerical calculation of modes of oscillation of the earth's core. *Geophysical Journal International*, 108(2):465–490, 1992. doi: 10.1111/j.1365-246X.1992.tb04629.x. URL `http://gji.oxfordjournals.org/content/108/2/465.abstract`.

D.E. Smylie and M.G. Rochester. Compressibility, core dynamics and the subseismic wave equation. *Physics of the Earth and Planetary Interiors*, 24(4):308 – 319, 1981. ISSN 0031-9201. doi: http://dx.doi.org/10.1016/0031-9201(81)90118-7. URL `http://www.sciencedirect.com/science/article/pii/0031920181901187`.

J.A. Stewartson, K.and Rickard. Pathological oscillations of a rotating fluid. *Journal of Fluid Mechanics*, null:759–773, 3 1969. ISSN 1469-7645. doi: 10. 1017/S002211206900142X. URL `http://journals.cambridge.org/article_S002211206900142X`.

K. Stewartson. On almost rigid rotations. *Journal of Fluid Mechanics*, 3:17–26, 10 1957. ISSN 1469-7645. doi: 10.1017/S0022112057000452. URL `http://journals.cambridge.org/article_S0022112057000452`.

K. Stewartson. On trapped oscillations of a rotating fluid in a thin spherical shell. *Tellus*, 23 (6):506–510, 1971. ISSN 2153-3490. doi: 10.1111/j.2153-3490.1971.tb00598.x. URL `http://dx.doi.org/10.1111/j.2153-3490.1971.tb00598.x`.

K. Stewartson. On trapped oscillations of a rotating fluid in a thin spherical shell ii. *Tellus*, 24(4):283–287, 1972. ISSN 2153-3490. doi: 10.1111/j.2153-3490.1972.tb01555.x. URL `http://dx.doi.org/10.1111/j.2153-3490.1972.tb01555.x`.

G. B. A. Thomas and R. L. A. Finney. *Calculus and Analytic Geometry*. ADDISON-WESLEY, 1992. ISBN 9780201529296. URL `http://books.google.at/books?id=7aWQqhNqKhIC`.

A. Toomre. On the nearly diurnal wobble of the earth. *Geophysical Journal of the Royal Astronomical Society*, 38(2):335–348, 1974. ISSN 1365-246X. doi: 10.1111/j.1365-246X.1974.tb04126.x. URL `http://dx.doi.org/10.1111/j.1365-246X.1974.tb04126.x`.

J.M. Wahr. A normal mode expansion for the forced response of a rotating earth. *Geophysical Journal of the Royal Astronomical Society*, 64(3):651–675, 1981. ISSN 1365-246X. doi: 10.1111/j.1365-246X.1981.tb02689.x. URL `http://dx.doi.org/10.1111/j.1365-246X.1981.tb02689.x`.

Wen-Jing Wu and M. G. Rochester. Core dynamics: the two-potential description and a new variational principle. *Geophysical Journal International*, 103(3):697–706, 1990. doi: 10.1111/j.1365-246X.1990.tb05681.x. URL http://gji.oxfordjournals.org/content/103/3/697.abstract.

J. XU, H. SUN, and R. FU. Variational approach to free motion in the earth's fluid outer core. *Chinese Journal of Geophysics*, 47(1):69–85, 2004. ISSN 2326-0440. doi: 10.1002/cjg2.456. URL http://dx.doi.org/10.1002/cjg2.456.

X.and Earnshaw P. Zhang, K.and Liao. On inertial waves and oscillations in a rapidly rotating spheroid. *Journal of Fluid Mechanics*, 504:1–40, 4 2004. ISSN 1469-7645. doi: 10.1017/S0022112003007456. URL http://journals.cambridge.org/article_S0022112003007456.

W. Zrn, P.A. Richter, B.and Rydelek, and J. Neuberg. Detection of inertial gravity oscillations in the earth's core with a superconducting gravimeter at brussels. *Physics of the Earth and Planetary Interiors*, 49(12):176 – 178, 1987. ISSN 0031-9201. doi: http://dx.doi.org/10.1016/0031-9201(87)90140-3. URL http://www.sciencedirect.com/science/article/pii/0031920187901403.

Appendix A

Appendix

A.1 Some of the Properties of the Spherical Harmonics

An essential mathematical tool for theories of the dynamical behavior of the nearly spherical Earth is that of surface spherical harmonics.Solving Laplace equation, $\nabla^2 V = 0$, with method of separation of variables using spherical polar coordinates $V = R(r)\Theta(\theta)\Phi(\phi)$. We can see that we find that Θ satisfies the associated Legendre equation, and the solutions are associated Legendre polynomials $P_n^m(\cos\theta)$, where

$$P_n^m(x) = \frac{(-1)^m(1-x^2)^{m/2}}{2^n n} \frac{d^{n+m}}{dx^{n+m}}(x^2-1)^n \tag{A.1}$$

A.1.1 Recurrence relations

We note two recurrence relations connecting associated Legendre functions of the same azimuthal order m:

$$xP_n^m(x) = \frac{n+m}{2n+1}P_{n-1}^m(x) + \frac{n+1-m}{2n+1}P_{n+1}^m(x) \tag{A.2}$$

$$(1-x^2)\frac{dP_n^m(x)}{dx} = \frac{(n+1)(n+m)}{2n+1}P_{n-1}^m(x) - \frac{n(n+1-m)}{2n+1}P_{n+1}^m(x) \tag{A.3}$$

Therefore, for $x = \cos\theta$ it can be shown that the following relations are valid, (Arfken, 1966)

$$\int \left(\frac{\partial P_q^m(\cos\theta)}{\partial\theta} \frac{\partial P_n^m(\cos\theta)}{\partial\theta} + m^2 \frac{P_q^m(\cos\theta)P_n^m(\cos\theta)}{\sin^2\theta} \right) \sin\theta d\theta$$
$$= n(n+1)\int P_q^m(\cos\theta)P_n^m(\cos\theta)\sin\theta d\theta = \frac{2n(n+1)}{2n+1}\frac{(n+m)!}{(n-m)!}\delta_{nq} \tag{A.4}$$

$$\int \left(\frac{P_q^m(\cos\theta)}{\sin\theta} \frac{\partial P_n^m(\cos\theta)}{\partial\theta} + \frac{\partial P_n^m(\cos\theta)}{\partial\theta} \frac{P_n^m(\cos\theta)}{\sin\theta} \right) \sin\theta d\theta = P_n^m(\cos\theta)P_q^m(\cos\theta)\Big|_0^\pi$$
$$(= 0 \ if \ m = 1) \tag{A.5}$$

$$2P_2(\cos\theta) = 3\cos^2\theta - 1$$
$$P_2^1(\cos\theta) = -3\,\sin\theta\cos\theta \tag{A.6}$$

Following properties can be derived using the method of integration by parts.

$$\int P_2^1 P_n^m \frac{dP_q^m}{d\theta}\sin\theta\,d\theta = \int -3\sin^2\theta\cos\theta P_n^m dP_q^m = 3\int P_q^m\,d(\sin^2\theta\cos\theta P_q^m)$$
$$= -\int P_2^1 P_q^m \frac{dP_n^m}{d\theta}\sin\theta\,d\theta + 6\int P_2 P_q^m P_q^m\,\sin\theta\,d\theta \tag{A.7}$$

$$\int \cos\theta\sin\theta\frac{\partial P_q^m}{\partial\theta}P_n^m\sin\theta d\theta = \int \cos\theta\sin^2\theta P_n^m dP_q^m$$
$$= -\int \cos\theta\sin^2\theta P_q^m dP_n^m - \int [2\cos^2\theta - \sin^2\theta]\sin\theta P_q^m P_n^m d\theta \tag{A.8}$$
$$= -\int \cos\theta\sin\theta P_q^m \frac{\partial P_n^m}{\partial\theta}\sin\theta\,d\theta - 2\int P_2 P_q^m P_n^m\sin\theta d\theta$$

$$\int \frac{\cos\theta}{\sin\theta}\frac{\partial P_q^m}{\partial\theta}P_a^m\sin\theta d\theta = \int \cos\theta P_a^m dP_q^m$$
$$= -\int \frac{\cos\theta}{\sin\theta}P_q^m \frac{\partial P_a^m}{\partial\theta}\sin\theta\,d\theta + \int P_q^m P_a^m\sin\theta d\theta \tag{A.9}$$

A.1.2 Orthogonality relations

Surface spherical harmonic of degree n and azimuthal order m, where $-n \le m \le$ n:

$$Y_n^m(\theta,\phi) = P_n^m(\cos\theta)e^{im\phi} \tag{A.10}$$

We have the orthogonality relations

$$\int_0^\pi \int_0^{2\pi} Y_n^m Y_q^{-p}\sin\theta\,d\theta d\phi = \frac{4\pi}{2n+1}(-1)^m \delta_{nq}\delta_{mp} \tag{A.11}$$

$$\int e^{i(m-k)\phi}d\phi = 2\pi\delta_{m,k} \tag{A.12}$$

We mentioned that the spherical harmonics are solutions of the Laplace equation as

$$\nabla^2 a = \frac{1}{r^2}\frac{\partial}{\partial r}\left(r^2\frac{\partial a}{\partial r}\right) + \frac{1}{r^2\sin\theta}\frac{\partial}{\partial\theta}\left(\sin\theta\frac{\partial a}{\partial\theta}\right) + \frac{1}{r^2\sin^2\theta}\frac{\partial^2 a}{\partial\phi^2} \tag{A.13}$$

Thus

$$\frac{1}{\sin\theta}\frac{\partial}{\partial\theta}\left(\sin\theta\frac{\partial Y_n^m}{\partial\theta}\right) + \frac{1}{\sin^2\theta}\frac{\partial^2 Y_n^m}{\partial\phi^2} = -n(n+1)Y_n^m \tag{A.14}$$

Finally, using (A.14) together with (A.12) we come up with two fundamental relations,

$$\sum\sum n(n+1)V_n^m(r)Y_n^m(\theta,\phi) = -\frac{1}{\sin\theta}\left[\frac{\partial}{\partial\theta}(\sin\theta\,u_\theta) + \frac{\partial u_\phi}{\partial\phi}\right] \tag{A.15}$$

$$\sum \sum n(n+1) W_n^m(r) Y_n^m(\theta, \phi) = \frac{1}{\sin \theta} \left[\frac{\partial}{\partial \theta}(\sin \theta \; u_\phi) - \frac{\partial u_\theta}{\partial \phi} \right] \qquad (A.16)$$

A.2 The Displacement Eigenvectors of s Stratified Core Model

A.3 Web of Characteristics

From the second-order derivative of the equation (2.44) the traces of the characteristic surface of the Poincaré hyperbolic equation in the meridional plane, (s, z), are two families of straight lines (Rochester, 1974)

$$z \pm \xi s = c_\pm \qquad (A.17)$$

where $\xi = \left(\sqrt{\frac{1}{\sigma^2} - 1} \right)$, c_-, c_+ are constants that respectively define coordinate of the characteristics of the positive and negative slopes. Recall that $\sigma = \omega/2\Omega$. From (A.17) these straight lines making angle γ with the **z** (rotation axis).

$$\gamma = \pm \arcsin(\sigma) \qquad (A.18)$$

Equation (2.44) may be extended in the characteristic coordinate as (Henderson, 1996)

$$\frac{\partial^2 P}{\partial c_+ \partial c-} + \frac{1}{2(c_+ - c_-)} \left(\frac{\partial P}{\partial c_+} - \frac{\partial P}{\partial c_-} \right) = 0 \qquad (A.19)$$

From (A.19), crossing the characteristic line c, derivative of the pressure $\partial P/\partial c$ is discontinues along an entire characteristic line.

Note that the discontinuity is in the gradient of the pressure and appear as a crease (and not as a shock) in the pressure contour. This is partially arise from numerical technique for calculating pressure field, and partially come from the function we used to interpolate the plots in TECPLOT software (see Figures A.3 and A.2).

Also, by finding the components of the displacement field in characteristic coordinate it may be seen that the the displacement normal to the characteristic line is continuous while tangential component of the displacement to the characteristic line is not continuous (Henderson, 1996). Note that because of the $exp(im\phi)$ dependence of the ϕ variables the results are valid for both axisymmetric or non-axisymmetric modes.
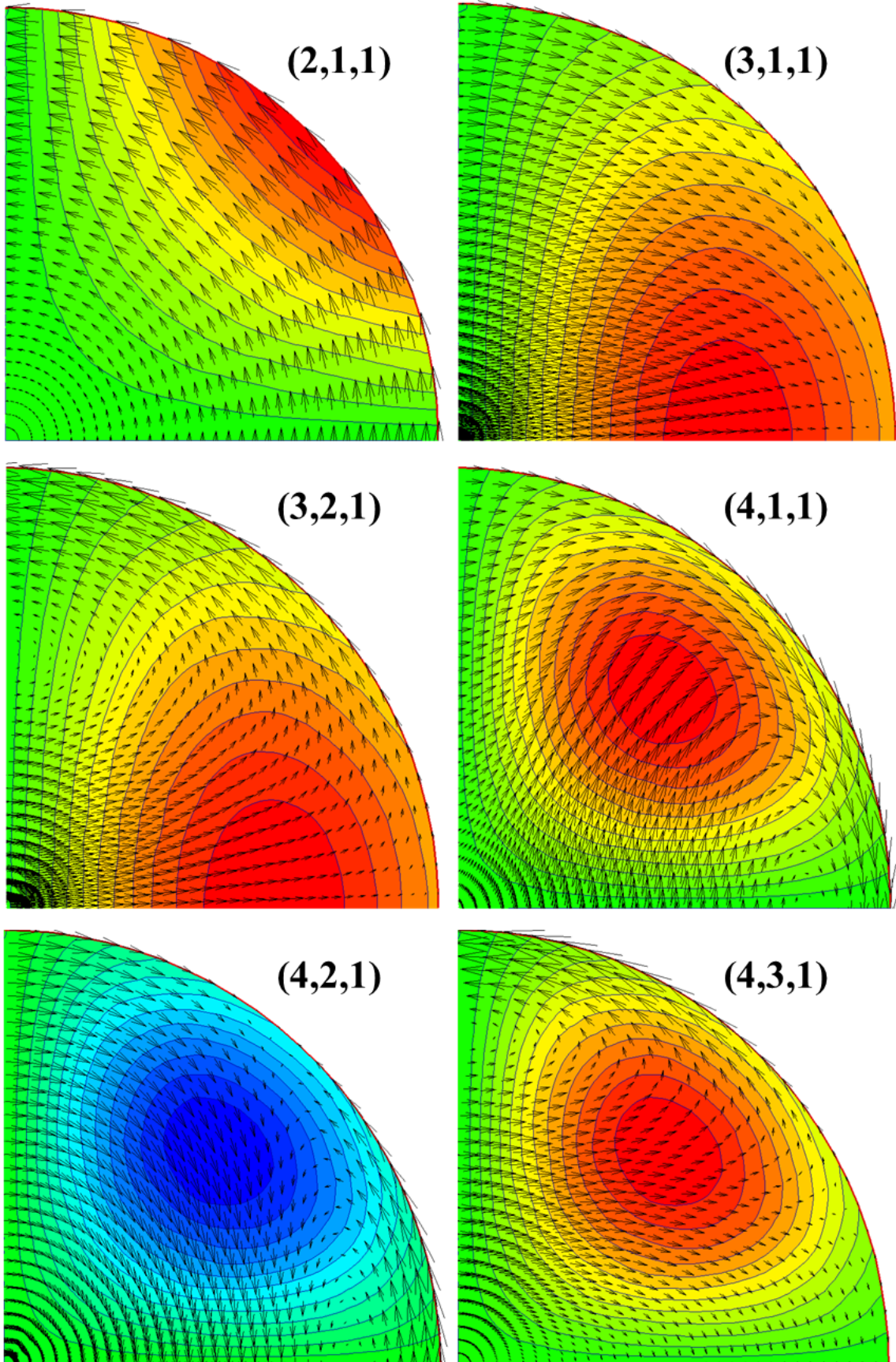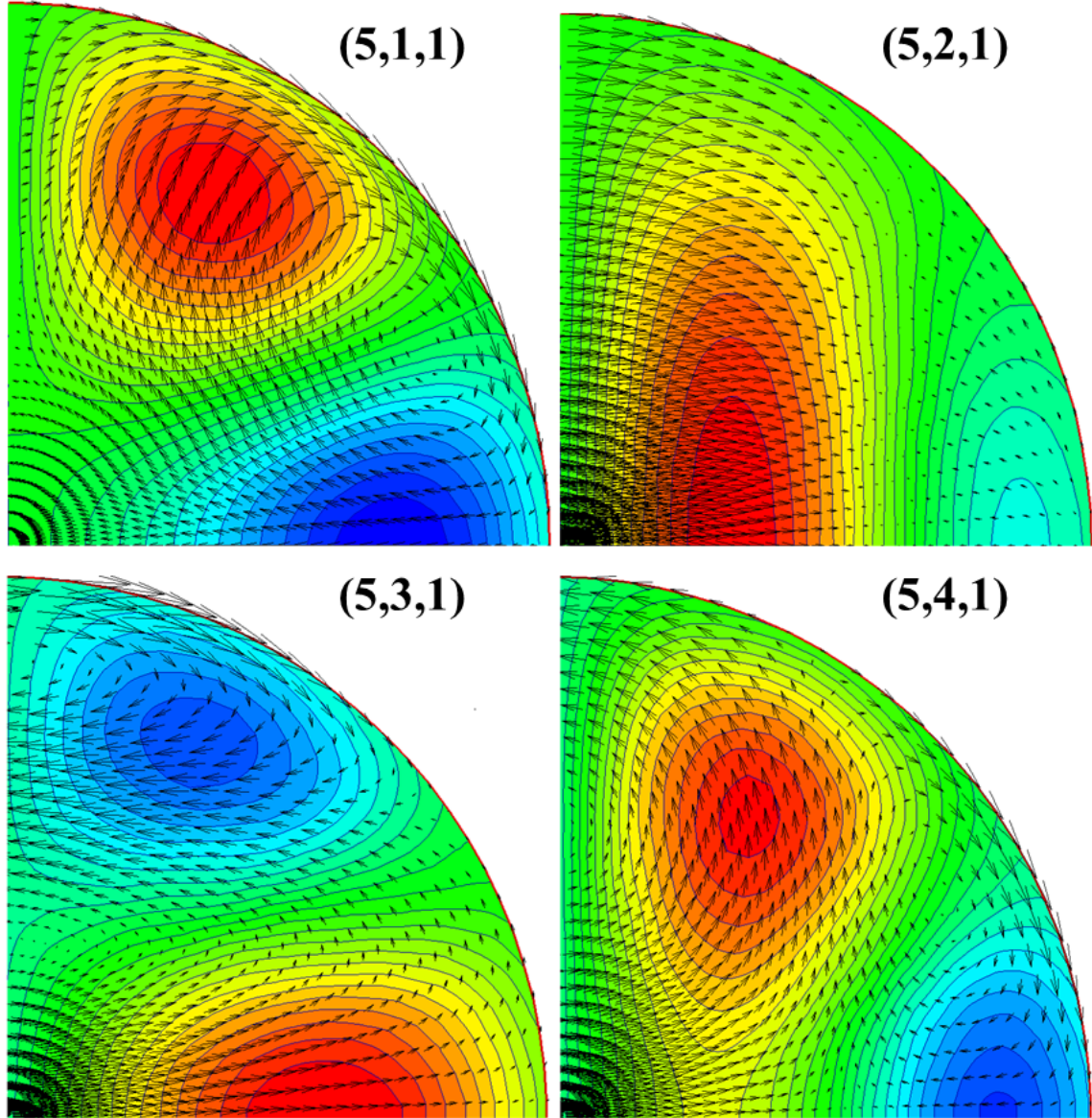
Figure A.1: The displacement eigenvectors **u** in a meridional plane, $\phi = 0$, for some of the low order, azimuthal wavenumbers, $m = 1$, of rotating stratified fluid in the full-spherical container with rigid boundaries. non-dimensional perturbation in gravitational potential, V_1 eigenfunctions are superimposed as contours. Note that for density statification we used modified PREM (Seyed-Mahmoud, 1994). The displacement patterns for a stratified fluid closely match those for a Poincaré model (Figure 4.2).
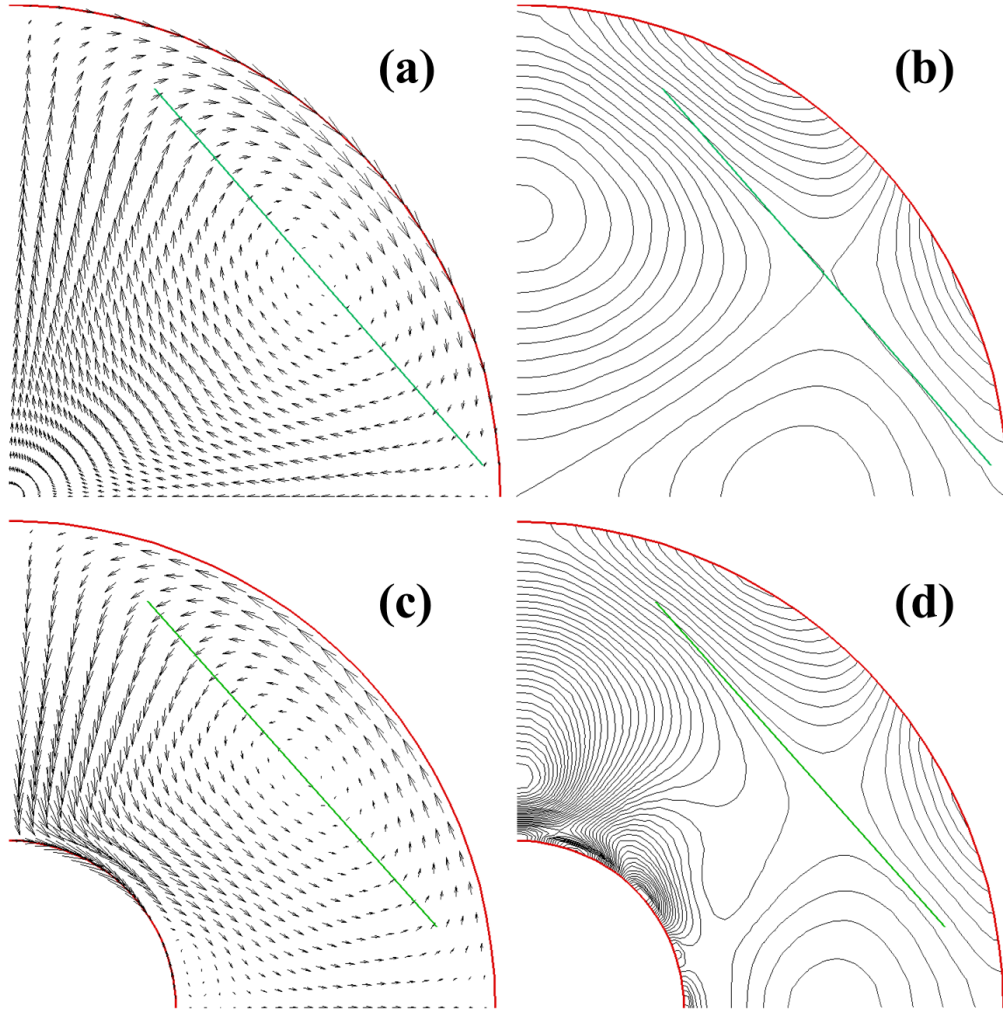
Figure A.2: The displacement eigenvectors **u** in a meridional plane, $\phi = 0$, foraxisymmetric (4,1,0) mode of rotating incompressible fluid in (a) the full-sphere and (c) Spherical shell containers with rigid boundaries. non-dimensional kinetic energy are as contours for the (b) full-sphere and (d) Spherical shell, respectively. Note that characteristic line calculated using equation (A.17) in which the frequency of the mode is $\sigma = 0.655$ and $\sigma = 0.664$ respectively for sphere and shell, and inner core outer core ratio $\eta = 0.351$.
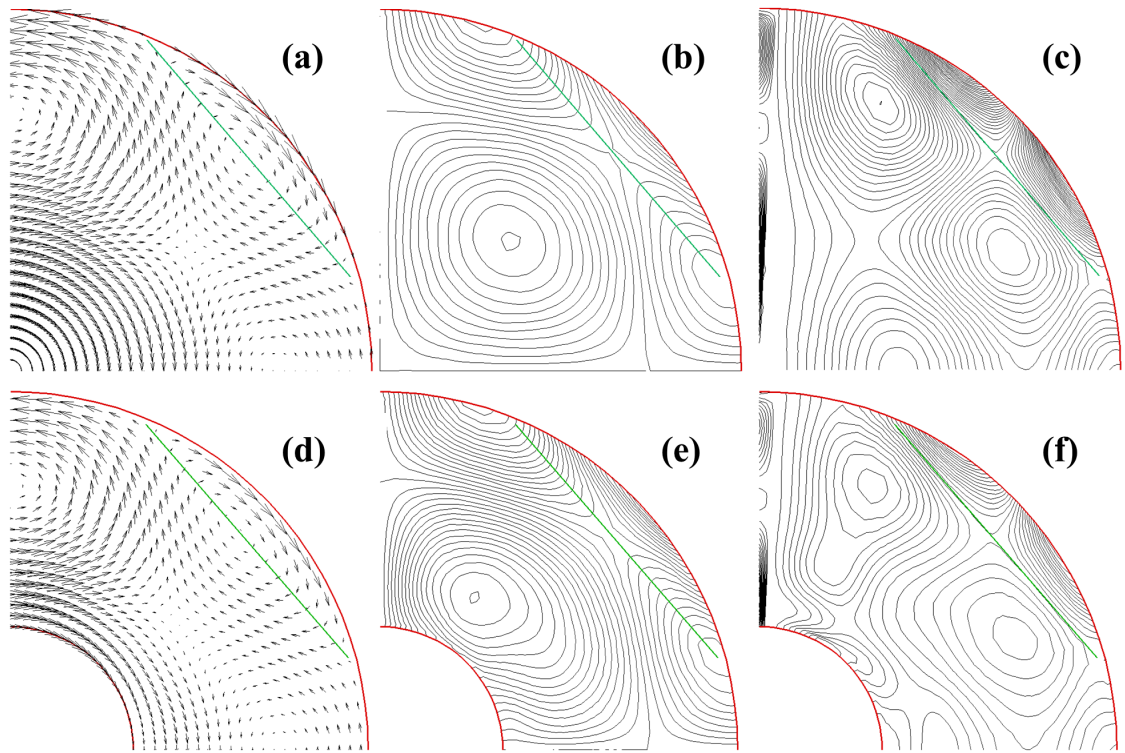
Figure A.3: The displacement eigenvectors **u** in a meridional plane, $\phi = 0$, for non-axisymmetric (6,4,1) mode of rotating incompressible fluid in (a) the full-sphere and (d) Spherical shell containers with rigid boundaries. non-dimensional (a) & (e) pressure eigenfunctions and (b) & (f) kinetic energy are as contours for the full-sphere and Spherical shell, respectively. The characteristic line calculated using equation (A.17) in which the frequency of the mode is $\sigma = 0.653$ and $\sigma = 0.659$ respectively for sphere and shell.